MOLECULAR ASSESSMENT OF RAPHIDOPHYTE SPECIES AND THEIR ASSOCIATION WITH *VIBRIO* IN DELAWARE'S INLAND BAYS

by

Christopher Robin Main

A dissertation submitted to the Faculty of the University of Delaware in partial fulfillment of the requirements for the degree of Doctor of Philosophy in Marine Studies

Fall 2014

ProQuest LLC.
789 East Eisenhower Parkway
P.O. Box 1346
Ann Arbor, MI 48106 - 1346

MOLECULAR ASSESSMENT OF RAPHIDOPHYTE SPECIES

AND THEIR ASSOCIATION WITH *VIBRIO*

IN DELAWARE'S INLAND BAYS

by

Christopher R. Main

Approved: _____

Mark A. Moline, Ph.D.
Director of the School of Marine Science and Policy

Approved: _____

Nancy M. Targett, Ph.D.
Dean of the College of Earth, Ocean, and Environment

Approved: _____

James G. Richards, Ph.D.
Vice Provost for Graduate and Professional Education

I certify that I have read this dissertation and that in my opinion it meets the academic and professional standard required by the University as a dissertation for the degree of Doctor of Philosophy.

Signed: _____

Kathryn J. Coyne, Ph.D.
Professor in charge of dissertation

I certify that I have read this dissertation and that in my opinion it meets the academic and professional standard required by the University as a dissertation for the degree of Doctor of Philosophy.

Signed: _____

Jennifer Biddle, Ph.D.
Member of dissertation committee

I certify that I have read this dissertation and that in my opinion it meets the academic and professional standard required by the University as a dissertation for the degree of Doctor of Philosophy.

Signed: _____

Dianne I. Greenfield, Ph.D.
Member of dissertation committee

I certify that I have read this dissertation and that in my opinion it meets the academic and professional standard required by the University as a dissertation for the degree of Doctor of Philosophy.

Signed: _____

Mark Warner, Ph.D.
Member of dissertation committee

ACKNOWLEDGMENTS

Several people contributed to the success and completion of this dissertation. I would like to thank Dr. Kathryn Coyne for the support and guidance over the process of research and writing. Her guidance in the varied molecular techniques has increased my passion for the various aspects of marine science. Secondly, I would like to thank Dr. Peggy Winter, who first introduced me to the world of phycology and fostered my interest in the study of algae and seaweeds over the years. Certainly, the former and current students of the Coyne lab who listened to my ramblings over the years: Dr. Kaytee Pokrzywinski, Dr. Charles Tilney, Katherine Lee, Colleen Bianco, Michelle Stuart, Dr. Josee Bouchard and Dr. Jennifer Stewart. I would also like to thank my committee members, Dr. Dianne Greenfield, Dr. Jennifer Biddle and Dr. Mark Warner for providing advice and direction. Finally, I thank everyone on the Lewes campus, in particular Dr. Edward Whereat and the participants of the University of Delaware's Citizen Monitoring Program, who without any of this research would not be possible.

I would like my family and friends who encouraged and supported me during my time at the University of Delaware and because of that deserve my eternal thanks and gratitude.

TABLE OF CONTENTS

LIST OF TABLES

LIST OF FIGURES

ABSTRACT

There is little information on the dynamics between bacteria and phytoplankton within the marine environment. One genus of bacteria, *Vibrio* is often found in association with eukaryotic organisms, forming relationships that range from mutualistic to pathogenic in nature.

In this dissertation, I investigated community-level and species-specific associations between *Vibrio* and three algal classes (diatoms, dinoflagellates, and raphidophytes) that form frequent blooms in Delaware's inland bays. Results demonstrated a significant correlation between particle-associated *Vibrio* abundance and all three algal classes. Further species-specific interactions were examined over the course of four days during a mixed bloom of the harmful algal bloom species (HABs) *Heterosigma akashiwo* (3.0-20 µm size fraction) and *Fibrocapsa japonica* (>20 µm size fraction). Results indicated a closer relationship for particle-associated *Vibrio* abundance with *H. akashiwo* abundance. Changes in the *Vibrio* community during the bloom were examined using automated ribosomal intergenic spacer analysis (ARISA) and showed differences between size fractions but not over time. Grazing experiments during a separate mixed raphidophyte bloom demonstrated that associations with different size fractions may provide refuge for certain members of the *Vibrio* community despite an increased grazing pressure on the total population.

Species-specific interactions were then examined showing that *V. cholerae* was the major species associated with *H. akashiwo*. The transcriptional response of *H.*

akashiwo to the presence of *V. cholerae* was evaluated using next generation sequencing, representing the first reported transcriptome of a raphidophyte species. This transcriptome was then used to examine differential expression of genes from *H. akashiwo* in response to the presence of *V. cholerae*. Genes related to antioxidant scavenging, amino acid transport, post-translation modification and translation were significantly up regulated, while those associated with energy production and conversion, and lipid transport and metabolism were down regulated.

Finally, direct comparison of quantitative real-time PCR (qPCR) and sandwich hybridization assay (SHA) was carried out using *H. akashiwo* as a model organism. The effects of diel cycle, growth stage, and macronutrient stress on enumeration of *H. akashiwo* was examined on both methods. A singular cellular homogenate was generated from each culture and split for analysis by qPCR and SHA. Results showed significantly greater rRNA content during lag and exponential phases compared to stationary phase for SHA, and a significant decrease in rRNA during the light cycle compared to the dark cycle. In contrast, there were no significant differences for qPCR over a diel cycle or during the different growth stages. However, under N stress both rRNA and DNA content per cell were significantly lower when compared to nutrient replete conditions.

This work increases our understanding of dynamics between harmful algal species and *Vibrio* spp. in Delaware's inland bays, as well as an understanding on the effects of diel cycle, growth stage, and macronutrient stress on enumeration of *H. akashiwo* using two molecular methods. Finally, results of this work are broadly applicable to the research and monitoring of HABs and *Vibrio* in the Mid-Atlantic region.

Chapter 1

INTRODUCTION

1.1 Algal Blooms

Algal blooms are naturally occurring phenomena in the world's oceans and under beneficial conditions, algal cells may proliferate into millions of cells per liter. Currently, there are 5000 extant species of phytoplankton in the marine environment (Sournia et al. 1991; Simon et al. 2009; Davidson et al. 2014). Among these, 300 species are known to cause harmful algal blooms (HABs), while 80 of these are known to produce toxins that can cause paralytic shellfish poisoning (PSP), diarrheic shellfish poisoning (DSP), amnesic shellfish poisoning (ASP), or neurotoxic shellfish poisoning (NSP) (Hallegraeff et al. 2003; Granéli & Turner 2007). A requirement for the monitoring of harmful algal blooms (HAB) is the accurate determination of both species and abundance. Several HAB species, including *Heterosigma akashiwo*, the subject of this dissertation, are difficult to enumerate by microscopy due to the fact that they cannot be easily preserved. Development of rapid molecular methods for both enumeration and detection of this and other HAB species can facilitate management practices in the coastal environment.

Over the last several decades the occurrence of HABs has increased in frequency and abundance (Anderson et al. 2012). The apparent increase of HABs may be related to several factors: anthropogenic eutrophication of coastal and inland waterways, increased aquaculture in coastal water or increased scientific focus on HABs (reviewed by Hallegraeff et al. 2003; Anderson et al. 2008). The association of

bacteria with phytoplankton also plays an important role in phytoplankton ecology and may impact HAB progression by either stimulating or inhibiting growth. These associations are likely species-specific, but little is known about bacterial:algal interactions in the natural environment, or how they shape microbial communities.

This dissertation investigates bacterial:algal interactions with respect to HABs and the ability to accurately quantify HAB species abundance using molecular methods. An overview of these topics is provided in this introductory chapter. This is not intended as a comprehensive review of the literature, but instead supplements material provided in each research chapter in order to place this research within the broader fields of microbial and HAB ecology.

1.2 *Vibrio*-algal Interactions

1.2.1 Marine bacteria

Marine bacteria exhibit two growth strategies in the aquatic environment: (i) free-living bacteria, or (ii) associated with particles or surfaces as a biofilm. The colonization of surfaces by bacteria and the formation of biofilms provides advantages including increased access to nutrients, refuge from predation and protection from environmental changes (Dang & Lovell 2000; Thompson et al. 2006; Asplund et al. 2011). In the marine environment, particle-associated bacteria represent approximately 10% of the total community (Middelboe et al. 1995) but may account for up to 90% of total bacterial production during blooms of phytoplankton (Smith et al. 1995). Phytoplankton cells often excrete organic compounds, predominantly carbohydrates, into the surrounding water (Takemura et al. 2014). By consuming extracellular material, particle-associated bacteria play an important role in the marine

microbial loop and the biogeochemical cycling of nutrients in the marine environment (Sapp et al. 2007; Cottrell & Kirchman 2004).

The dynamics between bacteria and phytoplankton in the marine environment are closely linked, with distinct correlations between bacterial and phytoplankton biomass (Rooney-Varga et al. 2005). However, little is known about how these communities interact at the species level in the natural environment (Rooney-Varga et al. 2005). Previous studies have provided evidence that species-specific interactions with bacteria may play a role in controlling phytoplankton growth (Lovejoy et al. 1998), through algicidal activity (Skerratt et al. 2002; Yang et al. 2013; Mayali & Azam 2004). In the dinoflagellate *Lingulodinium polyedrum*, for example, addition of proteases from marine bacteria resulted in decreased motility and changes in swimming behavior (Mayali et al. 2008). Temporary cyst formation has also been observed in *L. polyedrum* in the presence of bacterial strains from the Bacteroidetes (Mayali et al. 2007).

1.2.2 Bacterial Chemotaxis and the Phycosphere

Bacteria inhabit a heterogenous marine environment and must employ a range of strategies to exploit and navigate niches. Many bacteria are motile and can respond positively or negatively to external stimuli (taxis). The most studied response in bacteria is chemotaxis, the ability to sense and respond to chemical cues (Stocker & Seymour 2012). For example, several *Vibrio* species may use chemotaxis for colonization. *Vibrio cholerae* has been demonstrated to move towards intestinal mucosa (Freter et al. 1979), while *V. anguillarum* may migrate to the skin of fish (O'Toole et al. 1999). *V. alginolyticus* has been shown to positively migrate to exudates of *Heterosigma akashiwo* (Seymour et al. 2009). Grossart et al. (2001)

observed bacterial motility increased at the termination of a diatom bloom, suggesting release of DOM may elicit motility.

The ingestion, digestion, excretion and exudation of marine organisms produce a habitat characterized by microscale chemical gradients (Stocker & Seymour 2012). Phytoplankton, in particular, release significant amounts of amino acids, lipids, and simple sugars into the surrounding environment (Jones & Cannon 1986) that may be exploited by marine bacteria. Referred to as the phycosphere, the area immediately surrounding the phytoplankton cell represents a highly nutrient-enriched environment for marine bacteria (Stocker & Seymour 2012). The phycosphere can be several cell diameters surrounding the phytoplankton (Bell & Mitchell 1972) and may enhance the growth of bacteria near the phytoplankton (Mitchell et al. 1985; Bowen et al. 1993; Jackson 1987).

1.2.3 Cell-cell Communication

Quorum sensing (QS) is bacterial cell-cell communication that allows populations to alter gene expression patterns, allowing cells to respond individually or as a population to changes in the environment (Amin et al. 2012). Communication between bacterial cells may be carried out using *N*-acyl-L-homoserine lactones (AHL) which plays an important role in biofilm formation (reviewed by Dickschat 2010). For example, the plant pathogen *Pseudomonas syringae* requires AHL for the formation of extracellular polymeric substances (EPS) that aid in biofilm formation (Quiñones et al. 2005). Chemical communication has also been demonstrated in eukaryotes: pheromone based attraction of gametes in brown macroalgae has been demonstrated in *Ectocarpus* (Müller et al. 1971) and *Fucus* (Pohnert & Boland 2002). Interkingdom cell-cell signaling has been shown to initiate interactions between

species and is likely similar in the ocean (reviewed by Amin et al. 2012). Eukaryotes may also influence QS in bacteria. For example, Teplitski et al. (2004) demonstrated that colonies of *Chlamydomonas reinhardtii* and *Chlorella* spp. stimulated QS dependent luminescence in *Vibrio harveyi*. This ability to sense bacterial cells could allow phytoplankton to nurture specific bacteria in their phycosphere or facilitate attachment to the cell (reviewed by Amin et al. 2012).

1.2.4 Biofilm and attachment

Formation of bacterial biofilms is the process in which bacteria attach to abiotic and biotic surfaces in the aquatic environment, enhancing adaption and survival (Absalon et al. 2011). Attachment of bacterial cells is enabled by the production of extracellular polymeric substances (EPS) that forms the extracellular matrix that cells are embedded in. This matrix can account for up to 90% of the dry weight in biofilms (Flemming & Wingender 2010) and the matrix may be comprised of DNA, exopolysaccharides and proteins (Flemming & Wingender 2010; Absalon et al. 2011). The composition and structure of the biofilm matrix varies, but depends the resident species and environmental conditions (Dickschat 2010). Nutritional content, temperature, pH, iron availability and osmolarity are factors that can impact biofilm formation (O'Toole et al. 2000). Formation of the biofilm can also increase resistance to predation (Erken et al. 2011) and other environmental stressors (Sun et al. 2013).

In *Vibrio*, QS is used to determine population density and is used to control formation of biofilms (Yildiz & Visick 2009). Once a sufficient cell density has been reached the bacteria coordinate their behavior by production of small signal molecules called autoinducers. At a certain threshold of autoinducer concentration, target genes are activated for biofilm formation (Mieszkin et al. 2013). Cell structures may also

assist in formation of biofilms. For example, *V. cholerae* uses both the polar flagellum and mannose-sensitive hemagglutinin (MSHA) pili to mechanically scan a potential surface for initial attachment (Utada et al. 2014), after which production of *Vibrio* polysaccharides (VPS) begins (Lutz et al. 2013). Mannitol, a photosynthetic product of many marine algae, has been recently proposed to influence production of VPS and may play a role in habitat selection in *V. cholerae* (Ymele-Leki et al. 2013). VPS is positively regulated by VpsR and VpsT using c-di-GMP as a secondary messenger to control surface association of bacteria (Lutz et al. 2013). C-di-GMP concentration has been shown to be regulated by a phosphate responsive regulator (PhoB), which regulates the *acgAB* operon (Pratt et al. 2009). Induction of the *acgAB* operon in the late stages of infection may prepare the release of *V. cholerae* from the biofilm for dispersion in the aquatic environment (Pratt et al. 2009).

1.2.5 Predation

Predation on bacteria can induce biofilm formation, increasing production of external polysaccharides (Lutz et al. 2013; Matz et al. 2005). In *Vibrio cholerae*, the production of VPS has also been shown to increase resistance to predation (Sun et al. 2013). QS-deficient *V. cholerae* are more prone to grazing than the wild type but still retains some grazing resistance, suggesting that resistance is a combination of QS and other regulatory systems (Erken et al. 2011). Since grazing on bacteria is the largest source of bacterial mortality in the aquatic environment (Matz & Kjelleberg 2005), the capability to form biofilms may facilitate the survival and proliferation of bacteria (Matz & Kjelleberg 2005), and play a role in structuring microbial communities (Salcher et al. 2005).

1.2.6 *Heterosigma akashiwo*

The raphidophyte, *Heterosigma akashiwo*, is a cosmopolitan harmful alga, with increasing global impact on coastal environments (Li & Smayda 2000; Portune et al. 2009; O'Halloran et al. 2006; Kempton et al. 2008; Tyrrell et al. 2002). *H. akashiwo* has been implicated in fish killing blooms in China (Tseng et al. 1993), Japan (Honjo 1992), New Zealand (Chang et al. 1990), South Africa (Bates et al. 2004) and estuaries on the east (Kempton et al. 2008) and west (Rensel et al. 2010) coast of the United States. The raphidophytes have been shown to produce high levels of ROS (Marshall et al. 2002; Marshall et al. 2003; Kawano et al. 1996) which may contribute to their toxicity toward fish and shellfish (Yang et al. 1995; Oda et al. 1992; Oda et al. 1997; Kawano et al. 1996, but see Twiner et al. 2001). In photosynthetic organisms ROS are produced as byproducts of various metabolic pathways localized in the chloroplasts, peroxisomes, and mitochondria (Apel & Hirt 2004). ROS include superoxide anion radicals (O^{2-}), hydrogen peroxide (H_2O_2) and hydroxyl radicals ($OH^{\cdot}$). Photosynthetic organisms can generate ROS by activating various enzymes in response to environmental stressors, such as bacterial pathogens, drought, light intensity, and nutrient limitation (Liu et al. 2007). Studies examining factors involved in production of ROS by raphidophytes, however, have been contradictory. In *Chattonella marina*, for example, irradiance has been shown to play a role in the production of O^{2-}, with iron playing a role in suppressing production of O^{2-} (Marshall et al. 2002). Superoxide anion production in *C. marina* was also inhibited by the presence of the iron chelator deferoxamine (Kawano et al. 1996). In *Heterosigma akashiwo*, the opposite is true; iron depletion enhanced the production of ROS, with variation in light not affecting production (Twiner & Trick 2000).

One of the challenges in understanding *H. akashiwo* ecology is that the lack of a cell wall in this and other marine raphidophytes leads to difficulty in preserving and working with preserved samples. The addition of normal preservatives such as glutaraldehyde has been shown to lyse cells quickly so that enumeration by light microscopy is often not possible. Molecular methods, including both Quantitative Real-Time PCR (qPCR; Coyne et al. 2005; Handy et al. 2006; Demir et al. 2008; Portune et al. 2009) and the Sandwich Hybridization Assay (SHA; Tyrrell et al. 2002; Tyrrell et al. 2001; Greenfield et al. 2006; Greenfield et al. 2008; Preston et al. 2009) have been developed and independently validated for enumeration of *H. akashiwo* in laboratory culture and environmental samples. However, the direct comparison of these methods has only recently been carried out (Doll et al. 2014), demonstrating good correlation between results of qPCR and SHA for enumerating cell densities of several strains of *H. akashiwo* in laboratory culture. The extent to which these methods are able to accurately determine cell densities over a range of physiological conditions has not been evaluated.

1.2.7 Quantitative Real-Time PCR (qPCR)

Quantitative real-time PCR (qPCR) allows for quantification of products produced during the PCR reaction to be quantified in "real time" during each cycle of PCR. Reactions are done in a specialized thermocycler able to measure a fluorescent detector molecule. Two common fluorescent detectors are intercalating dyes, such as SYBR Green, or small probe sequences that fluoresce on hydrolysis, commonly called hydrolysis or TaqMan probes. TaqMan probes use the exonuclease activity of the Taq polymerase to degrade a non-extendable fluorescently marked probe during the hybridization and extension stages of PCR. The probe requires two different

fluorescent dyes, a reporter dye (such as FAM or HEX) and a quenching dye (such as BHQ). The reporter dye emission is transferred to the quencher dye by fluorescence-resonance energy transfer (FRET). Cleavage of reporter dye by Taq polymerase results in an increase in the fluorescence, which is captured by a CCD camera (Gibson et al. 1996). Species-specific probes allow for greater specificity during the PCR reaction and detection of fluorescence. The TaqMan method may also be multiplexed, using gene specific probes with different fluorescent reporter dyes to quantify multiple genes in a single reaction (VanGuilder et al. 2008; Handy et al. 2006).

Analysis of fluorescence is carried out by setting a critical/crossing threshold (C_T) during exponential amplification. The C_T is the number of cycles that it takes each reaction to reach the prescribed fluorescence level (VanGuilder et al. 2008). A standard curve of target DNA with known concentration is used along with samples. Linear regression is then used to determine relative abundance of target DNA in each sample. An exogenous control, such as pGEM plasmid, may be added to the extraction buffer to assess levels of inhibition in environmental samples. The abundance of the target gene is normalized to pGEM concentrations, correcting for errors in processing or due to inhibition of the PCR (Coyne et al. 2005).

1.2.8 Sandwich Hybridization Assay (SHA)

In contrast to qPCR, SHA uses direct detection of the ribosomal RNA (rRNA) from unpurified samples. SHA uses two oligonucleotide probes, a biotinylated species-specific capture probe immobilized on a support medium. The target sequence from a cellular homogenate is hybridized to the capture probe and then "sandwiched" between a signal probed conjugated with digoxygenin. The addition of an anti-digoxygenin horseradish peroxidase (HRP) substrate reacts with the sandwich

to produce colorimetric development. After color development the optical density is read and is directionally proportional to the amount of rRNA in the sample The abundance of *H. akashiwo* is determined through linear regression analysis of standards derived from either cultured or natural samples (Scholin et al. 1996; Miller & Scholin 1998; Greenfield et al. 2008; Doll et al. 2014).

1.3 Project Overview

This project has three components:

(1) In Chapter 2, I investigated community-level and species-specific associations between *Vibrio* spp. and algae within Delaware's inland bays. The abundance of particle-associated *Vibrio* spp. was measured in relation to diatom, dinoflagellate and raphidophyte abundance from three Delaware Inland Bay sites from 2009 – 2011. Species-specific associations and *Vibrio* community structure were then examined during a naturally occurring mixed bloom of two HAB species: *Fibrocapsa japonica* and *Heterosigma akashiwo*. Finally, I examined the hypothesis that association with algae provides a refuge from grazing for *Vibrio* spp. Microzooplankton grazing rates and changes in *Vibrio* community structure were measured for three size fractions of particle-associated and planktonic *Vibrio* populations during mixed blooms of *F. japonica* and *H. akashiwo*.

(2) Interactions between *Vibrio* and algal species were further investigated in Chapter 3 by examining the effects of *Vibrio cholerae* on the global transcriptome of the marine raphidophyte *Heterosigma akashiwo*. Changes in transcript levels for key enzymes related to stress response and mitigation of reactive oxygen species were verified by qPCR. This represents the first investigation of transcriptional responses of *Heterosigma akashiwo* to the presence of bacteria.

(3) Finally, in Chapter 4, I examined the effects of physiological status on the accuracy of qPCR for enumeration of *Heterosigma akashiwo*, and compared these results to SHA. Both qPCR and SHA target nucleic acids within the cell, but are distinctly different in that qPCR amplifies DNA fragments defined by a set of specific primers, while SHA measures the amount of captured rRNA within a cell lysate. Here, I evaluated the effects of diel cycle, growth phase and macronutrient (nitrogen and phosphorus) stress on the quantification of cell density by these two methods, using *Heterosigma akashiwo* as a model organism.

Chapter 2

COMMUNITY-LEVEL AND SPECIES-SPECIFIC ASSOCIATIONS BETWEEN PHYTOPLANKTON AND PARTICLE-ATTACHED *VIBRIO* SPECIES IN DELAWARE'S INLAND BAYS

2.1 Abstract

Vibrio are an abundant, naturally occurring and diverse group of bacteria in marine environments that can form associations with phytoplankton or other particles by forming a biofilm. Correlations between total *Vibrio* spp. abundance and phytoplankton abundance have been noted, suggesting that growth is enhanced by exudates produced during algal blooms and/or that association with phytoplankton cells may provide *Vibrio* with a refuge from predation. Here, we investigated community-level and species-specific associations between particle-associated *Vibrio* and phytoplankton species in size fractionated water samples collected from Delaware's inland bays (DIB), Delaware, in the mid-Atlantic region of the US. The relative abundances of particle-associated *Vibrio* and algal classes that form frequent blooms in the DIB (dinoflagellates, diatoms and raphidophytes) were determined using quantitative real-time PCR. Results demonstrated a significant correlation between particle-attached *Vibrio* abundance and all three classes of phytoplankton. Species-specific correlations were further examined over the course of four days during a mixed bloom of the harmful algal species (HABs) *Heterosigma akashiwo* and *Fibrocapsa japonica* (Raphidophyceae) where results indicated a closer relationship for particle-associated *Vibrio* abundance with *H. akashiwo*. Changes in the *Vibrio*

assemblages during the bloom were evaluated using automated ribosomal intergenic spacer analysis (ARISA) and revealed significant differences between each size fraction, but not over time. Grazing experiments during a separate mixed raphidophyte bloom showed that association with different size fractions may provide refuge for certain members of the *Vibrio* community despite an increased grazing pressure on the population as a whole. Results of this investigation demonstrate links between phytoplankton, including HAB species, and *Vibrio* that may lead to predictions of potential health risks and inform future management practices in this region.

2.2 Introduction

Bacteria within the genus *Vibrio* are naturally abundant in marine and estuarine environments (Grimes 1991), where they exhibit two alternative growth strategies: (i) association with particles as a biofilm or (ii) as free-living bacterioplankton (Yildiz & Visick 2009). Association with planktonic organisms plays an important role in the ecology of *Vibrio* (Turner et al. 2009) by providing an enriched microenvironment for *Vibrio* spp. (Huq et al. 2005; Eiler & Bertilsson 2006; Asplund et al. 2011). Previous research demonstrated that planktonic copepods, in particular, enhance the survival and distribution of *Vibrio* in temperate and tropical areas (Lizárraga-Partida et al. 2009; Tamplin et al. 1990). Associations with plankton may also provide a refuge from grazing by bacterivorous protozoa (Matz et al. 2005; Worden et al. 2006), which can be substantial in some areas (Beardsley et al. 2003). Matz et al. (2005), for example, showed that the cell density of *V. cholerae* within a biofilm remained stable in the presence of protozoa, whereas planktonic cells were rapidly eliminated. However, particle association may not always be advantageous as it may subject the

cells to sinking forces or losses through "collateral damage" when host cells are preyed upon (Worden et al. 2006).

In addition to copepods, *Vibrio* also form attachments to algal cells (Hood & Winter 1997), and it has been suggested that *Vibrio* preferentially attach to algal cells and detritus over whole copepods (Tamplin et al. 1990). Increases in *Vibrio* abundance have been associated with algal blooms, and in some cases, with specific algal groups. For example, Turner et al. (2009) showed a significant correlation between phytoplankton abundance and total culturable *Vibrio* abundance in the coastal waters of Georgia, and high *Vibrio* abundance has been noted to occur in diatom dominated phytoplankton assemblages in the Arabian Sea (Asplund et al. 2011). In another study, the abundance of particle-attached *Vibrio cholerae* increased rapidly (>4 doublings per day) during coastal algal blooms, despite intense protozoa grazing pressure (Worden et al. 2006). While previous studies have demonstrated a correlation between phytoplankton abundance and *Vibrio* concentrations in coastal waters, however, few studies have examined species-specific associations between *Vibrio* and phytoplankton in the natural environment. In one study, for example, Eiler et al. (2006) found a significant correlation between *V. cholerae* and *Prorocentrum* spp., suggesting that these interactions may be important determinants regulating intrageneric competition and growth of *Vibrio* in the marine environment.

Increased occurrences of algal blooms (Bricker et al. 2008) are one consequence of declining coastal water quality in the mid-Atlantic region of the United states (Kiddon et al. 2003). Eutrophication of Delaware's inland bays (DIB), which consist of Rehoboth Bay, Indian River Bay, and Little Assawoman Bay, has increased over the last several decades, with high concentrations of nutrient inputs

from agricultural and urban sources (Price 1998; Sallade & Sims 1997). Several harmful or potentially harmful algal bloom species (HABs) have been identified in the DIB, and blooms of harmful algal species occur frequently (Handy et al. 2008). Among these are several species of harmful dinoflagellates including *Gyrodinium instriatum* (Whereat 2013), *Karlodinium veneficum* (Whereat 2013), and *Prorocentrum minimum* (Warner & Madden 2007), as well as raphidophytes, a group of species distributed globally in temperate coastal waters and freshwater environments. Marine raphidophytes include genera which are known for fish kills, of which four species bloom annually in the DIB: *Heterosigma akashiwo*, *Chattonella subsalsa*, *Fibrocapsa japonica* and the recently described *Viridilobus marinus* (Coyne et al. 2005; Handy et al. 2006; Demir-Hilton et al. 2012; Whereat 2013).

Although there are extensive data on harmful algal species in the DIB, little is known about the ecology of *Vibrio* in mid-Atlantic estuaries (Johnson et al. 2012), or associations between *Vibrio* spp. and HABs or other phytoplankton groups in this region. Our goals were to examine community-level and species-specific relationships between particle-associated *Vibrio* spp. and phytoplankton groups in the DIB. Specifically, we examined correlations between the abundance of particle-associated *Vibrio* and three algal groups: diatoms, dinoflagellates, and raphidophytes at three sites in the DIB over three years. We also examined changes in abundance and community composition of particle-associated *Vibrio* spp. and HAB raphidophytes in size-fractionated water samples during a mixed bloom of *Heterosigma akashiwo* and *Fibrocapsa japonica*. In addition, the impacts of microzooplankton grazing on two size fractions of particle-associated and free-living planktonic assemblages of *Vibrio* were assessed during a separate mixed raphidophyte bloom. Results of this study are

broadly relevant to research and monitoring of *Vibrio* and interactions with HAB species in the Mid-Atlantic region.

2.3 Material and Methods

2.3.1 Field samples

Water samples were collected weekly from May to September in 2009 – 2011 from three sites within the Delaware Inland Bays: RB64 in Rehoboth Bay, IR32 in Indian River Bay and SB10E in Little Assawoman Bay (Figure 2.1). Temperature, salinity and dissolved oxygen (mg l^{-1}) were measured for each sample using a 556 MPS YSI meter (YSI Inc., Yellow Springs, OH). Dissolved nutrient (NH_4, NO_x, P and Si) concentrations were determined for water samples collected in 2010 and 2011 only, using a segmented flow auto-analyzer (Seal Analytical, Mequon, WI). Chlorophyll *a* (chl *a*) concentrations were measured after extraction in 90% acetone on a Turner 10AU fluorometer (Turner Designs, Sunnyvale, CA; Welschmeyer 1994).

Water samples were filtered under gentle vacuum (~380 mmHg) and size-fractionated on polycarbonate filters (Millipore Isopore, Billerica, MA) to retain the >3.0 μm size fraction. Filters were immediately placed in CTAB buffer consisting of 100 mM Tris–HCl (pH 8), 1.4M NaCl, 2% (w/v) cetyltrimethylammonium bromide (CTAB), 0.4% (v/v) 2-mercaptoethanol, 1% (w/v) polyvinylpyrrolidone and 20 mM EDTA (Dempster et al. 1999), amended with 20 ng ml^{-1} pGEM plasmid (Promega, Madison, WI) as an internal standard (Coyne et al. 2005). Filtered samples were stored at -80°C until extraction. Before extraction, all samples were heated at 65 °C for 10 minutes.

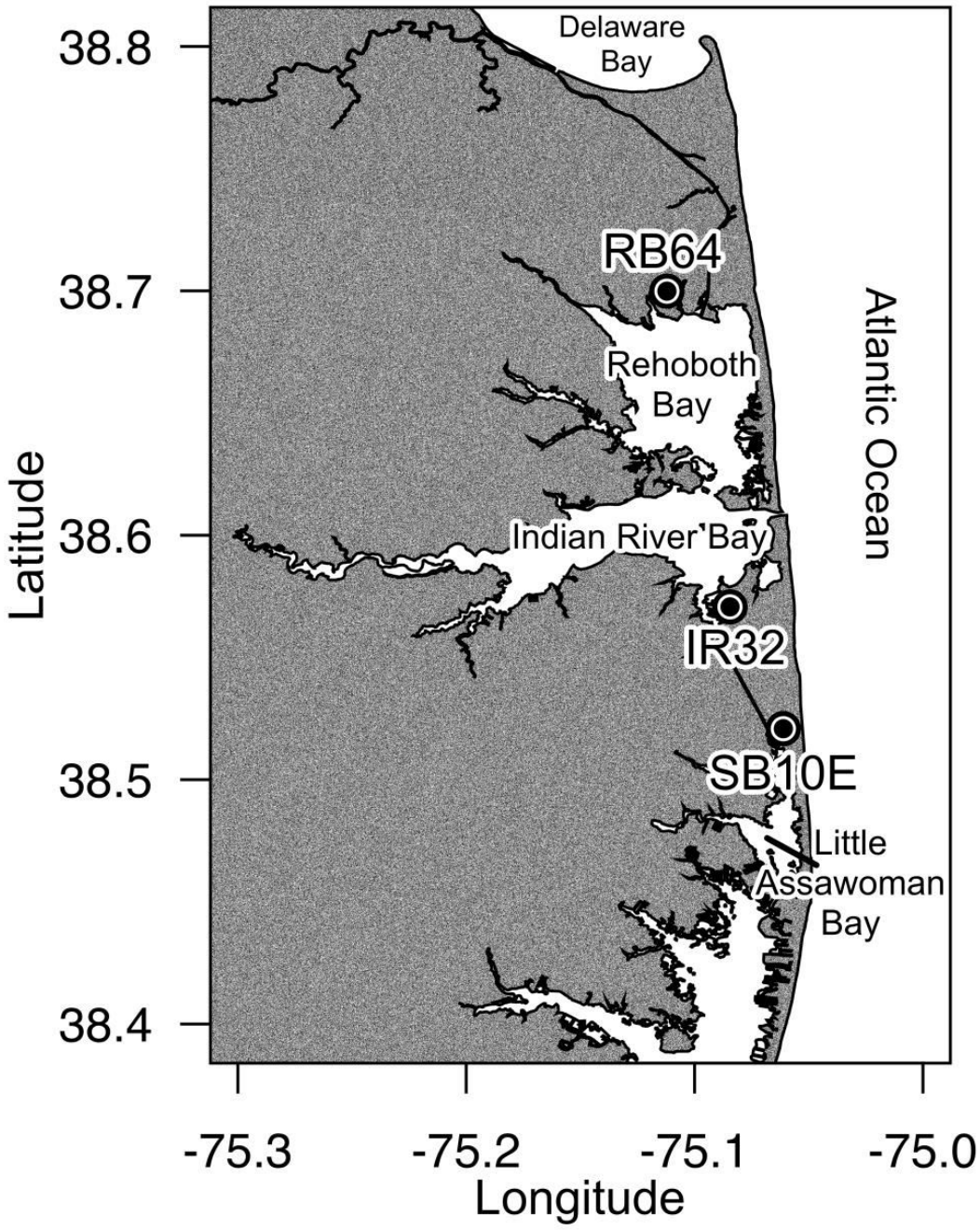

Figure 2.1 Sampling sites within the Delaware Inland Bays: Rehoboth Bay at Torquay (RB64); Indian River Bay at Holly Terrace Acres Canal (IR32); and Little Assawoman Bay at South Bethany: Russell Canal East (SB10E).

DNA was extracted as described in Coyne et al. (2001) and resuspended in LoTE (3 mM Tris- HCl, 0.2 mM EDTA, pH 7.5) (Coyne et al. 2001; Dempster et al. 1999). DNA concentration was determined by spectrophotometry and samples were diluted to approximately 25 ng μl^{-1} for molecular analysis.

Primers (Table 2.1) for the RNA polymerase subunit A (*rpoA*), a single copy gene within the *Vibrio* genome, were previously described in Dalmasso et al. (2009). Concentrations of algal class-specific primers (Table 2.1) targeting the 18S rDNA for raphidophytes, dinoflagellates and diatoms were optimized for qPCR as described in Coyne et al. (2005). DNA from size-fractionated water samples was amplified by qPCR in triplicate 10 µl reactions consisting of 5 µl of SYBR Green Master Mix (Applied Biosystems), 0.9 µM each primer targeting *Vibrio rpoA* or algal 18S rRNA sequences (Table 2.1), and 1 µl diluted DNA template (~25 ng). Reaction conditions for amplification of *Vibrio rpoA* consisted of 2 min at 50 °C, 10 min at 95 °C, followed by 40 cycles at 95 °C for 15 s, 53 °C for 30 s and 72 °C for 1 min, with added dissociation analysis. Reaction conditions for algal groups were 2 min at 50 °C, 10 min at 95 °C, followed by 40 cycles at 95 °C for 15 s, 56 °C for 30 s and 72 °C for 1 min, with added dissociation analysis. Quantification of the internal pGEM plasmid standard was carried out using a TaqMan®-based assay in triplicate 10 µl reactions consisting of 5 µl of TaqMan Universal Master Mix (Applied Biosystems), 0.9 µM of each primer, 0.2 µM TaqMan probe (Table 2.1), and 1 µl of diluted DNA template. Reaction conditions consisted of 2 min at 50 °C, 10 min at 95 °C, followed by 40 cycles at 95 °C for 15 s, 56 °C for 30 s and 72 °C for 1 min. The relative abundance of *Vibrio* and algal groups were determined by linear regression analysis using a standard curve generated from *rpoA* plasmid and 18S rDNA plasmid from each algal

group. *rpoA* and 18S rDNA abundance in each sample was normalized to the abundance of pGEM and reported as relative abundance per volume of water filtered.

2.3.2 Intensive sampling

Samples were collected during a mixed raphidophyte bloom of *Heterosigma akashiwo* (10 – 15 µm in size) and *Fibrocapsa japonica* (20 – 30 µm in size), at site RB64 on 13 – 16 September 2011. Initial cell concentrations for *H. akashiwo* were 2.99×10^7 cells l^{-1}, while *F. japonica* cell concentrations were 4.1×10^5 cells l^{-1}. Samples were collected from just below the surface at replicate Sites 1 and 2, approximately 10 meters apart, at 10:14 a.m. on 13 September 2011 (T_0), and at 4, 26, 47 and 70 hours after T_0 (T_4, T_{26}, T_{47}, and T_{70}, respectively). Physical parameters, chl *a*, and nutrient concentrations were measured as above for each time point. Water was pre-filtered on site using a 150 µm filter to remove detritus and zooplankton. Prefiltered samples were then transported to the laboratory and size fractionated onto polycarbonate filters to collect the >20 µm, 3.0-20, and 0.2-3.0 µm size fractions (which contained the planktonic or "free-living" *Vibrio*) within 1 hour of collection. DNA was extracted from each size fraction as described above. The relative abundance of *H. akashiwo* (3.0-20 µm size fraction) and *F. japonica* (>20 µm size fraction) were determined using a TaqMan®-based assay in triplicate 10 µl reactions consisting of 5 µl of TaqMan Universal Master Mix (Applied Biosystems), 0.9 µM of species-specific primers (Table 2.1), 0.2 µM TaqMan probe (Table 2.1), and 1 µl of diluted DNA template (~25 ng). Reaction conditions were 2 min at 50 °C, 10 min at 95 °C, followed by 40 cycles at 95 °C for 15 s, 56 °C for 30 s and 72 °C for 1 min. Quantification of *Vibrio* spp., dinoflagellates (>20 µm size fraction only), and the pGEM internal standard were carried out as above.

Table 2.1 Primer and probe sequences used in this study

Target	Primer	Sequence (5' - 3')
Heterosigma akashiwo 18S rDNA[1]	Hs 1350F	CTAAATAGTGTCGGTAATGCTTCT
	Hs 1705R	GGCAAGTCACAATAAAGTTCCAT
	Hs Probe	HEX-CAACGAGTAACGACCTTTGCCGGAA-IBFQ1
Fibrocapsa japonica 18S rDNA[2]	Fj 1350F	CCCAGTCACGACGTTGTAAAACG
	Fj 1705R	TGTGTGGAATTGTGAGCGGA
	Fj Probe	FAM-CACTATAGAATACTCAAGCTTGCATGCCTGCA-IBFQ1
pGEM plasmid DNA[1]	M13F	CCCAGTCACGACGTTGTAAAACG
	pGEM R	TGTGTGGAATTGTGAGCGGA
	pGEM Probe	FAM-CACTATAGAATACTCAAGCTTGCATGCCTGCA-IBQF1
Vibrio spp. *rpoA*[3]	*rpoA* 294F	AAATCAGGCTCGGGCCCT
	rpoA 535R	GCAATTTTRTCDACYGG
Diatom[4]	Diatom 1256F	TAGTGAGGATTGACAGATTGAG
	Diatom 1637R	CGTAATCATTGCAGTTTGATGAAC
Dinoflagellate[5]	Dino 1662F	CCGATTGAGTGWTCCGGTGAATAA
	Euk B	GATCCWTCTGCAGGTTCACCTAC
Raphidophyte[6]	BTG005C	ATCATTACCACACCGATCC
	Raphid-ITS-R	YGCCAGGTGCGTTCGAA

Table 2.1 continued

Target	Primer	Sequence (5' - 3')
Vibrio spp. ITS[7]	16S.6	ACTGGGGTGAAGTCGTAACA
	23S.1	CTTCATCGCCTCTGACTGC

[1]From (Coyne et al. 2005)
[2]From (Demir et al. 2008)
[3]From (Dalmasso et al. 2009)
[4]From (Tilney et al. 2014)
[5]From (Handy et al. 2008)
[6]Modified from (Connell 2002)
[7]From (Hoffmann et al. 2010)

Vibrio assemblages were also evaluated in each size fraction by automated ribosomal intergenic spacer analysis (ARISA) using *Vibrio*-specific primers (Table 2.1; Hoffmann et al. 2010). The 23S rRNA primer was modified with the fluorescent probe hexachlorofluorescein (HEX). ARISA patterns were generated from DNA extracted from known cultured *Vibrio* species (kindly provided by Dr. Gary Richards, USDA ARS, Delaware State University, Dover, DE) for comparison and to identify peaks. DNA was amplified after an initial denaturation for 5 min at 94 °C for 16 cycles of 94 °C for 1 min, 72 °C for 1 min (decreased 0.5 °C per cycle), 72 °C for 1 min, followed by 22 cycles of 94 °C for 1 min, 64 °C for 1 min and 72 °C for 1 min. PCR products were then denatured at 94 °C for 1 min followed by a 1 min incubation at 84 °C and a 5 min incubation at 72 °C. To reduce heteroduplex formation, PCR products were diluted 10-fold in fresh reaction mixture and subjected to 5 additional cycles of 94 °C for 1 min, 64 °C for 1 min and 72 °C for 1 min (Thompson et al. 2002). 1 µL of the PCR product was combined with 18 µL HiDi formamide (Applied Biosystems) and 1 µL GeneScan-2500 Size Standard (Applied Biosystems) and denatured at 95º C for 3 minutes. HEX-labeled PCR products were detected and sized with an ABI Prism 310 Genetic Analyzer (Applied Biosystems) using GeneScan v. 3.1 software (Applied Biosystems). Results were imported into PeakScanner v.2.0 software (Applied Biosystems) for analysis and peaks between 50 and 1000 bases in length were binned at a width of 1 nt. Peaks were aligned and standardized to the total of all peak heights within each sample for comparison between ARISA profiles using T-Rex (Culman et al. 2009).

2.3.3 Microzooplankton grazing

Samples were collected from RB64 during a mixed *Heterosigma akashiwo* and *Fibrocapsa japonica* bloom on 23 Aug. and 25 Aug., 2011, for two separate grazing studies. Samples were pre-filtered on site through a 150 μm filter to remove zooplankton and detritus. Initial cell concentrations for Experiment 1 were $4.3x10^6$ cells l^{-1} for *Heterosigma akashiwo* and $2.66x10^4$ cells l^{-1} for *Fibrocapsa japonica*. For Experiment 2, initial cell concentrations were $1.15x10^7$ cells l^{-1} and $1.32x10^4$ cells l^{-1} for *H. akashiwo* and *F. japonica* respectively. For each grazing study, an aliquot of the water sample (T_0) was size fractionated to achieve >20 μm, 3.0 – 20 μm and 0.2 – 3.0 μm (free-living) size fractions for both chl *a* and qPCR analyses. Site water was also filtered through a 0.2 μm filter (Whatman Polycap Disposable Capsules, GE Healthcare, Piscataway, NJ) for dilution of whole water (Demir et al. 2008) to achieve dilutions consisting of 25, 50 and 100% of whole water. Diluted samples (N=4) were enriched with f/2 nutrients (Demir et al. 2008). Bottles were incubated at 25 °C for 24 hr at a light intensity of 228 μmol m^{-2} sec^{-1}. Samples were then size fractionated to collect >20 μm, 3.0-20 μm and 0.2-3.0 μm (free-living) size fractions for both chl *a* and DNA extractions as described above. The relative abundance of *H. akashiwo*, *F. japonica* and *Vibrio* spp. were determined using qPCR parameters as above. *Vibrio* growth rate (μ) per day was calculated as follows:

$$\mu=[\ln(\text{relative abundance at } T_{24})-\ln(\text{relative abundance at } T_0)] \times \text{day}^{-1}$$

Vibrio apparent growth and grazing rates were calculated by plotting the growth rate of *Vibrio* vs. dilution factor. The negative slope of this relationship is the grazing rate and the y-intercept is the apparent growth rate (Landry & Hassett 1982; Demir et al. 2008), reported as per day (day $^{-1}$).

The free-living and particle attached *Vibrio* assemblages within each size fraction for the 100% (undiluted) treatments were evaluated by ARISA as described above.

2.3.4 Statistical analysis

Statistical comparisons were performed using the R statistical package (R Core Team 2012). Relative abundances determined by qPCR were transformed using a square root square root transformation before calculating Pearson's correlations between *Vibrio* spp. abundance and environmental factors or algal groups. A difference was considered significant if the P-value was < 0.05. If a significant relationship was detected, a Tukey honest significant differences (TukeyHSD) post-hoc test was conducted to determine relationships. Principal Component Analysis (PCA) was carried out using the PRIMER 6.1.16 (Primer-E, Ivybridge, UK) software package to identify factors contributing to differences between sites or years with respect to environmental factors.

Multivariate analysis of ARISA data was carried out using the PRIMER 6.1.16 software package. Standardized peak heights from ARISA were subjected to a square root transformation before analysis. The transformed data was then used to produce a Bray-Curtis similarity matrix. Multidimensional scaling (MDS) diagrams were produced from the similarity matrix using the Kruskal fit scheme of 1, with 25 restarts and a minimum stress of 0.01. The Analysis of Similarity (ANOSIM) function in PRIMER was used to examine relationships between the particle-associated *Vibrio* community structure in the Intensive Sampling and Grazing experiments. ANOSIM compares similarities between samples within each group to similarities between groups and generates a value of R between -1 and +1, such that a value of 0 supports

the null hypothesis. In the intensive sampling experiment, ANOSIM was used to test the null hypotheses that *Vibrio* communities were not significantly different (i) between sites, (ii) between size fractions, or (iii) over time. For the grazing experiments, we used ANOSIM to test the null hypotheses that *Vibrio* communities were not significantly different (i) between size fractions, (ii) between experiments for each size fraction, or (iii) between T_0 and T_{24} within each size fraction. When ANOSIM revealed a significant difference, the Species Contributions to Similarity (SIMPER) was used to identify *Vibrio* species or operational taxonomic units (OTUs) which contributed to differences in assemblages (Moore et al. 2004). The Biota-Environment STepwise (BEST) matching function in PRIMER was conducted to identify environmental variables that were correlated *Vibrio* community structure in the Intensive Sampling experiment. The BEST analysis calculates the Spearman rank correlation coefficient (ρ) from combinations of variables to find the subset with the highest value of ρ for the Bray-Curtis similarity matrix. For this test, transformed and normalized environmental data was used to construct a Euclidean distance matrix, followed by computation of the rank correlation comparison to the biotic (ARISA) similarity matrix (Garren et al. 2006). BEST analysis generated a rank correlation coefficient (Rho) such that a value of 0 supports the null hypothesis that the environmental data was not correlated to the biotic data.

2.4 Results

2.4.1 Field samples

Altogether, 148 samples were analyzed from three sites in the DIB between 2009 and 2011 (Table 2.6). Temperature during the collection period ranged from

18.4 – 31.4 °C, salinity ranged from 9.3 – 37, and extracted chl *a* ranged from 2.82 – 386.8 µg l^{-1}. Average temperature (24.8 °C), salinity (22.9), and chl *a* (162.9 mg l^{-1}) for 2009 were significantly different from those in 2010 (26.7 °C, 26.2, and 58.1 mg l^{-1}) and 2011 (26.5 °C, 23.4 and 18.7 mg l^{-1}) ($P < 0.001$). Average salinity in 2011 was also significantly lower (23.4) than in 2010 (26.2) ($P < 0.01$). Dissolved NO_x during the 2010 – 2011 collection period ranged from 0.14 – 49.6 µM, NH_4 ranged from 0.3 – 37.5 µM, and PO_4 ranged from 0.09 – 2.82 µM. Average concentrations of NO_x and PO_4 were significantly higher in 2011 (7.4 and 0.7 µM respectively) when compared to 2010 (2.7 and 0.4 µM respectively) ($P < 0.001$). Principal Component Analysis (PCA) show an increased influence of NO_X (PC1: 0.491, PC2: 0.206), N:P ratio (PC1: 0.390, PC2: 0.534) and salinity (PC1: -0.380, PC2: 0.353) on the variability between water samples collected in 2010 versus 2011, with 37.4% variation accounted for on PC1 and 15.3% accounted for on PC2.

Samples that yielded low pGEM values in qPCR analysis were eliminated due to possible inhibition, leaving a total of 132 samples, with 41 samples from IR32, 47 samples from RB64 and 44 samples from SB10E over the three years. The relative abundance of particle-associated *Vibrio* in the >3 µm size fraction as determined by qPCR was significantly correlated to the relative abundance of diatoms (Fig. 2.2B) and raphidophytes (Fig. 2.2C) ($r = 0.745$ and 0.768 respectively, $P < 0.001$; Table 2.2) for all three years combined. The correlation between particle-associated *Vibrio* abundance and dinoflagellates (Fig. 2.2A) was lower, though still significant ($r = 0.560$, $P < 0.001$; Table 2.2) for all three years combined. Pearson's correlations within collection years showed the highest correlation between particle-associated *Vibrio* and diatom abundance for 2009 and 2011 (2009: $r = 0.764$; 2011: $r = 0.779$),

while correlations between *Vibrio* and raphidophytes were highest in 2010 ($r = 0.855$; Table 2.2). Correlations between particle-associated *Vibrio* abundance and dinoflagellates were significant only in years 2010 and 2011. Pearson's correlations of particle-associated *Vibrio* spp. abundance and each phytoplankton group were not significantly different between sites (Fig. 2.2A – C). However, particle-associated *Vibrio* abundance in the >3 μm size fraction for all three years combined was significantly correlated to salinity ($r = 0.202$, $P < 0.05$; Table 2.2) and chl *a* concentrations ($r = 0.343$, $P < 0.001$; Table 2.2) but not with temperature, dissolved oxygen concentrations or nutrient concentrations.

2.4.2 Intensive sampling

Sampling was conducted on four consecutive days (13-16 Sept., 2011) for a total of ten samples from two replicate sampling locations during a mixed raphidophyte bloom at RB64. Temperature ranged from 22.9 – 27.2 °C, salinity ranged from 24.2 – 24.8, and dissolved oxygen ranged from 0.74 – 2.41 mg l^{-1}. chl *a* in the >20 μm fraction ranged from 12.8 – 30.0 μg l^{-1}, while the 3.0-20 μm fraction ranged from 11.4 – 21.6 μg l^{-1}. Dissolved nutrients ranged from 0.69 – 2.3 μM NO_x, 1.45 – 4.61 μM NH_4, and 0.17 – 0.56 μM PO_4 (Fig. 2.3). Cell counts ranged from $2.99x10^7$ – $1.39x10^8$ cells l^{-1} for *Heterosigma akashiwo* and $2.37x10^5$ – $4.1x10^5$ cells l^{-1} for *Fibrocapsa japonica* (Fig. 2.3). A significant correlation (Table 2.3) was identified between particle-associated *Vibrio* and *H. akashiwo* abundance in the 3.0-20 μm fraction for combined replicate samples ($r = 0.788$, $P < 0.001$; Fig. 2.4A). Dinoflagellates (>20 μm) were also observed microscopically during the mixed raphidophyte bloom, and particle-associated *Vibrio* abundance in the >20 μm size fraction was more highly correlated with dinoflagellate abundance than with *F.*

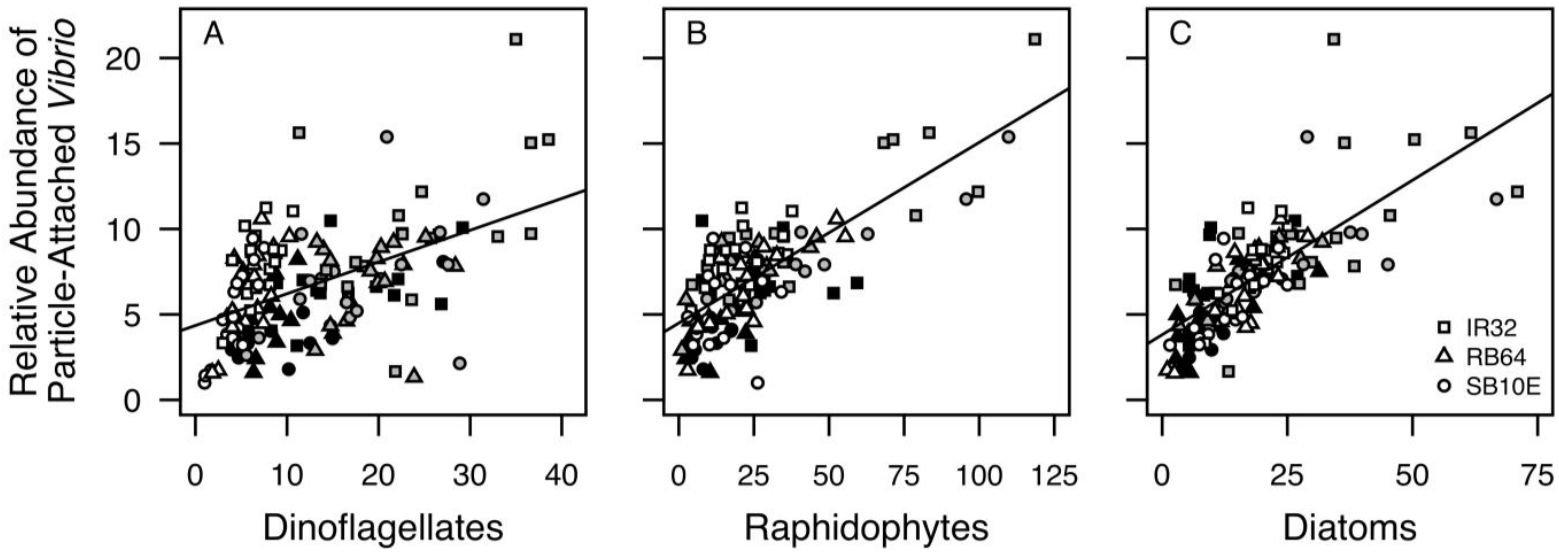

Figure 2.2 Community-level analysis of the relative abundance of particle-associated (>3µm) *Vibrio* vs. dinoflagellates (A), diatoms (B), and raphidophytes (C). Relative abundances were square root square root transformed and reported on a per volume filtered basis. Years are represented by colored symbols: Black: 2009; Grey: 2010; Open: 2011.

Table 2.2 Correlations between relative abundances of particle-associated *Vibrio* spp. with algal groups or environmental factors.

	Pearson's correlation coefficient					
Vibrio	Diatom	Dinoflagellate	Raphidophyte	Temperature	Salinity	Chlorophyll a
All Years	0.745***	0.560***	0.768***	0.105	0.202*	0.343***
2009	0.764***	0.231	0.513**	0.258	0.135	0.535*
2010	0.657***	0.550***	0.855***	0.074	0.293*	0.646***
2011	0.779***	0.760***	0.560***	-0.051	-0.121	0.241

Significance levels are indicated as follows: *, $P < 0.05$; **, $P < 0.01$; ***, $P<0.001$.

japonica (Figure 2.4C). Pearson's correlations between particle-associated *Vibrio* abundance in the >20 µm fraction and environmental factors were significantly positive and negative for temperature and salinity, respectively (Table 2.3). However, neither temperature nor salinity were significantly correlated to the 3.0-20 µm fraction of particle-associated *Vibrio* abundance (Table 2.3).

2.4.3 Analysis of *Vibrio* community structure during intensive sampling

Changes in *Vibrio* assemblages in each size fraction at Sites 1 and 2 were examined using ARISA. ARISA analysis of amplified DNA isolated from *Vibrio* cultures showed major peaks for *Vibrio parahaemolyticus* at 389 bp, *V. tubiashii* at 412 bp, *V. cholerae* at 542 bp and *V. vulnificus* at 396 bp. Relationships between *Vibrio* assemblages were investigated by multivariate analysis based on Bray Curtis similarity matrices implemented in PRIMER and trends were visualized by construction of a non-metric multi-dimensional scaling (MDS) ordination plot from the matrix (Fig. 2.5). Statistical analysis by ANOSIM showed that the *Vibrio* assemblages were not significantly different between sites or over time, but that there was a significant difference in assemblages between size fractions (R=0.571, P=0.001). SIMPER analyses indicated an average dissimilarity of 28.73, 62.07 and 47.66% between assemblages in the free-living and 3.0-20 µm fraction, free-living and >20 µm fraction and 3.0-20 and >20 µm fractions, respectively. The OTU at 389 bp, identified as *V. parahaemolyticus*, contributed most (28.37%) to the dissimilarity between the *Vibrio* assemblage in the free-living fraction and the 3.0-20 µm fraction, where the average relative abundance increased from 1.43 in the free-living fraction to 4.61 in the 3.0-20 µm fraction. The average relative abundance of *V. parahaemolyticus* also increased to 5.32 in the 20 µm fractions, contributing 15.49%

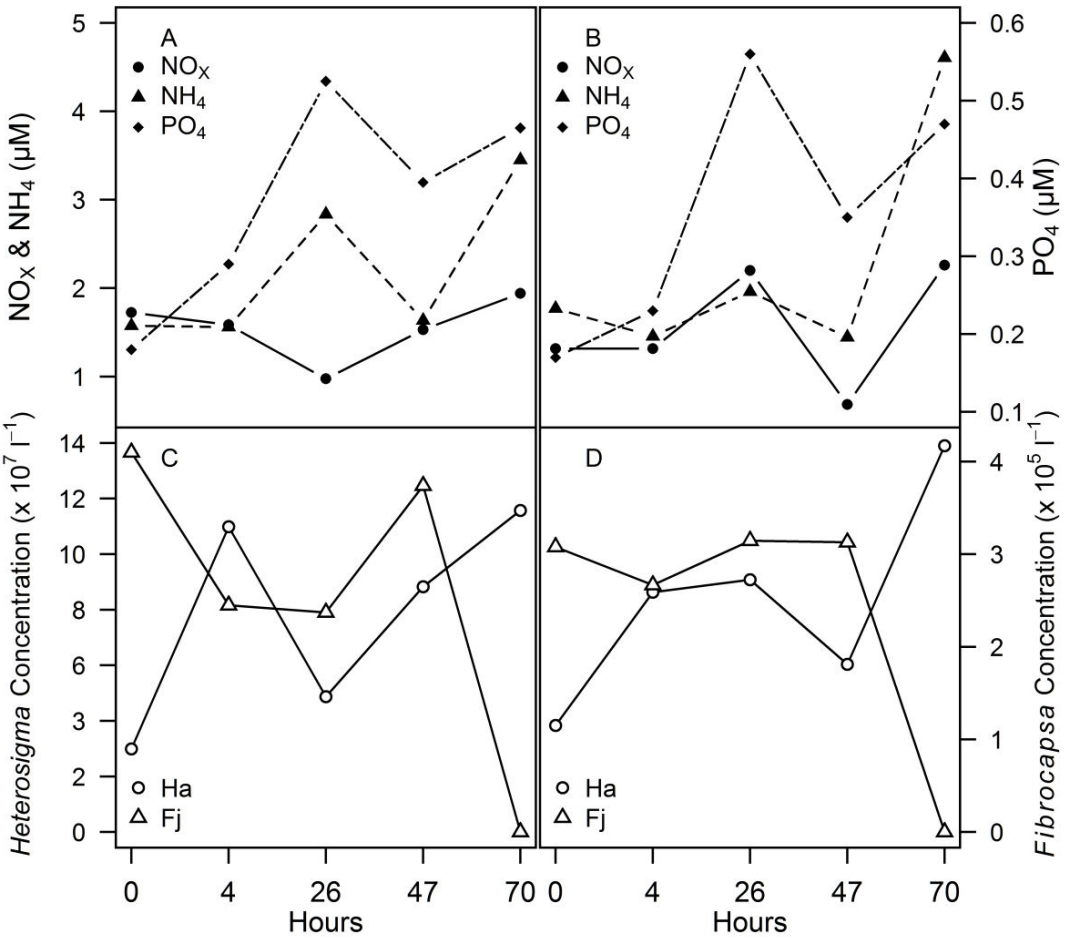

Figure 2.3 Environmental parameters during intensive sampling of a mixed bloom at RB64. (A), (B) temperature (°C) and salinity for Sites 1 and 2, respectively; (C), (D) nutrient concentrations (µM) for Sites 1 and 2, respectively.

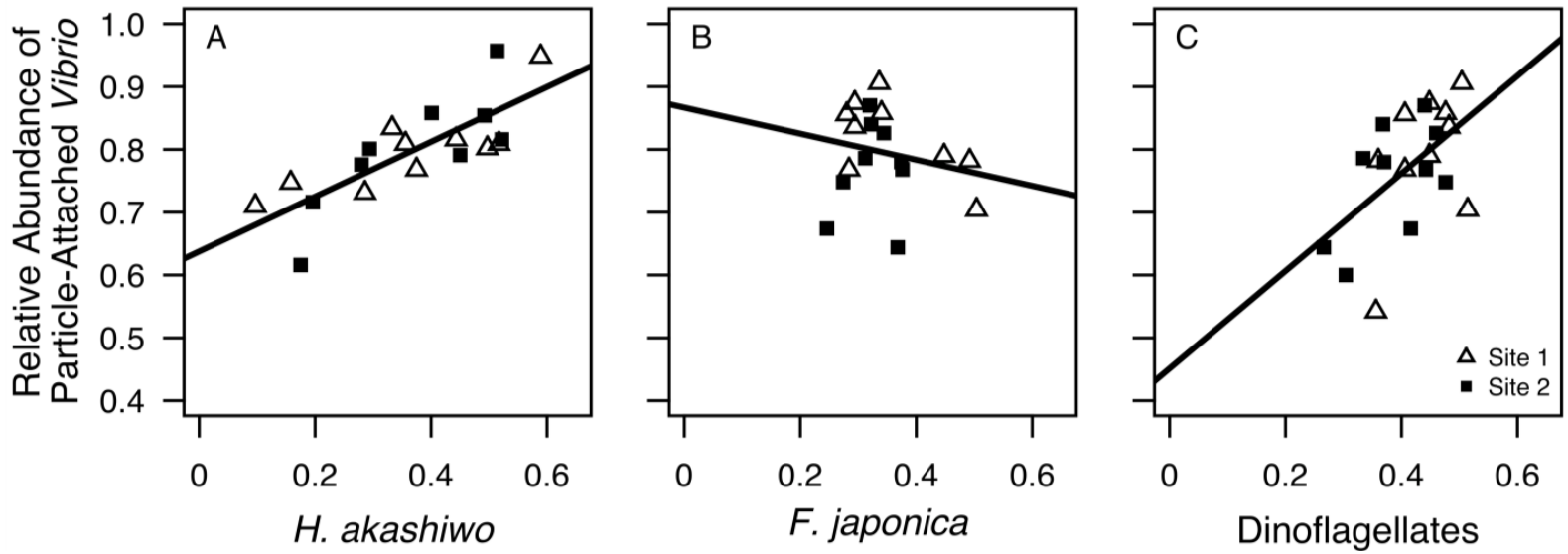

Figure 2.4 Relative abundance of particle-associated *Vibrio* vs. *Heterosigma akashiwo* in the >3 µm size fraction (outlier removed) (A), *Fibrocapsa japonica* in the >20 µm size fraction (B), and dinoflagellates in the >20 µm size fraction (C). Relative abundances were square root square root transformed and reported on a per volume filtered basis.

Table 2.3 Correlations between relative abundances of particle-associated *Vibrio* spp. with *Heterosigma akashiwo*, *Fibrocapsa japonica*, Dinoflagellates, or environmental factors from the Intensive Sampling Experiment.

	Pearson's correlation coefficient				
Vibrio	*Heterosigma*	*Fibrocapsa*	Dinoflagellates	Temperature	Salinity
3.0-20 µm fraction	0.788***			0.015	-0.133
>20 µm fraction		-0.212	0.543*	0.541*	-0.463*

Significance levels are indicated as follows: *, P < 0.05; **, P < 0.01; ***, P<0.001.

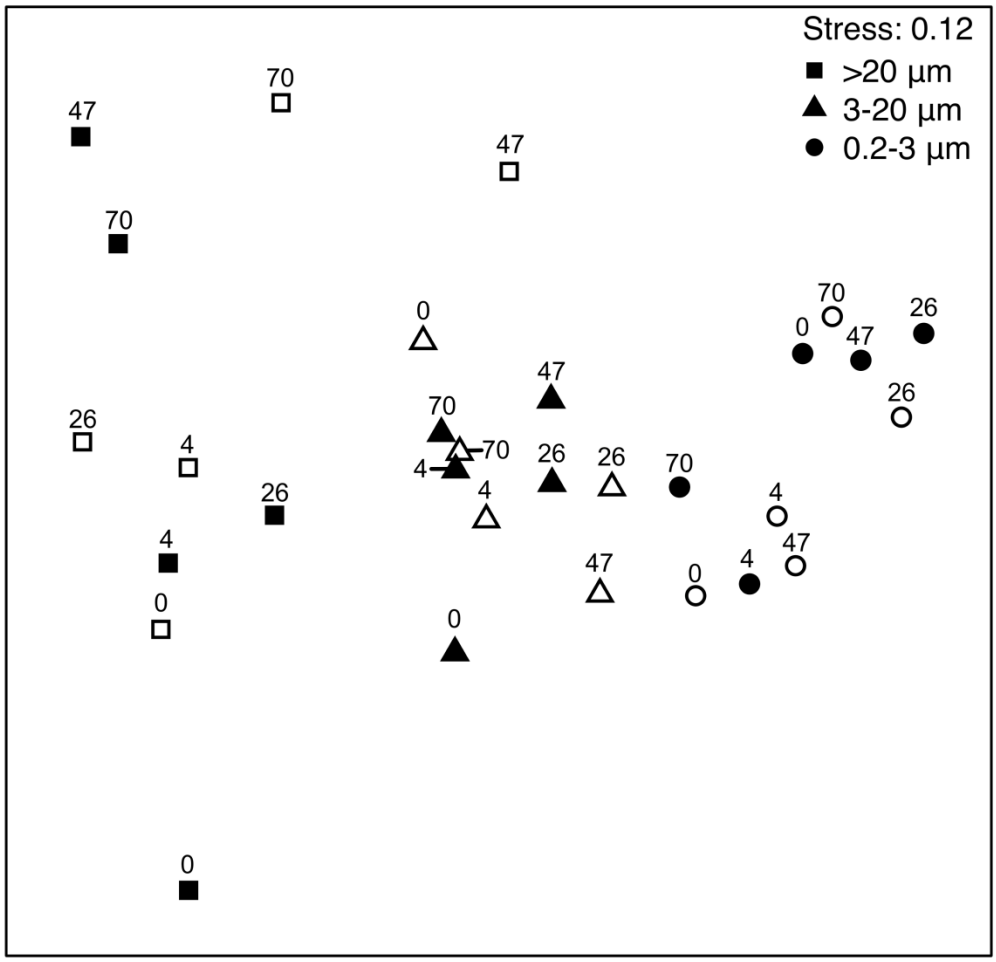

Figure 2.5 MDS plot of ARISA analysis of *Vibrio* assemblages from the Intensive Sampling Experiment during a mixed raphidophyte bloom in September, 2011. Symbols are labeled with the time in hours. Open symbols – Site 1, closed symbols – Site 2.

to the dissimilarity between these size fractions. The OTU at 311 bp contributed 14.53% of the dissimilarity between particle-associated *Vibrio* size fractions where the average relative abundance decreased from 4.59 in the 3.0-20 μm size fraction to 1.53 in the >20 μm size fraction.

2.4.4 Microzooplankton grazing

Two grazing experiments were conducted on consecutive days during a mixed bloom of *Heterosigma akashiwo* and *Fibrocapsa japonica* in August 2011. For both grazing experiments, environmental parameters at the collection site were similar with regards to temperature and salinity, however dissolved oxygen was lower at collection time for Experiment 2 (Table 2.4). chl *a* concentrations (Table 2.4) at the start of Experiment 1 (T_0) were 27.6 μg l^{-1} for the >20 μm size fraction, 19.2 μg l^{-1} for the 3.0-20 μm size fraction and 9.2 μg l^{-1} for the free-living μm size fraction. In Experiment 1, grazing rates on *Vibrio*, as determined by qPCR, ranged from 1.98 to 5.37 day^{-1} and were not significantly different between size fractions (Fig. 2.6A – C; $P > 0.05$; Table 2.5). After 24 hours, the relative abundance of *Fibrocapsa japonica* in the 100% whole water, >20 μm size fraction increased by 155% after 24 hours, whereas in the 3.0-20 μm size fraction, *Heterosigma akashiwo* decreased in relative abundance by 43%. Grazing rates on the total phytoplankton community, based on chl *a* concentrations, ranged from -0.036 day^{-1} in the >20 μm size fraction to 0.337 day^{-1} in the free-living size fraction for Experiment 1 and were significantly higher for the free-living fraction compared to the >20 μm and 3.0-20 μm size fractions (Fig. 2.7A-C; $P < 0.05$ and $P < 0.0001$ respectively; Table 2.5).

In Experiment 2, chl *a* concentrations at T_0 were 31.9 μg l^{-1} for the >20 μm size fraction, 9.1 μg l^{-1} for the 3.0-20 μm size fraction and 10.8 μg l^{-1} for the free-

living size fraction (Table 2.4). Grazing rates on *Vibrio* during this experiment were significantly different between size fractions with the highest predation on *Vibrio* in the 3.0-20 μm size fraction and lowest in the free-living size fraction (Fig. 2.6D – F; $P < 0.05$ Table 2.5). After 24 hours, the relative abundance of *H. akashiwo* in the 100% whole water 3.0-20 μm size fraction increased by 126%, while *F. japonica* decreased in the >20 μm size fraction by 5%. Grazing rates on the total phytoplankton community for Experiment 2 were significantly lower in the >20 μm size fraction compared to the free-living and 3.0-20 μm size fractions (Fig. 2.7D-F; $P < 0.05$ and $P< 0.01$ respectively; Table 2.5).

When comparing Experiments 1 and 2, grazing rates on *Vibrio* were significantly lower in Experiment 2 for the free-living size fraction ($P < 0.001$) and significantly higher in Experiment 2 for the 3.0-20 μm fractions ($P < 0.01$), while grazing rates between the >20 μm fractions were not significantly different. The relative abundance of *H. akashiwo* increased by 268% at the beginning of Experiment 2 compared to Experiment 1, while the relative abundance of *F. japonica* was 201% greater in Experiment 1 compared to Experiment 2. For the total phytoplankton community, grazing rates were significantly higher in Experiment 2 for the >20 and 3.0-20 μm size fractions when compared to Experiment 1 ($P < 0.001$; Table 2.5).

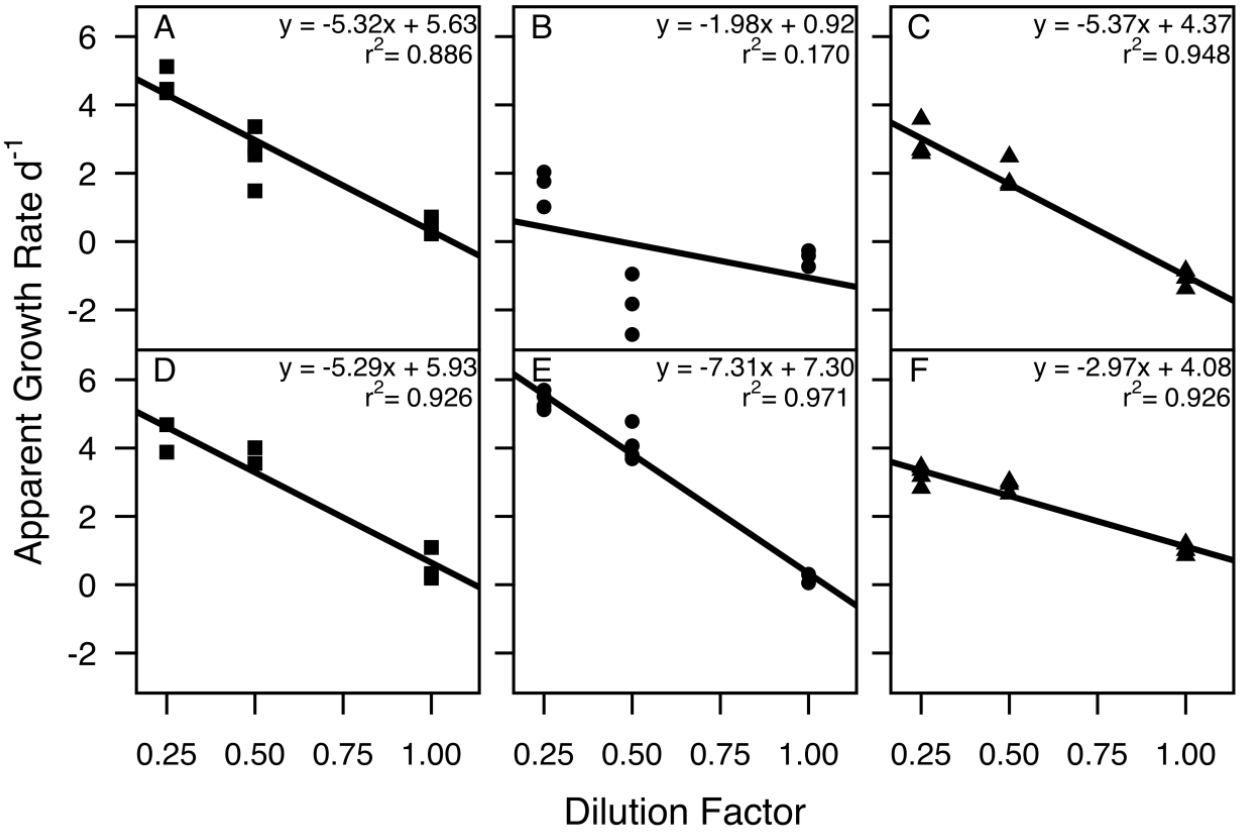

Figure 2.6 Microzooplankton grazing on size-fractionated *Vibrio* during a mixed raphidophyte bloom. (A-C) Experiment 1; (D-F) Experiment 2. (A, D) >20 µm size fraction; (B, E) 3.0-20µm size fraction; (C,F) 0.2-3.0 µm (free-living) size fraction.

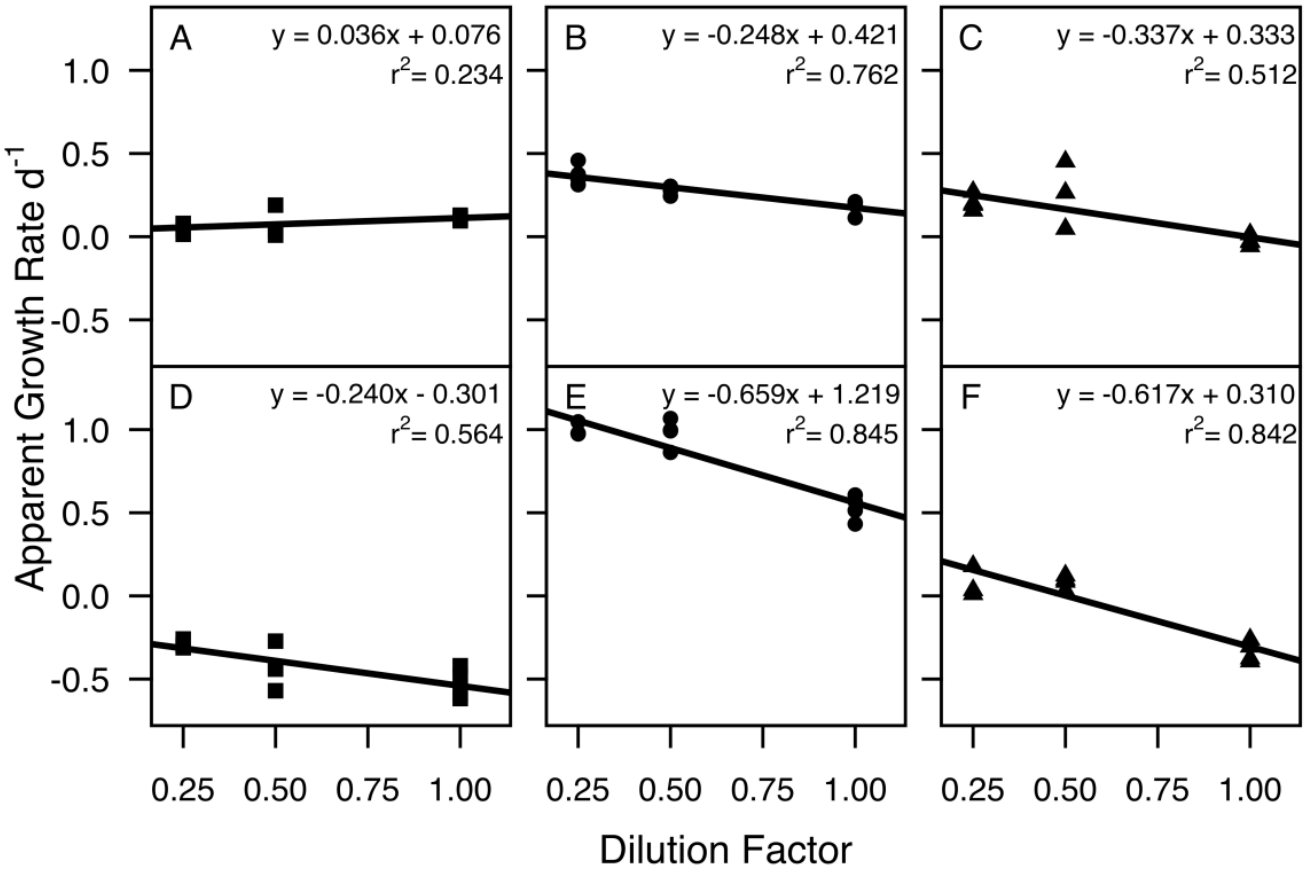

Figure 2.7 Microzooplankton grazing on size-fractionated total phytoplankton community during a mixed raphidophyte bloom. (A-C) Experiment 1; (D-F) Experiment 2. (A, D) >20 µm size fraction; (B, E) 3.0-20µm size fraction; (C,F) 0.2-3.0 µm (free-living) size fraction.

Table 2.4 Environmental parameters for grazing experiments. DO, dissolved oxygen.

					Chlorophyll *a* ($\mu g\ l^{-1}$)		
Experiment	Temperature (°C)	Salinity	DO ($mg\ l^{-1}$)	% DO	>20 μm	3.0-20.0 μm	Free-living
1	29.09	26.77	6.64	101.3	27.6	19.2	9.2
2	27.03	27.06	2.85	43	31.9	9.1	10.8

Table 2.5 Grazing rate and apparent growth (day^{-1}) for grazing experiments.

	Experiment 1	
	Vibrio	Chl *a*
Size Fraction	Grazing Rate (Apparent Growth)	Grazing Rate (Apparent Growth)
Free-living	5.37 (4.37) day^{-1}	0.337 (0.333) day^{-1}
3.0-20 μm	1.98 (0.92) day^{-1}	0.248 (0.421) day^{-1}*
>20 μm	5.32 (5.63) day^{-1}	-0.036 (0.076) day^{-1}***

	Experiment 2	
	Vibrio	Chl *a*
Size Fraction	Grazing Rate (Apparent Growth)	Grazing Rate (Apparent Growth)
Free-living	2.97 (4.08) day^{-1}***	0.617 (0.310) day^{-1}
3.0-20 μm	7.31 (7.30) day^{-1}***	0.659 (1.219) day^{-1}*
>20 μm	5.29 (5.93) day^{-1}*	0.240 (-0.301) day^{-1}**

Significance levels are indicated as follows: *, $P < 0.05$; **, $P < 0.01$; ***, $P<0.001$.

2.4.5 Analysis of *Vibrio* community structure during the grazing experiments

ARISA analysis was used to examine the changes in the *Vibrio* community structure during the two grazing experiments. ARISA analysis identified a total of 23 distinct OTUs for both experiments. Analysis of Experiment 1 by ANOSIM indicated a significant difference between the free-living size fraction and both 3.0-20 and >20 μm size fractions (R=0.544, P=0.008; R=0.492, P=0.016 respectively) for the T_0 and T_{24} samples combined. However, there was no significant difference between *Vibrio* assemblages in the 3.0-20 μm and >20 μm size fractions. SIMPER analysis indicated that the OTU with a peak at 336 bp contributed the greatest dissimilarity between the free-living and particle-associated size fractions, with a change in average abundance of 0.98 in the 3.0-20 μm size fraction to 7.09 in the free-living size fraction and from 1.64 in the >20 μm size fraction to 7.09 for the free-living population. When comparing between size fractions at T_{24} only, there was also a significant difference in *Vibrio* assemblages between the free-living size fraction and both 3.0-20 and >20 μm size fractions (R=0.833, P=0.029; R=0.677, P=0.029 respectively). The OTU with a peak at 336 bp again contributed the greatest dissimilarity between the free-living and 3.0-20 μm size fractions (18.26%) and between the free-living and >20 μm size fractions (17.50%) for samples at T_{24} only.

For Experiment 2, there was also a significant difference between the free-living and both 3.0-20 and >20 μm size fractions (R=0.214, P=0.048; R=0.260, P=0.024 respectively) and also between the 3.0-20 and >20 μm size fractions (R=0.364, P=0.04) at both time points. The OTU at peak 318 bp contributed the most (12.65%) dissimilarity between the free-living size fraction, where it was not detected, and the 3.0-20 μm size fraction where its average abundance was 3.97. In contrast,

this OTU contributed only 3.38% to the dissimilarity between the free-living and >20 μm size fractions. Instead the OTU at 471 bp contributed 10.76% of the dissimilarity between these two size fractions. When comparing between the two particle-associated size fractions, the OTU at 318 bp contributed 11.19% dissimilarity with average abundance decreasing from 3.97 in the 3.0-20 μm size fraction to 1.01 in the >20 μm size fraction. However, the OTU at 389 bp contributed the most (11.88%) dissimilarity between the particle-associated size fractions, with average abundance decreasing from 4.09 in the 3.0-20 μm size fraction to 1.07 in the >20 μm size fraction. When comparing between size fractions at T_{24} only, there was also a significant difference between the free-living and 3.0-20 size fractions (R=0.417, P=0.029; >20: R=0.271, P=0.029) as well as between the 3.0-20 and >20 μm size fractions (R=0.844, P=0.029). The OTU at 318 bp contributed the most dissimilarity between the free-living and the 3.0-20 μm size fractions (15.05%) where it increased from undetected to an average abundance of 4.97 in 3.0-20 μm size fraction, and between the 3.0-20 and >20 μm size fraction (14.71%) where again it was undetected. In contrast, the OTU at 471 bp contributed the most (12.66%) dissimilarity between the free-living and >20 μm size fractions where it increased in average abundance from 3.52 in free-living size fraction to 6.14 in the >20 μm size fraction.

Vibrio assemblages in Experiments 1 were significantly different from assemblages in Experiment 2 for all size fractions combined (R=0.161; P=0.005). However, when comparing within a size fraction, there was a significant difference in *Vibrio* assemblages only between the 3.0-20 μm size fractions (R=0.719, P=0.029). The OTU at 389 bp contributed the most (15.15%) dissimilarity in this size fraction where it increased in average abundance from undetected in Experiment 1 to 5.11 in

Experiment 2. Despite significant difference between 3.0-20 μm size fractions in Experiment 1 and 2, similarities included OTUs at 318 and 471 bp, which contributed 24.52% and 20.81% of the similarity respectively between *Vibrio* assemblages in this size fraction.

There was no significant difference between the *Vibrio* assemblages in T_0 and T_{24} for the free-living and 3.0-20 μm size fractions. In the >20 μm size fraction, however, there was a significant difference in the *Vibrio* assemblages between T_0 and T_{24} (R=0.513, P=0.044). The OTU at 318 bp contributed the most (13.48%) dissimilarity between T_0 and T_{24} for both Experiment 1 and 2 combined, decreasing in average abundance from 4.51 to undetected after 24 hours for both experiments combined. Though there were no significant differences between *Vibrio* assemblages at T_0 and T_{24} for each size fraction within each experiment, changes in the average relative abundance of several OTUs in the same size fraction were consistent for both experiments. The OTU at 471 bp decreased in relative abundance in the free-living size fraction for both experiments, while the OTUs at 356, 425, and 542 bp decreased in abundance in the 3.0-20 μm size fraction for both experiments. In the >20 μm size fraction, the OTUs at 356 and 318 decreased in abundance while the OTU at 557 bp increased in abundance for both experiments at T_{24}. A few OTUs consistently increased in one size fraction while decreasing in another size fraction for each of the experiments. For example, the OTU at 318 bp increased in average abundance in the 3.0-20 μm size fraction from undetected in both experiments to 3.06 and 4.97 in Experiments 1 and 2, respectively. The same OTU decreased in abundance in the >20 μm size fraction from 3.99 and 5.04 in Experiments 1 and 2, respectively, to undetected at T_{24} in both experiments.

2.5 Discussion

In the marine environment, bacteria that are associated with particles represent approximately 10% of the total community (Middelboe et al. 1995) but may account to up to 90% of total bacterial production during blooms of phytoplankton (Smith et al. 1995). Although there is a distinct correlation between bacterial and phytoplankton biomass, however, little is known about how these communities interact at the species level (Rooney-Varga et al. 2005). Several studies suggest that species-specific interactions with bacteria may play a major role in controlling phytoplankton population dynamics (Lovejoy et al. 1998; Rooney-Varga et al. 2005). For example, bacterial attachment has been shown to stimulate the growth of some dinoflagellates, such as *Gambierdiscus toxicus* (Sakami et al. 1999), *Alexandrium fundyense* (Ferrier et al. 2002), and *Pfiesteria* spp. (Alavi et al. 2001), while other bacterial species have been shown to have algicidal effects on phytoplankton (Yang et al. 2013; Skerratt et al. 2002; Mayali & Azam 2004). Furthermore, survival, growth and abundance of particle-attached bacterioplankton, such as *Vibrio*, may be positively affected by the release of bioavailable dissolved organic substances (DOM) from phytoplankton (Eiler et al. 2006; Eiler et al. 2007). Increased growth of pathogenic members of the bacterioplankton due to DOM from phytoplankton may have serious implications for human and ecosystem health. The growth of *V. cholerae*, for example, increased with amendment of phytoplankton derived dissolved organic matter to levels that were 3 orders of magnitude higher than an infectious dose (Mouriño-Pérez et al. 2003).

The objectives of this study were to examine the community-level and species-specific relationships between particle-associated *Vibrio* and phytoplankton populations in Delaware's inland bays, the influence of environmental factors on these relationships, and the role of microzooplankton grazing in structuring particle-

associated *Vibrio* assemblages. Environmental factors such as temperature (Lobitz et al. 2000; Huq et al. 2005; Eiler et al. 2007; Singleton et al. 1982; Froelich et al. 2013) and salinity (Randa et al. 2004; Motes et al. 1998; Singleton et al. 1982; Froelich et al. 2013) have been shown to explain the majority of variance in total *Vibrio* populations compared to other physical parameters (Reviewed by Takemura et al. 2014; Blackwell & Oliver 2008). Salinity within the DIB (Zhang et al. 2006) is affected by tidal cycles, evaporation and rainfall. During 2010, the average salinity was higher than other years with a lower range of salinity distributions, and was significantly correlated to the higher relative abundance of particle-associated *Vibrio* spp. in this year compared to 2009 or 2011 ($R = 0.293$; Table 2.2). In contrast, water temperatures were not significantly correlated to abundances of particle-associated *Vibrio* spp. ($R = 0.105$; Table 2.2) for any of the years tested. While NO_x and N:P were shown to have the greatest influence on differences between 2010 and 2011, neither were significantly correlated to abundances of particle-associated *Vibrio*.

At the community level, the abundance of particle-associated *Vibrio* spp. in the >3 µm size fraction was significantly correlated with both diatom and the raphidophyte abundances in samples collected in all three years (Table 2.2), while correlations with dinoflagellate abundance were significant only in years 2010 and 2011. With the exception of the 2009 dinoflagellate-*Vibrio* correlation, the abundance of particle-associated *Vibrio* was more highly correlated to abundance of each phytoplankton class than to any of the environmental parameters collected. Group- or species-specific associations between *Vibrio* spp. and raphidophytes or diatoms may be due to production of algal exudates which activate biofilm formation in *Vibrio*. Mannitol, for example, is a common exudate from marine phytoplankton (Dittami et

al. 2011) and has been shown to induce transcription of the biofilm matrix genes in *Vibrio cholerae* (Ymele-Leki et al. 2013). Other exudates may be involved in species-specific interactions. Chitin, produced as component of the diatom frustule in some species (Frischkorn et al. 2013), has been shown to stimulate expression of functional type IV pili in *V. parahaemolyticus*, resulting in an increase in adherence (Frischkorn et al. 2013). In addition, Seymour et al. (2009), demonstrated a positive chemotactic response by *V. alginolyticus* to exudates from laboratory cultures of *H. akashiwo*, while other bacterial species tested showed no response. Other studies have investigated antagonistic interactions between *Vibrio* and raphidophyte species in laboratory culture. For example, algicidal activity by a South Carolina isolate of *Vibrio* spp. resulted in cell lysis of *Chattonella subsalsa*, *Fibrocapsa japonica*, and *Heterosigma akashiwo* (Liu et al. 2008). In another study, Kim et al. (1999) demonstrated that the raphidophyte *Olisthodiscus luteus* inhibited the growth of *V. alginolyticus* by reactive oxygen species-mediated processes. In addition, the bioluminescence of *V. fischeri* was inhibited 5-fold by the cellular exudate of *F. japonica* (van Rijssel et al. 2007). While these laboratory culture experiments suggest a mechanism for species-specific associations, they don't provide much information about the role of these interactions in structuring *Vibrio* assemblages in the natural environment.

In our study, we investigated species-specific associations between *Vibrio* and two raphidophytes, *F. japonica* and *H. akashiwo*, during mixed blooms of these species in the DIB. These raphidophytes and their associated *Vibrio* assemblages were separated by size fractionation, with *H. akashiwo* retained in the 3-20 µm fraction and *F. japonica* in the >20 µm fraction. Cross-contamination between size fractions was

minimal as verified by PCR analysis. Results of our Intensive Sampling Experiment, in which samples were collected from two replicate locations over the course of four days, demonstrated a significant positive correlation between the abundance of particle-associated *Vibrio* spp. and *H. akashiwo* (R = 0.788) (Fig. 2.4).

Changes in the particle-associated *Vibrio* assemblages during the Intensive Sampling Experiment were also evaluated using data from ARISA. ARISA patterns are generated due to heterogeneity of the *Vibrio* ITS length, allowing for discrimination of *Vibrio* strains (Hoffmann et al. 2010). ANOSIM analysis of ARISA patterns produced by the *Vibrio* community showed a significant difference in *Vibrio* population structure associated with each size fraction, supporting the hypothesis that associations between *Vibrio* spp. and phytoplankton are species-specific. In addition, cluster analysis demonstrated a higher level of similarity within the 0.2-3.0 µm size fraction, which contained planktonic or "free-living" *Vibrio* assemblages (79.71% similar) and those in the 3.0-20 µm size fraction (67.96% similar) compared to the >20 µm size fraction (28.98% similarity) (Fig. 2.6). There were no significant differences within each size fraction over time, or with respect to changes in environmental parameters. Pairwise comparisons of *Vibrio* assemblages by SIMPER indicated that two peaks in the ARISA analysis were partially responsible for differences between size fractions for all time points (389 and 311 bp). ARISA analysis of cultured *Vibrio* species tentatively identified the peak at 389 bp as *V. parahaemolyticus*. However heterogeneity of sequence lengths between strains of the same species may increase the complexity of mixed community analysis (Crosby & Criddle 2003).

Attachment of *Vibrio* to particles, specifically algal cells, in the marine environment may provide refuge from predation (Worden et al. 2006), however

attachment may also influence the microzooplankton grazing community (Caron 1987). Here, we extended this hypothesis to investigate the effects of grazing on *Vibrio* assemblages associated with size-fractionated phytoplankton populations during a mixed raphidophyte bloom. Overall, our results indicate that loss to grazing in the particle-associated *Vibrio* population may be equal to or even greater than losses in the free-living population (Fig. 2.6; Table 2.5). However, growth rates of the particle-associated *Vibrio* population were consistently higher in the >20 μm size fraction compared to the free-living population, so that in Experiment 1, at least, the increased growth conferred by this association may outweigh the consequences of predation. From the data collected here, we are not able to identify phytoplankton in the >20 μm size fraction that are associated with *Vibrio*. Demir et al. (2008) found little grazing on *F. japonica* in the DIB, suggesting that association with this species may provide *Vibrio* with a refuge from predation. However, growth and grazing on *Vibrio* were not correlated to the relative abundance of *Fibrocapsa japonica*, which increased in abundance (155%) at T_{24} in Experiment 1, but decreased (5%) in Experiment 2. Results of the grazing experiments along with the Intensive Sampling experiment, suggest that the abundance of *F. japonica* has no impact on growth or grazing of particle-associated *Vibrio* in the natural environment.

In contrast, both growth and grazing rates significantly increased for *Vibrio* in the 3.0-20 μm size fraction between Experiments 1 and 2 (Fig. 2.6B, E), corresponding to an increase (119%) in the relative abundance of *Heterosigma akashiwo* in this size fraction. Demir et al. (2008) showed higher microzooplankton grazing pressure on *H. akashiwo* from the DIB compared to other raphidophyte species, implying that *Vibrio* that are associated with *Heterosigma* will also face this

increased grazing pressure. It is notable, though, that growth rates for *Vibrio* were also highest for this size fraction in Experiment 2. These results support the idea that *Vibrio* assemblages exhibit multiple growth strategies, as suggested in Worden et al. (2006), where free-living *Vibrio* may rapidly grow (Fig. 2.6C, F) utilizing nutrients so that association with particles in the environment can also be beneficial, resulting in an increased growth rate (Fig. 2.6A, D, E) despite increased grazing pressure.

The effects of grazing on the population structure of free-living and particle-associated *Vibrio* revealed differential impacts on *Vibrio* species, such that association with particles confer protection for some species over others. Furthermore, several species or OTUs, as noted above, consistently increased or decreased within the same size fraction for both experiments, supporting the hypothesis that associations between *Vibrio* and phytoplankton are species-specific. One OTU, at 318 bp, also increased in average abundance in the 3.0-20 μm size fraction but decreased in abundance in the >20 μm size fraction for both experiments. It's possible that *Vibrio* species remained within the same size fraction for the duration of the experiment, in which case specific association with phytoplankton that are more heavily grazed within the >20 μm size fraction would result in a decrease in the relative abundance of some *Vibrio* species, while these associations within the 3.0-20 μm size fraction confers protection for the same species. Alternatively, a concurrent increase of some OTUs within one size fraction and decrease in another may be due to a remobilization of *Vibrio* cells from one size fraction to another to avoid increased grazing pressure. In either case, species-specific associations between *Vibrio* and phytoplankton may provide some species with a clear advantage in periods of high grazing pressure.

Enhanced growth of some species even in the presence of increased grazing pressure may have significant human health impacts. The OTU at 389 bp, for example, was tentatively identified as *V. parahaemolyticus*, a human pathogen responsible for gastroenteritis and wound infection (Blackwell & Oliver 2008; Johnson et al. 2012). This OTU was a large portion of the free-living size fraction at the beginning of Experiment 2, but decreased in relative abundance in this fraction while increasing in the 3.0-20 μm size fraction (Table 2.5; Fig. 2.7E). In a similar manner, the OTU at 412, tentatively identified as *Vibrio tubiashii*, an oyster pathogen (Hada et al. 1984), increased in the >20 μm size fraction in both experiments, while it decreased in abundance in the 3.0-20 μm size fraction in Experiment 1. These results suggest that association with particles may provide some *Vibrio* species, including potential pathogens, with a growth advantage over other members of the community, in spite of increased grazing pressure on the population as a whole.

Results of this investigation may lead to predictions of potential outbreaks of *Vibrio* by association with algal bloom species. Distinct differences between *Vibrio* assemblages associated with different size fractions of phytoplankton in the DIB suggest that blooms are not only a vector for *Vibrio*, but that species-specific associations may determine the risk potential to human and ecosystem health. Specifically, our investigation points to associations that favor interactions between *Vibrio* and *H. akashiwo* over *F. japonica*, while results of microzooplankton grazing experiments also demonstrate that these associations may benefit some species of *Vibrio* while at the same time result in greater loss to the population as a whole due to grazing.

Chapter 3

TRANSCRIPTIONAL RESPONSE OF *HETEROSIGMA AKASHIWO* TO THE PRESENCE OF *VIBRIO CHOLERAE*

3.1 Abstract

Here we identified *V. cholerae* as a major species associated with *H. akashiwo*. Using next generation sequencing, we examined the transcriptional response of *H. akashiwo* to the presence of *V. cholerae*. A reference transcriptome was assembled *de novo*, representing the first reported transcriptome of a raphidophyte species. The reference transcriptome was then used to identify differentially expressed genes in response to the presence of *V. cholerae*. We identified 12698 contigs for the reference transcriptome with 1560 contigs significantly differentially expressed. Genes related to extracellular structures, energy production and conversion, and lipid transport and metabolism were down regulated in the presence of *V. cholerae*, while those associated with amino acid transport, post-translation modification, and translation were up regulated. In addition, transcripts associated to antioxidant scavenging were up regulated suggesting an increase in ROS production by *H. akashiwo*. Microscopic evaluation showed an increase in EPS which may lead to an increase in toxicity of *H. akashiwo*. The results of this investigation will lead to a greater understanding of interactions between harmful algal bloom species and associated bacterial populations.

3.2 Introduction

Heterosigma akashiwo Hada ex Hara et Chihara (Raphidophyceae) is a small naturally wall-less, bi-flagellate, pleomorphic marine alga (Hara & Chihara 1987). This cosmopolitan harmful alga (Bowers et al. 2006; Cattolico et al. 2008) has had an increasing impact on coastal environments (Li & Smayda 2000; Portune et al. 2009; O'Halloran et al. 2006; Kempton et al. 2008; Tyrrell et al. 2002; Handy et al. 2006; Demir et al. 2008). *H. akashiwo* has been implicated in fish killing blooms in China (Tseng et al., 1993), Japan (Honjo, 1992), New Zealand (Chang et al., 1990), South Africa (Bates et al., 2004) and estuaries on the east (Kempton et al. 2008; Coyne et al. 2005) and west (Rensel et al., 2010) coasts of the United States. Currently the mechanisms for toxicity are unknown, but may be related to toxic compounds within the extracellular matrix (Ling & Trick 2010; Twiner et al. 2005), or due to the high levels of reactive oxygen species (ROS) produced by raphidophytes in general (Marshall et al. 2002; Marshall et al. 2003; Kawano et al. 1996; Yang et al. 1995; Oda et al. 1992; but see Twiner et al. 2001). Studies examining factors involved in production of ROS by raphidophytes, however, have been contradictory. In *Chattonella marina*, for example, irradiance has been shown to increase the production of O_2^- (Marshall et al. 2002). Superoxide anion production in *C. marina* was also inhibited by the presence of the iron chelator deferoxamine suggesting that iron is required for the generation of superoxide (Kawano et al. 1996). In *Heterosigma akashiwo*, the opposite is true; iron limitation enhanced the production of ROS, with variation in light having no effect (Twiner & Trick 2000).

Interactions with bacteria within the *Vibrionaceae* may also have an effect on toxin production in raphidophyte species. There was an increase in toxicity for *Heterosigma carterae* when co-cultured with *Vibrio* sp., (Carrasquero-Verde 1999),

although the identity of toxins or toxic mechanisms was not further investigated. Cell-surface interactions likely play a role in toxicity, however: Kim et al. (2000) for example, showed that production of ROS in *C. subsalsa* and *H. akashiwo* increased in the presence of galacturonic acid, a major constituent of lipopolysaccharides found on the cell surface of *V. parahaemolyticus* and *V. cholerae* (Kondo et al. 1991).

Portune et al. (2011) examined ROS production and the activities of superoxide dismutase (SOD) and catalase (CAT) in three raphidophyte species at different phases of growth. Highest ROS production occurred during exponential phase and significant correlations between O_2^- and SOD activity were noted for *Chattonella* spp. and for *H. akashiwo*. In contrast, CAT activity was not correlated to H_2O_2 production in *H. akashiwo*, suggesting that other antioxidant pathways are activated in response to ROS. Investigations of ROS production or antioxidant activities in mixed species cultures can be difficult to interpret, however, since both species are capable of producing ROS, as well as antioxidant enzymes that scavenge ROS, altering their concentrations in culture.

Species-specific effects of microbial interactions including those between bacteria and phytoplankton have been investigated using next generation sequencing (NGS) approaches (for example: Moustafa et al. 2010; Martinez-Garcia et al. 2012; Su et al. 2012; Frias-Lopez et al. 2008; Gifford et al. 2013). NGS provides a comprehensive and quantitative view of changes in transcript levels that can be used to identify genes that are up or down regulated in the presence of another species. In the dinoflagellate *Alexandrium tamarense*, for example, Moustafa et al. (2010) identified 487 unique signatures in the *Alexandrium* transcriptome when cultured in the presence of bacteria, supporting the hypothesis that the presence of bacteria can have a

significant impact on algal transcript levels. Of particular interest was the discovery that ascorbate peroxidase (APX), a photosynthesis related enzyme for scavenging of oxidative radicals (e.g. H_2O_2) was down regulated in the presence of the bacteria (Moustafa et al. 2010).

Previous research by Main et al. (Chapter 2 of this dissertation) demonstrated significant correlations between particle-associated *Vibrio* spp. and raphidophytes in Delaware's inland bays (DIB). The highest correlation was with *H. akashiwo* during a mixed bloom of this species with *Fibrocapsa japonica*. Analysis of the *Vibrio* assemblages associated with different size fractions supported the hypothesis that *Vibrio*:algal interactions are species-specific, and that these associations may provide a growth advantage for some members of the *Vibrio* community despite increased grazing pressure.

Here we identified *Vibrio* species that are specifically associated with *H. akashiwo* cells in environmental water samples during blooms of this species, and confirmed these associations by spiking cultured *H. akashiwo* into a natural bacterioplankton population from the DIB. Our results indicated that *V. cholerae*, a common inhabitant of bacterioplankton populations in temperate coastal waters, was the major *Vibrio* species associated with *H. akashiwo* in both natural bloom samples and spiked samples. We then examined the transcriptional response of *H. akashiwo* to the presence of *V. cholerae* using NGS. A *Heterosigma* reference transcriptome was assembled *de novo* and then used as a template to identify differentially expressed genes in response to the presence of *Vibrio cholerae*. Our results demonstrated a significant increase in transcripts related to antioxidant scavenging in the presence of *V. cholerae*, suggesting an increase in ROS production by this species. In addition,

genes related to lipid transport and metabolism, energy production and conversion, and extracellular structures were down regulated in the presence of *V. cholerae*, while those associated with translation, ribosomal structure and biogenesis, amino acid transport and metabolism, post-translation modification, and transcription were up-regulated. Microscopic examination of *H. akashiwo-Vibrio cholerae* mixed cultures suggested that interactions between these species enhance production of extracellular polymeric substances (EPS), which may increase toxicity while also providing a mechanism for the transport of *H. akashiwo* cells out of the euphotic zone.

3.3 Material and Methods

3.3.1 Cultures

Heterosigma akashiwo, National Center for Marine Algae and Microbiota strain CCMP2393, was previously isolated from Torquay Canal, Bald Eagle Creek in Rehoboth Bay, Rehoboth Beach, Delaware, USA (38.6991° N, 75.1097° W). Cultures of *H. akashiwo* were maintained in sea water amended with *f*/2 nutrients (Guillard & Ryther 1962) at a salinity of 20. Cultures were maintained at 25 °C with 140 μE m^{-2} s^{-1} irradiance on a 12:12 hour light:dark cycle. To reduce bacterial growth, kanamycin (50 μg ml^{-1}) was added over multiple transfers. For all experiments, *H. akashiwo* was grown semi-continuously to maintain cultures in mid to late log phase.

Vibrio cholerae SG7 was transformed with a GFP containing plasmid conferring kanamycin resistance (kindly provided by F. Fidelma Boyd, University of Delaware). *V. cholerae* was grown at 37 °C on LB 1% NaCl (Martinez et al. 2010) agar plate with 50 μg ml^{-1} kanamycin overnight. A single colony was picked and placed into LB 1% NaCl liquid medium and grown at 37 °C overnight on an orbital

shaker at 150 rpms. Cell density of *V. cholerae* was measured on a Nanodrop2000c (ThermoScientific, Wilmington, DE) using the optical density (600 nm) setting. An OD of 0.300 equates to ~$3x10^9$ colony forming units (CFU) ml^{-1}. *V. cholerae* grown overnight was diluted in fresh LB medium and grown at 37 °C for several hours to a density of ~$3x10^9$ CFU ml^{-1}.

3.3.2 Identification of *Vibrio-Heterosigma* associations in the natural environment

To examine attached *Vibrio* community, water was collected on August 29, 2012 from Torquay Canal (RB64: 38°41'59.6"N, 75°06'43.6"W) during a *Heterosigma akashiwo* bloom where cell density was $1x10^6$ cells l^{-1}. Water was sorted using a BD FACSCalibur (BD Biosciences, San Jose, CA) to collect *H. akashiwo* cells and associated bacteria. Parameters for sorting were established based on cultures of *Heterosigma akashiwo*. Contamination of other algal species on sorted samples of *Heterosigma akashiwo* was examined by PCR using primers for diatoms and dinoflagellates (Tilney et al. 2014). Confirmation of *H. akashiwo* was examined by PCR using primers for *H. akashiwo* (Coyne et al. 2005). Side scatter, indicative of cell granularity, size and shape, and fluorescence from chlorophyll *a* (FL3) were used to limit cell sorting to that of *Heterosigma*. Collected samples were filtered onto 3.0 µm polycarbonate filters (Millipore Isopore). Filters were immediately placed in CTAB buffer consisting of 100 mM Tris–HCl (pH 8), 1.4M NaCl, 2% (w/v) cetyltrimethylammonium bromide (CTAB), 0.4% (v/v) 2-mercaptoethanol, 1% (w/v) polyvinylpyrrolidone and 20 mM EDTA (Dempster et al. 1999). Filtered samples were stored at -80°C until extraction. Before extraction, all samples were heated at 65 °C for 10 minutes. DNA was extracted as described in Coyne et al. (2001) and

resuspended in LoTE (3 mM Tris- HCl, 0.2 mM EDTA, pH 7.5) (Coyne et al. 2001; Dempster et al. 1999). DNA concentration was determined by spectrophotometry and samples were diluted to approximately 25 ng μl^{-1} for molecular analysis.

For the Spike Experiment, water was collected from RB64 on 12 October, 2012 and filtered through a 20 µm polycarbonate filter (Millipore Isopore, Billerica, MA) to remove micro- and meso- grazers. The filtered water, containing the bacterial population, was aliquoted into 1-L polycarbonate bottles (n=4). Cultured *H. akashiwo* of a starting cell density of 215000 cells ml^{-1} was incubated on a 12:12 light:dark cycle at ~228 µmol m^{-2} sec^{-1} at 25 °C in site filtered water. After 24 hour incubation, samples were sorted using a BD FACSCalibur (BD Biosciences) to collect *H. akashiwo* cells and associated bacteria. Samples were filtered and extracted as above.

Analysis of the *Vibrio* community associated with *H. akashiwo* from the Spike Experiment and bloom sampling was carried out using *Vibrio*-specific primers previously designed to amplify a ~120 bp fragment of the 16S rRNA gene, 567F and 680R (Eiler & Bertilsson 2006; Thompson et al. 2004). DNA was amplified in 20 µl reactions consisting of 2 µl of 10X reaction buffer (Sigma-Aldrich, St. Louis, MO), 1 µM each primer, 200 µM dNTPs (New England BioLabs, Ipswich, MA), 2.5 mM $MgCl_3$, 0.5 units of JumpStart Taq (Sigma-Aldrich), and 1 µl diluted DNA template. DNA was amplified after an initial denaturation for 5 min at 94 °C for 16 cycles of 94 °C for 1 min, 72 °C for 1 min (decreased 0.5 °C per cycle), followed by 22 cycles of 94 °C for 1 min, 64 °C for 1 min and 72 °C for 1 min. PCR products were then denatured at 94 °C for 1 min followed by a 1 min incubation at 84 °C and a 5 min incubation at 72 °C. To reduce heteroduplex formation, PCR products were diluted 10-fold in fresh reaction mixture and cycled for 5 extra cycles (Thompson et al. 2002).

Temporal temperature gel electrophoresis (TTGE; Ogier et al. 2002) was carried out using a 10% (wt/vol) polyacrylamide gel with 7M urea in TAE buffer (20 mM Tris, 10mM acetate, 0.5mM Na_2EDTA; pH 7.4). The temperature gradient was determined using the MeltINGENY software package (IGENY, The Netherlands) using sequences of the 16S rRNA PCR fragment for *V. cholerae*, *V. parahaemolyticus* and *V. vulnificus*. PCR products (200 – 300 ng of DNA) from each sample were applied to individual lanes and electrophoresed at 130V for 8 hours. The temperature was increased at a rate of 1.5 °C per hour from 56 to 68 °C. Bands on the gel were excised, reamplified, and sequenced for identification (Muyzer et al. 1993; Coyne et al. 2001).

3.3.3 Culture conditions for transcriptome construction

Prior to the start of the experiment, cultures were diluted to 150,000 cells ml^{-1} and acclimatized for 24 hours in *f*/2 medium with 1 μM Fe and EDTA. This concentration of iron is approximately 0.1x *f*/2 concentrations and is similar to concentrations in Delaware's inland bays (Ma et al. 2006). Cultures (n=3) were inoculated with *Vibrio cholerae* at a ratio of 1:100 *Heterosigma*:*Vibrio* cells (n=3). An equal volume of LB medium was added to controls. Cultures were incubated for 24 hours at 25 °C on a 12:12 light:dark cycle at a light intensity of 228 μmol m^{-2} sec^{-1}. After 24 hours (5 hours after lights on), cultures were filtered under gentle vacuum (~380 mmHg) onto 3.0 μm filters (Millipore Isopore) and immediately placed into 0.6 ml of ice cold RLT buffer (Qiagen, Germantown, MD). Filters were stored at -80 °C until extraction.

3.3.4 Fluorescent microscopy

To examine attachment of *Vibrio cholerae* to *Heterosigma akashiwo*, samples were collected from the surface of treatment cultures at the end of the transcriptome experiment. Samples were visualized on an EVOS Fl Auto Cell Imaging System (Life Technologies, Grand Island, NY). Visualization of *V. cholerae* was performed using a GFP filter (AMEP4651, Excitation: 470/22 Emission: 525/50). Visualization of *H. akashiwo* was performed using a Texas Red filter for autofluorescence (AMEP4655, Excitation: 585/29 Emission: 624/40). Additional staining was carried out using DAPI (4′6′diamidino-2-phenolindole, final concentration 2 µg ml^{-1}) and filtered onto 0.2 µm polycarbonate black membrane filters.

3.3.5 Sample prep for RNA-Seq and quantitative PCR (qPCR)

Filtered cells in RLT buffer were heated at 55 °C for 3 minutes. Total RNA was isolated using the RNeasy Mini kit (Qiagen) using the manufacturer's instructions. DNA was removed from 2-3 µg of extracted RNA using DNase I (Invitrogen, Frederick, MD) following the manufacturer's instructions. RNA was quantified using a Nanodrop2000c (ThermoScientific) and removal of DNA was visualized by electrophoresis. A total of 3 µg of RNA was used for library construction using the Illumina TruSeq RNA Sample Preparation Kit (Illumina, San Diego, CA), according to manufacturer's instructions and performed at the Delaware Biotechnology Institute (DBI; Newark, DE, USA) sequencing facility. Sequencing of 50 base pair single end reads for each library was performed on duplicate lanes on an Illumina HiSeq 2000 (Illumina) at DBI.

3.3.6 *De novo* assembly

Raw reads of 50 bp were trimmed to remove poor quality reads and Illumina adaptors using the Trimmomatic software package with a sliding window of 6 through 20, and a minimum accepted length of 25 base pairs (Bolger et al. 2014). After trimming, reads with less than 20 bp were discarded prior to analysis. Reads for all samples were pooled into a single transcriptome and *de novo* assembly of the pooled samples was conducted using the Trinity (version 20140413) software package with default options (--seqType fq -JM 24G --single --CPU 2 --min_contig_length 200) (Haas et al. 2013). Expression levels for each transcript were estimated using the bundled RSEM software (-e remove_rsem.fasta -c 10) (Haas et al. 2013), and contigs with <10 Fragments Per Kilobase of transcript per Million mapped reads (FPKM) were removed. After filtering, the assembled contigs were clustered using the UCLUST algorithm as part of the USEARCH (v.7.0.101) software package (Edgar 2010) with a cutoff of 90% identity. Finally, those contigs ≥200 bp were retained for analysis.

3.3.7 Annotation

Annotation of the assembled transcriptome was carried out using the Trinotate (20140708) (Haas et al. 2013) (http://trinotate.sourceforge.net/) or BLASTx (Sun et al. 2011) search against the Marine Microbial Eukaryotic Transcriptome Sequencing Project (MMETSP) (Keeling et al. 2014), discarding results with associated e-value ≥ 1e-06. The Trinotate software package uses several methods for functional annotation by comparison to known sequences (NCBI-BLAST), protein domains (HMMER/Pfam), and curated databases (EMBL, Uniprot, eggnog, and GO pathways) (Haas et al. 2013). Functional annotation by the euKaryotic Orthologous Groups

(KOG) (Tatusov et al. 2003) database was carried out using WebGMA webserver (Wu et al. 2011) discarding results with associated e-value ≥ 0.001.

3.3.8 Differential expression (DE)

To discover possible contamination of reads from *Vibrio cholerae*, reads were first mapped against the *V. cholerae* 623 genome (Broad Institute). The remaining high quality reads were mapped to assembled contigs using the aligner software Bowtie2 (2.2.3) (Langmead et al. 2009). Gene expression levels were estimated as FPKM values using Cufflinks, v.2.2.1 (Trapnell et al. 2012; Trapnell et al. 2010). To examine differential gene expression of *Heterosigma akashiwo* in the presence of *Vibrio cholerae*, Cuffdiff (Trapnell et al. 2013) part of the Cufflinks software package was employed. The *Q*-value, false-discovery rate (FDR) p-value using the Benjamini-Hochberg correction for multiple-testing, was derived from Cuffdiff. A *Q*-value of ≤ 0.01 was used to determine a significantly differentially expressed gene. Genes were functionally annotated using the Mercator pipeline (Lohse et al. 2014), and significantly expressed genes were visualized using the MapMan (3.6.0RC1; Thimm et al. 2004). Briefly, the Mercator pipeline within MapMan bins ontology using a set of 34 tree-structured bins that describe metabolism and other cellular processes specifically tailored to plant pathways and processes (Klie & Nikoloski 2012). MapMan bin enrichment was examined on DE contigs using Fisher's exact test implemented in the Mefisto software (Giorgi 2012).

3.3.9 qPCR

To validate Cufflinks assemblage and results of Cuffdiff analysis of differential expression, several significantly up- or down-regulated genes were

examined and validated using qPCR. cDNA was synthesized using the Superscript III First-Strand Synthesis Kit (Invitrogen) from 500 ng of total RNA, isolated above, following the manufacturer's protocol using random hexamers. Reverse-transcribed cDNAs were diluted 1:20 in LoTE (3 mM Tris-HCl, 0.2 mM EDTA, pH 7.5) prior to qPCR analysis. qPCR was performed using an Applied Biosystems 7500 Real Time PCR System (Applied Biosystems, Grand Island, NY). Primers were designed for plasma membrane iron permease, fucoxanthin-chlorophyll a-c binding protein F, peroxidase, glutathione peroxidase, glutaredoxin, 60 kDa chaperonin 2, and mitochondrial elongation factor Ts 1 (Table 3.1) using the PRIMER-Blast tool (Ye et al. 2012). Primer concentrations were optimized using a diluted 1:20 cDNA as template. cDNA was amplified by qPCR in triplicate 10 µl reactions consisting of 5 µl of SYBR Green Select Master Mix (Applied Biosystems), 0.3 µM each primer, and 1 µl diluted cDNA template. A series of standards, prepared from 10-fold dilutions of cDNA from one sample were run concurrently. Reaction conditions for amplification consisted of 2 min at 50 °C, 10 min at 95 °C, followed by 40 cycles at 95 °C for 15 s, and 60 °C for 1 min, with added dissociation analysis. Expression was normalized to the housekeeping gene Glyceraldehyde-3-phosphate dehydrogenase (GAP) as described in Coyne (2010). Differential expression was calculated by using the $\log_2$ of normalized expression for treatment vs. control and compared to fold-change as determined by Cuffdiff.

3.4 Results

3.4.1 *Vibrio* community of Spike Experiment and bloom

The *Vibrio* community associated with isolated *H. akashiwo* cells from the Spike Experiment and bloom collection was examined using TTGE. Isolated cells of *Heterosigma* for the Spike Experiment were 3,232 cells ml^{-1}, while isolated cells from the bloom were 1,618 cells ml^{-1}. TTGE analysis and sequencing of bands from the bloom at RB64 confirmed *V. cholerae* and *V. parahaemolyticus* was associated with *Heterosigma akashiwo* (Fig. 3.1A, Lanes 1 and 2), while bands from the sorted samples showed similar results (Fig. 3.1A, Lanes 3 and 4). TTGE analysis of the second *Heterosigma* bloom demonstrated *V. cholerae* associated with *H. akashiwo* (Fig. 3.1B, Lanes 1 and 2), while the Spike experiment indicated *V. cholerae* associated with *H. akashiwo* in the sorted samples (Fig. 3.1B, Lanes 3 and 4). Identification of sequenced band (1) was determined with a BLAST search of GenBank (Altschul et al. 1990; Fig. 3.2).

3.4.2 Fluorescent microscopy

Examination of treatments cultures, *Heterosigma akashiwo* + *Vibrio cholerae*, using fluorescent microscopy GFP and autofluorescence overlay revealed association of *V. cholerae* in the EPS, with attachment to the algal cell (Fig.3.3B). Overlay of GFP and autofluorescence demonstrated localization of *V. cholerae* near the flagellar pore of *H. akashiwo* as well as being encased by EPS (Fig. 3.3B). DAPI staining revealed localized attachment of *V. cholerae* to the flagellar pore without EPS (Fig. 3.3C).

3.4.3 *Heterosigma akashiwo* transcriptome assembly and annotation

From a total of 2.4 x 10^8 Illumina HiSeq2000 cDNA reads, the final set consisted of 2.1 x 10^8 reads of 50 bp after filtering and trimming. Prior to assembly, mapping to the *Vibrio cholerae* genome resulted in only a few reads being mapped. Trinity assembly produced 73,109 contigs with a N50 of 868 and median contig length of 401 bp. After filtering, 12,698 contigs $\geq$200 bp remained with a N50 of 1,315 and median contig length of 849 bp. A BLASTx against the UniProtKB Swiss-Prot (Boeckmann et al. 2005) database using the Trinotate software package led to annotation of 44.8% of the transcriptome (Table 3.2). A search against the eggNOG and GO pathways database lead to annotation of 23.3% and 38.9% respectively. Classification of contigs against the KOG database by BLAST (Wu et al. 2011) returned 5,801 annotated contigs (Fig. 3.4). Of the 5,801 annotated contigs, 2,526 belong to the cellular process and signaling group (Fig. 3.4), with signal transduction and posttranslational modification, protein turnover and chaperones consisting of the majority of those contigs. Contigs associated with metabolism were the second largest grouping, with carbohydrate transport and metabolism, and inorganic ion transport metabolism the largest number of contigs associated with those classes (Fig. 3.4).

Table 3.1 Primers used for qPCR validation of transcriptome assembly and Cuffdiff analysis.

	Contig	Amplicon Size (bp)		Primers (5'-3')
Plasma membrane iron permease	comp31333_c0_seq1	199	F	CCCACAACCATACCCAGAATAC
			R	CCATGATCAAGATGGCGAAGA
Fucoxanthin-chlorophyll a-c binding protein F	comp28818_c0_seq1	233	F	GCACATTTTCGAGTGGCACA
			R	AACCAGCAGGGTCGAAGAAA
Peroxidase	comp27526_c0_seq1	200	F	TAAAGAGGAGCTGGACCAAAC
			R	CTCTTCACAGTGGGCTAGTAAAT
Glutathione peroxidase	comp14318_c0_seq1	217	F	CTCTGTGGACTCCAGAACTACTA
			R	GATGGGTGATCTGGATGTGATG
Glutaredoxin	comp28752_c0_seq1	207	F	CCTATGGTCTGTCCAGCAATAAA
			R	TGGAGGATTTCATCAACGAGAC
60 kDa chaperonin 2	comp5770_c0_seq1	202	F	TCACCAGCCGATTTGTCAGA
			R	ATCAACAAGGTGGCCAATGC
Elongation factor Ts 1, mitochondrial	comp25831_c0_seq1	158	F	TCTTTGAGCGCCTTGCTGTA
			R	GGCCGGTTGAATAAGTACCTG

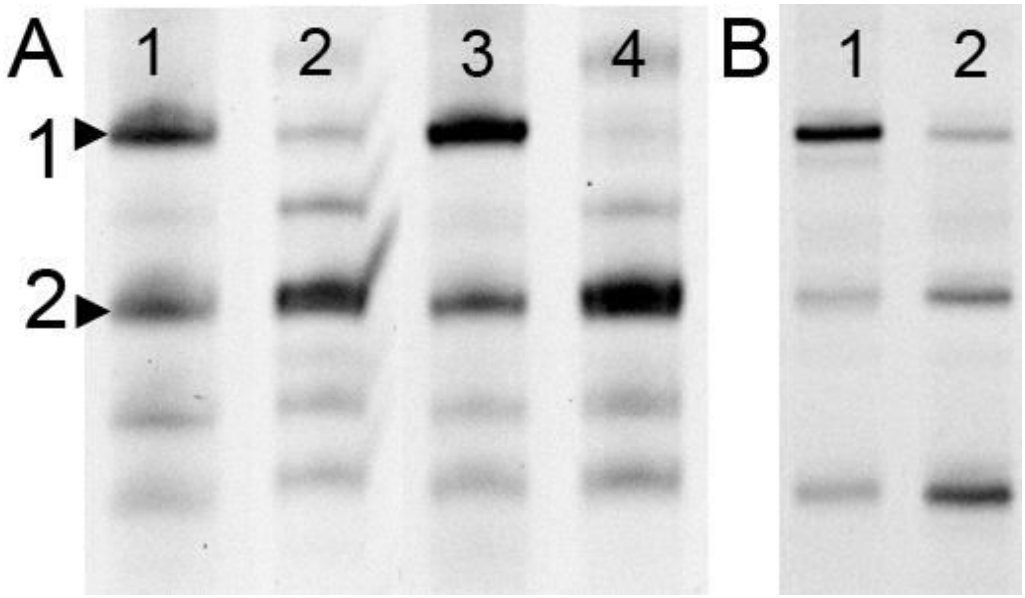

Figure 3.1 TTGE analysis of *Vibrio* communities. A) Lane 1: *Vibrio* community associated with RB64 Bloom >3.0 µm fraction, Lane 2: *Vibrio* community associated with RB64 Bloom 0.2-3.0 µm fraction, Lane 3: *Vibrio* community associated with sorted *Heterosigma akashiwo* >3.0 µm fraction, Lane 4: *Vibrio* community associated with 0.2-3.0 µm fraction B) Lane 1: *Vibrio* community associated with sorted *H. akashiwo* in the Spike Experiment, Lane 2: *Vibrio* community in the 0.2-3.0 µm fraction from Spike Experiment. 1. *V. cholerae*, 2. *V. parahaemolyticus*

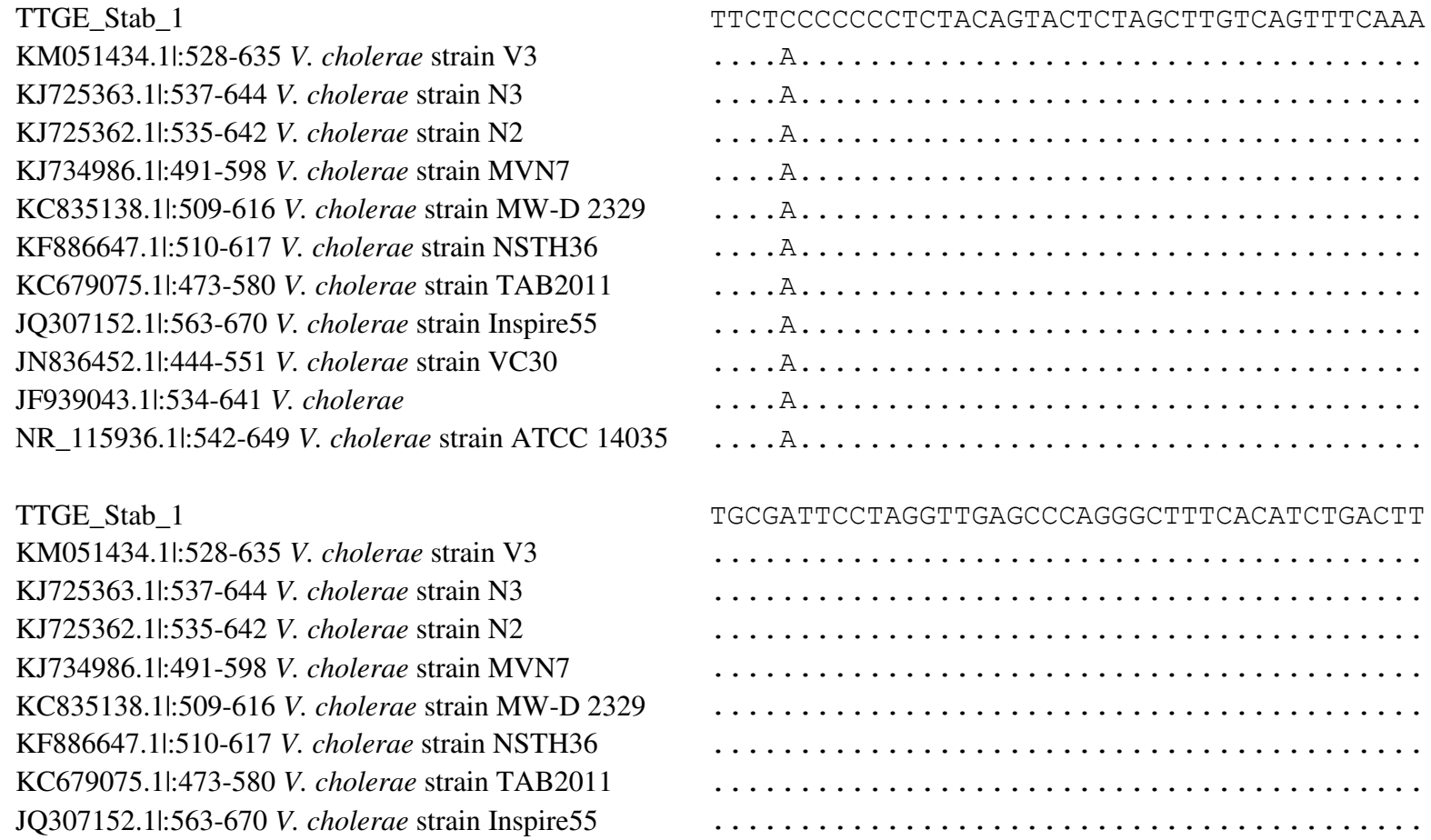

Figure 3.2 Sequence alignment of TTGE Band from 082914 RB64 bloom and *Vibrio cholerae* sequences from GenBank

TTGE_Stab_1	TGCGATTCCTAGGTTGAGCCCAGGGCTTTCACATCTGACTT
JN836452.1|:444-551 V. cholerae strain VC30	. . . . .
JF939043.1|:534-641 V. cholerae	. . . . .
NR_115936.1|:542-649 V. cholerae strain ATCC 14035	. . . . .

TTGE_Stab_1	AACAAACCACCTGCATGCGCTTTACG
KM051434.1|:528-635 *V. cholerae* strain V3	. . . . .
KJ725363.1|:537-644 *V. cholerae* strain N3	. . . . .
KJ725362.1|:535-642 *V. cholerae* strain N2	. . . . .
KJ734986.1|:491-598 *V. cholerae* strain MVN7	. . . . .
KC835138.1|:509-616 *V. cholerae* strain MW-D 2329	. . . . .
KF886647.1|:510-617 *V. cholerae* strain NSTH36	. . . . .
KC679075.1|:473-580 *V. cholerae* strain TAB2011	. . . . .
JQ307152.1|:563-670 *V. cholerae* strain Inspire55	. . . . .
JN836452.1|:444-551 *V. cholerae* strain VC30	. . . . .
JF939043.1|:534-641 *V. cholerae*	. . . . .
NR_115936.1|:542-649 *V. cholerae* strain ATCC 14035	. . . . .

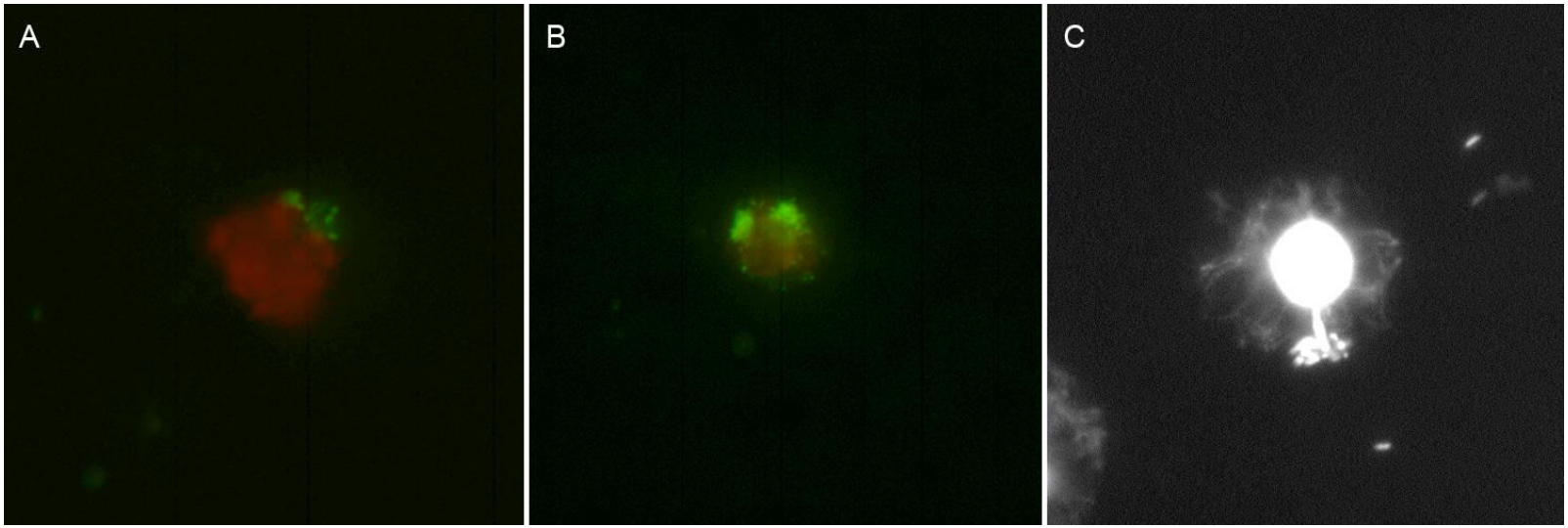

Figure 3.3 Fluorescent microscopy of treatment cultures, *Heterosigma akashiwo* + *Vibrio cholerae*. A) GFP and autofluorescence of *V. cholerae* and *H. akashiwo,* respectively; B) Localized *V. cholerae* around flagellar pore encased in EPS; C) DAPI stain localized *V. cholerae* to flagellar pore.

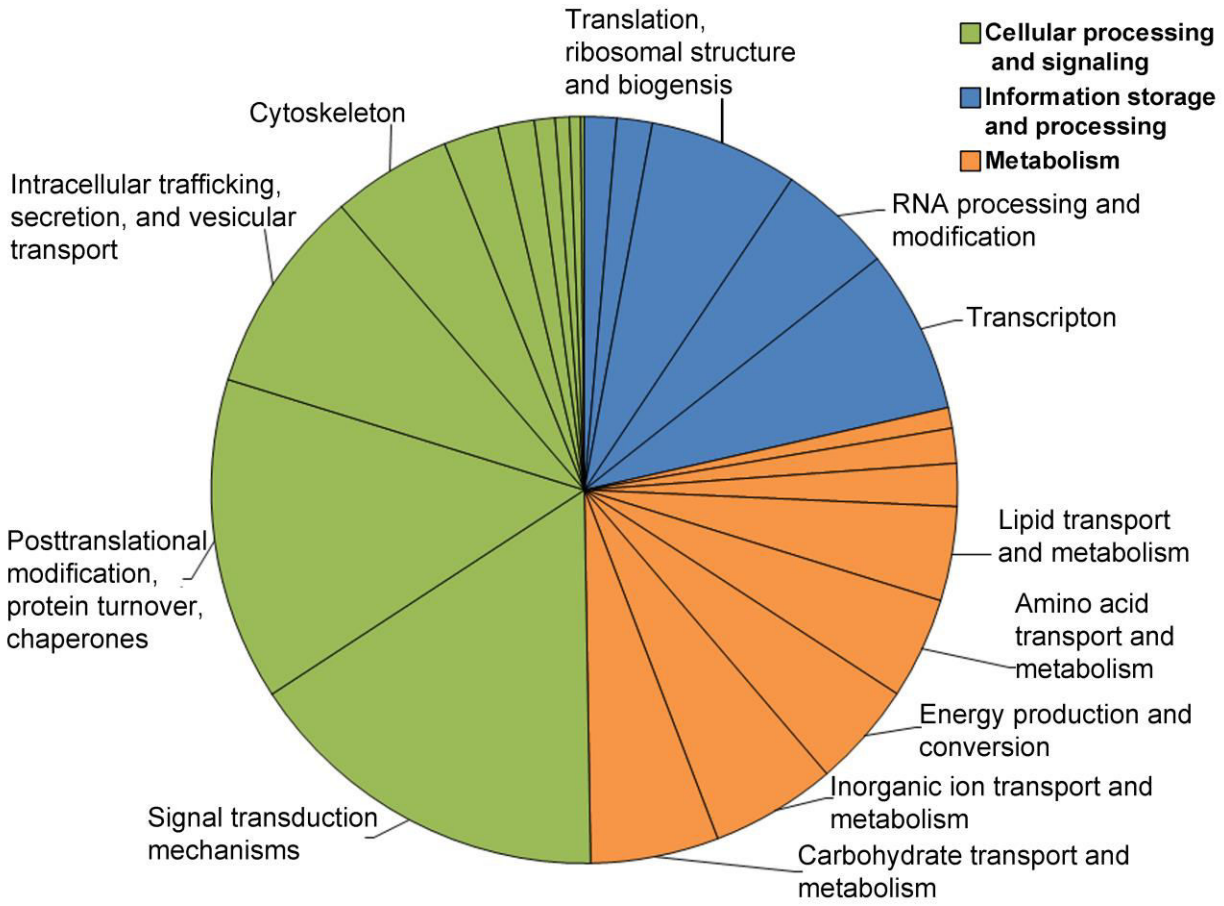

Figure 3.4 KOG analysis of transcriptome. A total of 5801 contigs were identified. Contigs without significant hits (e-value > 0.01) are not displayed.

3.4.4 Differential expression and KOG analysis

Of the 12,698 contigs, 1,560 were differentially expressed (DE) between the Controls and Treatments at a Q-value of ≤ 0.01. Of the 1,560 DE contigs, 1,001 contigs were up-regulated and 559 were down-regulated in the presence of *Vibrio cholerae* (Fig. 3.5), with 48.1% of the DE contigs annotated with Trinotate (Table 3.2). Classification of differentially expressed contigs against the KOG database by BLAST returned 474 annotated contigs (Table 3.3). Gene categories down-regulated in *Heterosigma akashiwo* in the presence of *Vibrio cholerae* were highly populated in lipid transport and metabolism (I), and energy production and conversion (C) (Table 3.3). Gene categories highly up-regulated were translation, ribosomal structure and biogenesis (J), amino acid transport and metabolism (E), post-translation modification, protein turnover and chaperones (O), signal transduction mechanisms (T), and transcription (K) (Table 3.3).

3.4.5 MapMan analysis

Classification of DE contigs using the Mercator pipeline assigned contigs to 1194 bins, with some contigs assigned to multiple bins for a total of 1287 assignments. Highly down- regulated MapMan bins were in photosystem (bin 1) and lipid metabolism (bin 11) bins, while highly up-regulated transcripts were represented in stress response (bin 20), tetrapyrrole synthesis (bin 19), development (bin 33), signaling (bin 30), RNA processing (bin 27), redox response (bin 21), protein processing (bin 29), DNA processing (bin 28), cell division, cell cycle and cellular organization (bin 31), amino acid metabolism (bin 13) and N-metabolism (bin 12) (Table 3.5). All DE transcripts in the stress response bin (20) were up regulated in the

Table 3.2 Assembly metrics and annotation statistics for transcriptome assembly.

Total Reads	$2.4x10^8$
Final number of contigs	12698
Maximum contig Length (bp)	16750
Mean contig Length (bp)	1019
N50	1315
Number of contigs with significant BLASTx hits	5693
% of contigs with significant BLASTx hits	44.8
Number of differentially expressed contigs*	1560
Number of significantly up-regulated contigs	1001
Number of significantly down-regulated contigs	559
Number of DE contigs with significant BLASTx Hits	750
% of DE contigs with significant BLASTx hits	48.1

* Q-value ≤ 0.01

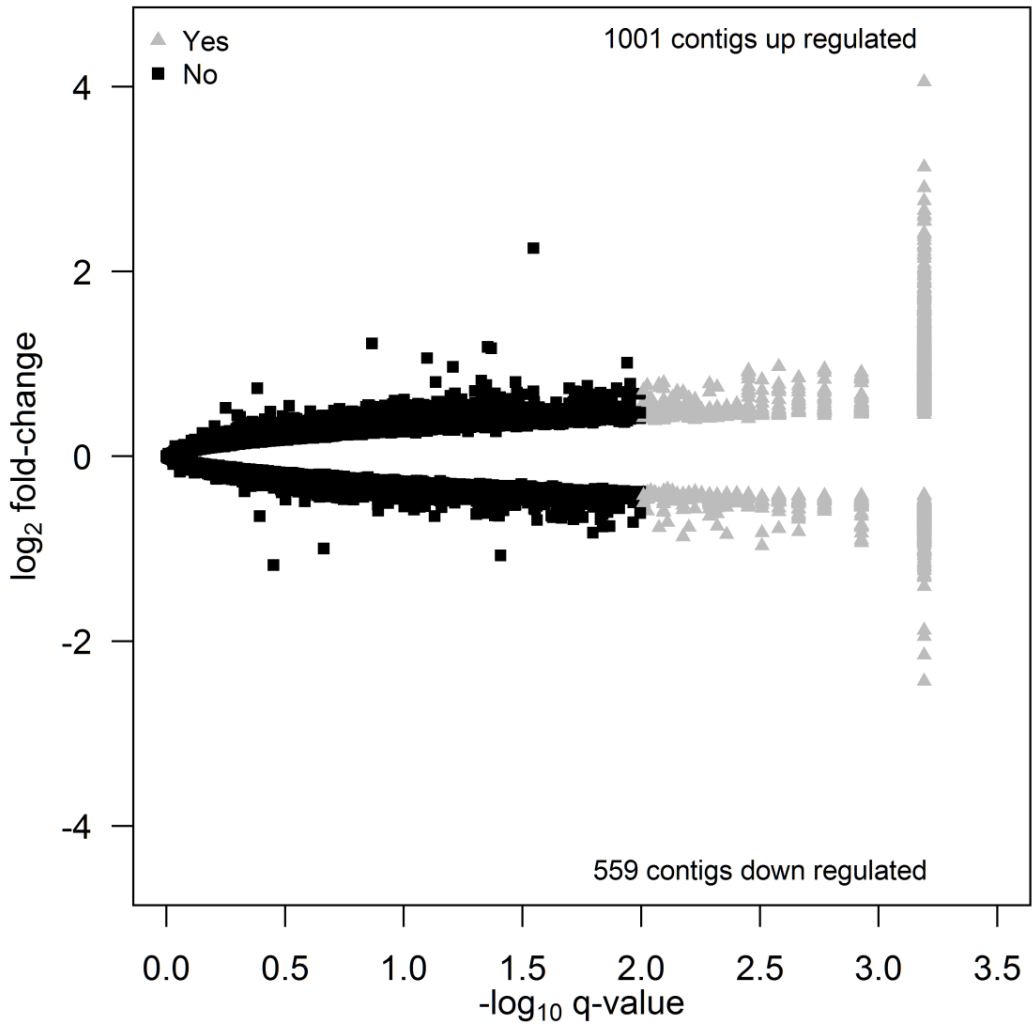

Figure 3.5 Log_2 fold-change between *Heterosigma* + *Vibrio* (Treatment) versus *Heterosigma* (Control) for all contigs. Grey symbols: Q-value ≤ 0.01.

Table 3.3 Contigs per KOG class and percent up- or down-regulated (in parentheses) sequences for differentially expressed contigs.

KOG Category	KOG Description	# Up Regulated	# Down Regulated
Information storage and processing			
J	Translation, ribosomal structure and biogenesis	81 (98.8)	1 (1.2)
K	Transcription	29 (93.5)	2 (6.5)
A	RNA processing and modification	19 (86.4)	3 (13.6)
L	Replication, recombination and repair	8 (88.9)	1 (11.1)
B	Chromatin structure and dynamics	6 (100)	0 (0)
Metabolism			
E	Amino acid transport and metabolism	31 (75.6)	10 (24.4)
G	Carbohydrate transport and metabolism	18 (78.3)	5 (21.7)
P	Inorganic ion transport and metabolism	18 (90)	2 (10)
C	Energy production and conversion	6 (46.2)	7 (53.8)
H	Coenzyme transport and metabolism	9 (90)	1 (10)
I	Lipid transport and metabolism	4 (40)	6 (60)
Q	Secondary metabolites biosynthesis, transport and catabolism	5 (100)	0 (0)
F	Nucleotide transport and metabolism	4 (100)	0 (0)
Cellular process and signaling			
O	Posttranslational modification, protein turnover, chaperones	43 (84.3)	8 (15.7)
T	Signal transduction mechanisms	32 (86.5)	5 (13.5)
Z	Cytoskeleton	14 (73.7)	5 (26.3)
U	Intracellular trafficking, secretion, and vesicular transport	16 (94.1)	1 (5.9)

Table 3.3 continued

KOG Category	KOG Description	# Up Regulated	# Down Regulated
M	Cell wall/membrane/envelope biogenesis	4 (66.7)	2 (33.3)
W	Extracellular structures	2 (50)	2 (50)
V	Defense mechanisms	1 (33.3)	2 (66.7)
D	Cell cycle control, cell division, chromosome partitioning	2 (100)	0 (0)
Y	Nuclear structure	1 (100)	0 (0)
Poorly characterized			
R	General function prediction only	37 (80.4)	9 (19.6)
S	Function unknown	11 (91.7)	1 (8.3)

presence of *V. cholerae*, with 11 of the 17 transcripts identified as members of the heat shock protein 70 family (Table 3.5; Fig. 3.5). In bin 21, redox response, the majority of sequences were up-regulated. These were identified as chloroplast-specific enzymes, thioredoxin and peroxiredoxin (Table 3.5; Fig. 3.5). In bin 30, signaling response, a blue light photoreceptor was down regulated (Fig. 3.6). DE contigs in bin 30.3, calcium regulation, were up regulated in the presence of *V. cholerae*. Three of the contigs were identified as proteins involved in calmodulin regulation, while 2 contigs were identified as calcium-transporting ATPase (Fig. 3.6). Contigs involved in RNA regulation (bin 27.3) were up-regulated except for 3 contigs, of which one was identified as encoding a subunit of the RNA polymerase located in the chloroplast (Fig. 3.6). All contigs in bin 19, tetrapyrrole synthesis, responsible for chlorophyll and other pigment synthesis, were up regulated in presence of *V. cholerae* (Table 3.5). In contrast, the chlorophyll a-b binding and fucoxanthin-chlorophyll binding proteins were all down regulated (Fig. 3.7). Enrichment analysis of all contigs by MapMan indicated 45 bins were enriched (Table 3.6).

3.4.6 qPCR validation

Differential expression of 7 significantly expressed transcripts as determined by qPCR results verified the results of Cuffdiff analysis (Table 7), although the magnitude of expression differed for some. qPCR analysis of the plasma membrane iron permease (comp31333_c0_seq1) underestimated DE by 35% when compared to Cuffdiff. Likewise, qPCR analysis of glutathione peroxidase (comp14318_c0_seq1) underestimated DE by 57% when compared to Cuffdiff. In contrast, qPCR analysis overestimated DE for Fucoxanthin-chlorophyll a-c binding protein F by 349% (Table 3.7).

Table 3.4 Distribution of functional assignments across MapMan bins for differentially expressed contigs.

Bin Code	Bin Name	Contigs classified	% Up Regulated	% Down Regulated
1	Photosystem	23	8.7	91.3
2 & 3	Carbohydrates metabolism	6	66.7	33.3
4	Glycolysis	11	72.7	27.3
6	Gluconeogenesis/glyoxylate cycle	1	0.0	100.0
7	Oxidative Pentose Phosphate Cycle	3	33.3	66.7
8	TCA/org. transformation	7	42.9	57.1
9	Mitochondrial electron transport/ATP synthesis	4	25.0	75.0
10	Cell wall	3	100.0	0.0
11	Lipid metabolism	17	35.3	64.7
12	N-metabolism	5	80.0	20.0
13	Amino acid metabolism	26	80.8	19.2
14	S-assimilation	3	100.0	0.0
15	Metal handling	3	66.7	33.3
16	Secondary metabolism	11	63.6	36.4
18	Cofactor and vitamin metabolism	4	50.0	50.0
19	Tetrapyrrole synthesis	8	100.0	0.0
20	Stress	19	100.0	0.0
21	Redox	17	88.2	11.8
23	Nucleotide metabolism	8	62.5	37.5
25	C1-metabolism	3	100.0	0.0
27	RNA	34	91.2	8.8
28	DNA	15	86.7	13.3
29	Protein	168	87.5	12.5
30	Signaling	28	96.4	3.6
31	Cell	19	84.2	15.8
33	Development	7	100.0	0.0
34	Transport	52	69.2	30.8

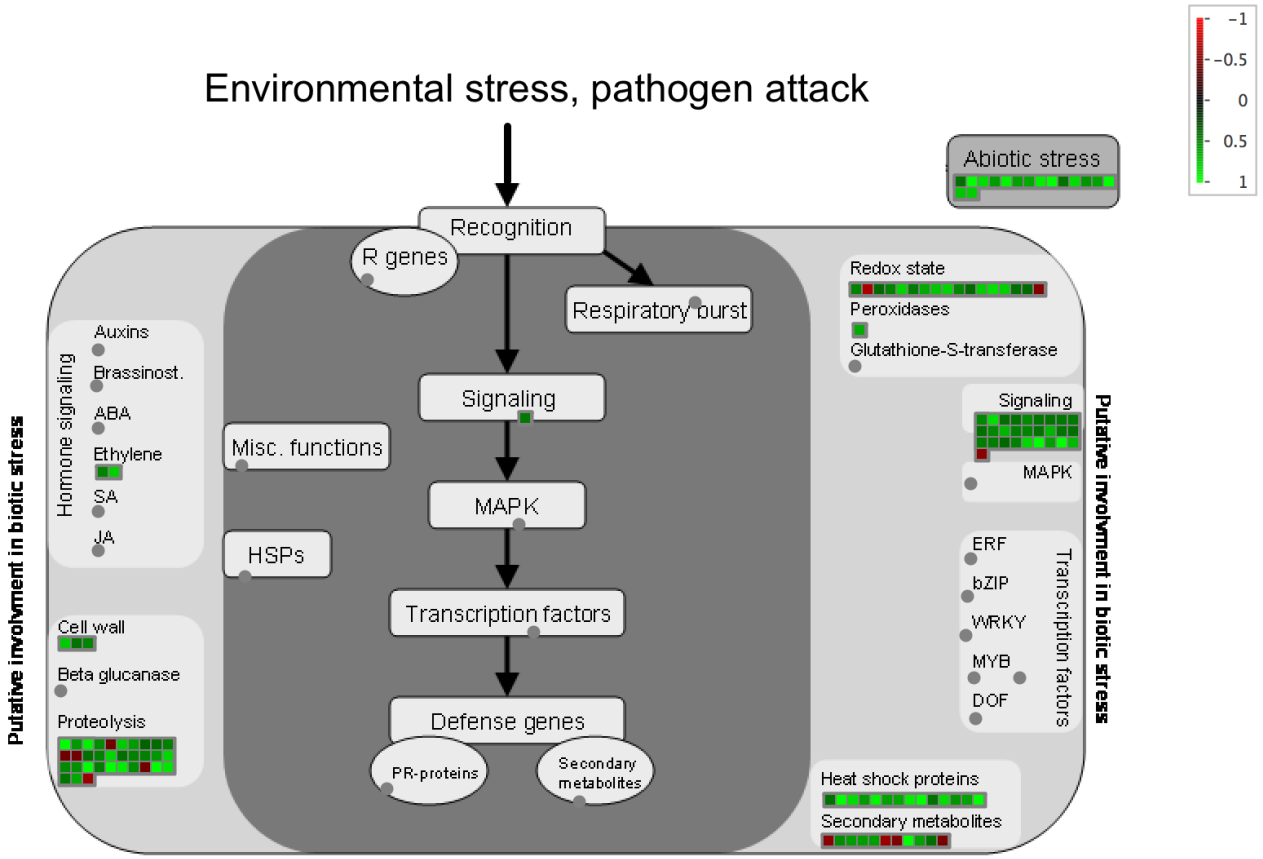

Figure 3.6 The biotic stress response of *Heterosigma akashiwo* to *Vibrio cholerae* using MapMan bins of significantly DE contigs, based on $\log_2$ fold-change determined using Cuffdiff.

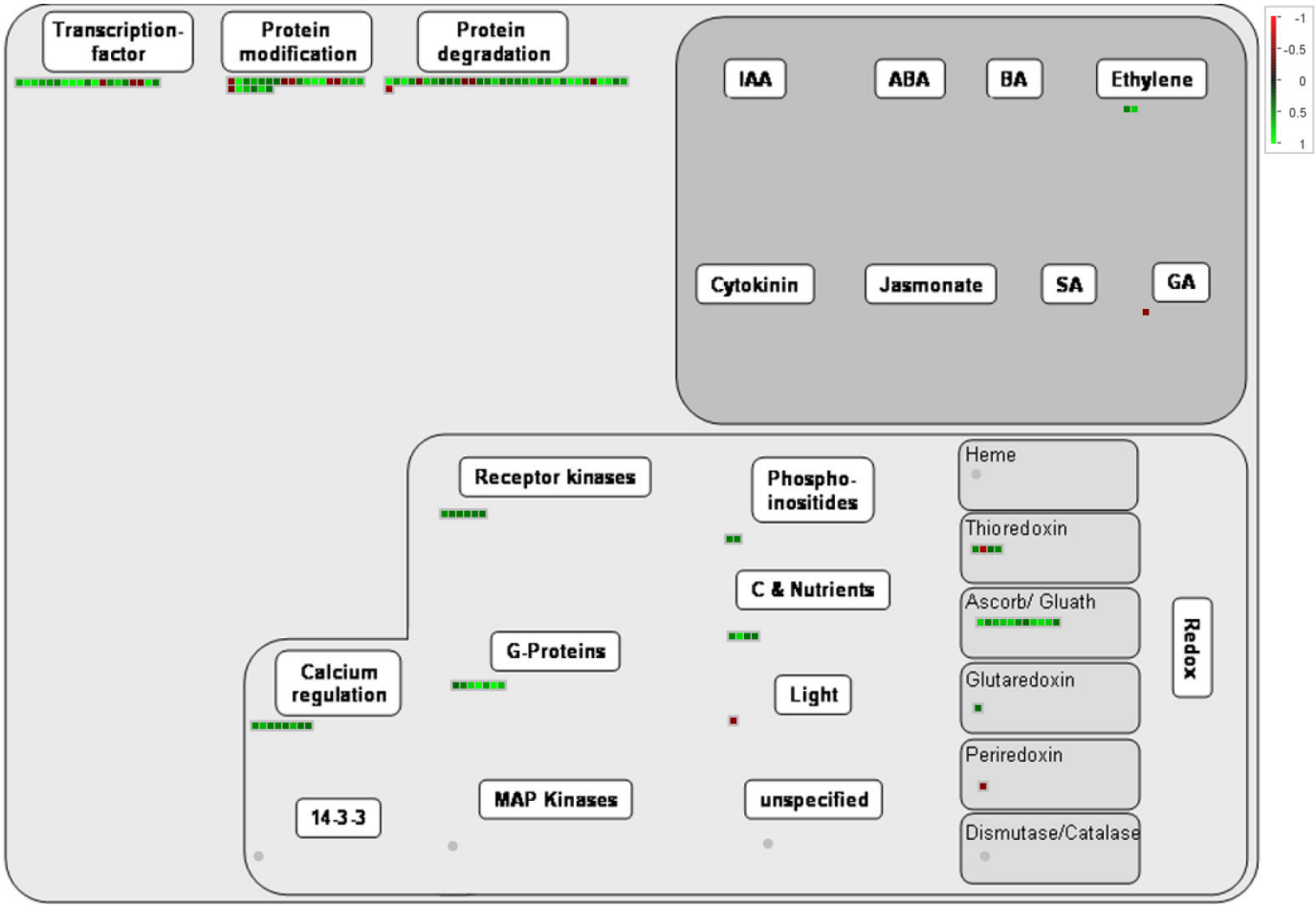

Figure 3.7 Overview of regulation of *H. akashiwo* in response to *Vibrio cholerae* using MapMan bins of significantly DE contigs, based on $\log_2$ fold-change determined using CuffDiff.

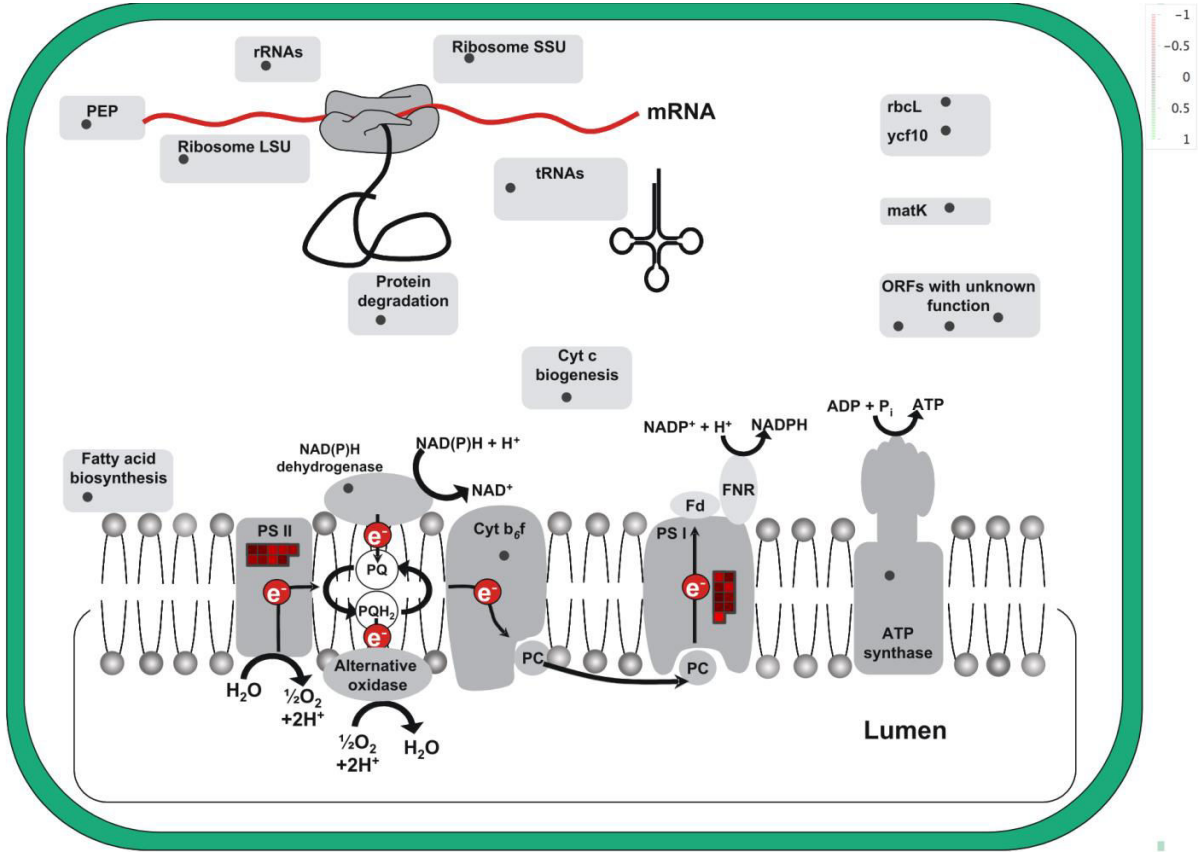

Figure 3.8 Transcriptional response of chloroplast of *H. akashiwo* to *V. cholerae* using significantly DE MapMan bins, based on $\log_2$ fold-change determined using Cuffdiff.

Table 3.5 Enrichment of contigs in MapMan terms for DE contigs.

Bin	BinName	Fisher's exact test *P*-value (Bonferroni-corrected)
1	Photosynthesis	1.67E-05
1.2	PS.photorespiration	3.77E-03
1.3	PS.calvin cycle	2.34E-02
2	Major carbohydrates metabolism	1.19E-11
2.1	Major carbohydrates metabolism.synthesis	2.45E-10
2.1.1	Major carbohydrates metabolism.synthesis.sucrose	5.16E-09
2.2	Major carbohydrates metabolism.degradation	1.34E-02
3	Minor carbohydrates metabolism	7.75E-36
3.3	Minor carbohydrates metabolism.sugar alcohols	1.74E-11
3.99	Minor carbohydrates metabolism.misc	2.87E-33
8	TCA / org transformation	2.69E-06
8.1	TCA / org transformation.TCA	3.35E-03
8.2	TCA / org transformation.other organic acid transformations	1.18E-03
10	Cell wall	1.69E-09
10.2	Cell wall.cellulose synthesis	1.14E-15
11	Lipid metabolism	5.86E-38
11.8	Lipid metabolism.exotics(steroids, squalene etc.)	1.34E-06
13	Amino acid metabolism	1.10E-16
13.1	Amino acid metabolism.synthesis	1.46E-15
13.1.2	Amino acid metabolism.synthesis.glutamate family	8.63E-03
13.1.3	Amino acid metabolism.synthesis.aspartate family	2.21E-02
13.1.5	Amino acid metabolism.synthesis.serine-glycine-cysteine group	2.73E-02
13.1.6	Amino acid metabolism.synthesis.aromatic aa	1.76E-02
13.1.6.3	Amino acid metabolism.synthesis.aromatic aa.phenylalanine	1.66E-02
16	Secondary metabolism	2.78E-122
16.1	Secondary metabolism.isoprenoids	1.18E-23
16.2	Secondary metabolism.phenylpropanoids	1.51E-69
16.1.2	Secondary metabolism.isoprenoids.mevalonate pathway	1.12E-14

Table 3.5 continued

Bin	BinName	Fisher's exact test *P*-value (Bonferroni-corrected)
16.2.1	Secondary metabolism.phenylpropanoids.lignin biosynthesis	5.16E-09
16.4	Secondary metabolism.N misc	3.28E-07
16.1.3	Secondary metabolism.isoprenoids.tocopherol biosynthesis	8.63E-03
16.4.1	Secondary metabolism.N misc.alkaloid-like	1.82E-06
17	Hormone metabolism	1.53E-09
17.2	Hormone metabolism.auxin	6.06E-05
18	Co-factor and vitamin metabolism	2.26E-02
22	Polyamine metabolism	4.92E-04
23	Nucleotide metabolism	1.31E-20
23.1	Nucleotide metabolism.synthesis	3.92E-23
23.1.1	Nucleotide metabolism.synthesis.pyrimidine	6.67E-11
23.2	Nucleotide metabolism.degradation	2.94E-05
23.1.2	Nucleotide metabolism.synthesis.purine	1.79E-13
27	RNA	2.75E-03
29	Protein	1.50E-15
29.5	Protein.degradation	2.25E-03
34	Transport	2.29E-03

Table 3.6 qPCR validation of transcriptome assembly compared to Cuffdiff analysis.

	Sequence	qPCR	CuffDiff
Plasma membrane iron permease	comp31333_c0_seq1	0.229	0.646
Fucoxanthin-chlorophyll a-c binding protein F	comp28818_c0_seq1	-1.700	-0.486
Peroxidase	comp27526_c0_seq1	0.763	0.911
Glutathione peroxidase	comp14318_c0_seq1	0.476	0.835
Glutaredoxin	comp28752_c0_seq1	0.836	1.146
60 kDa chaperonin 2	comp5770_c0_seq1	2.398	2.615
Elongation factor Ts 1, mitochondrial	comp25831_c0_seq1	2.130	1.969

3.5 Discussion

Full genome sequencing for eukaryotic phytoplankton is rare, and the few exceptions are only available as single isolates within a species (Keeling et al. 2014). Recently, full genomes have been described for *Aureococcus anophagefferens* (Gobler et al. 2011), *Synechococcus* sp. (Marsan et al. 2014), *Thalassiosira pseudonana* (Armbrust et al. 2004) and *Nannochloropsis gaditana* (Radakovits et al. 2012). Without a genome, *de novo* assembly of global transcripts is a powerful alternative for examination of strain difference and expression analysis (Frischkorn et al. 2014). The number of transcripts for several *Pythium* species has been reported to range from 11,958 to 15,323 (Adhikari et al. 2013). For the diatom *Thalassiosira pseudonana*, the reported number of protein-coding genes is 11,426 (Armbrust et al. 2004). However for *Aureococcus anophagefferens* the number of assembled contigs ranged from 31,473 to 53,886 depending on method of assembly (Frischkorn et al. 2014). Similarly, in *Alexandrium tamarense* the number of transcripts ranged from 38,000 to 39,000 depending on culture treatment (Moustafa et al. 2010). Our *de novo* assembled transcriptome contained 12,698 contigs after filtering out lowly expressed transcripts and those less than 200 bases in length (Table 3.2), well within the range of genes expressed in other single cellular stramenopiles.

Here, we examined the transcriptional and cellular response of *Heterosigma akashiwo* to the presence of *Vibrio cholerae*. Importantly, we identified *V. cholerae* as the major *Vibrio* species associated with *H. akashiwo* cells during natural blooms of this species and confirmed these observations using laboratory cultures spiked into environmental water (Fig. 3.1). Physical attachment of *V. cholerae* to *H. akashiwo* cells was also observed by microscopy (Fig. 3.3), suggesting the potential for inter-

kingdom signaling between these species that may lead to establishment of a stable association. In addition, *Vibrio* cells were often localized near the flagellar pore of *H. akashiwo*, perhaps due to specific structures or cell-surface carbohydrate moieties (Rosenbaum & Witman 2002) associated with this region. Recently, *H. akashiwo* has been described as a mixotroph (Jeong 2011) on bacteria only. Two potential means to engulf bacterial cells exist in raphidophytes, a funnel-shaped groove with two flagella and mucocyst pores (Jeong 2011; Hara & Chihara 1987).

Functional annotation of genes that were differentially expressed in *H. akashiwo* helps to characterize the cellular response to the presence of *V. cholerae*. We found that annotated genes related to translation, transcription, RNA processing, posttranslational modification, signal transduction and cytoskeleton were generally up regulated in the presence of *V. cholerae*, while those involved in energy production and lipid transport were down regulated (Table 3.3, 3.4). Gene enrichment analysis indicated that in the presence of *Vibrio cholerae*, transcripts were highly enriched in secondary metabolism, lipid metabolism, carbohydrate metabolism, protein metabolism, and cell wall modification pathways (Table 3.6). Changes in lipid metabolism can mediate important environmental actions, including grazing (Miralto et al. 1999), response to viral infection (Vardi et al. 2009) and toxicity (Deeds & Place 2006). In *Thalassiosira pseudonana*, lipid metabolism changes in response to *Karenia brevis* allelopathy included a decrease in phospholipids and mannan (Poulson-Ellestad et al. 2014). However, transcripts for enzymes involved in sulfolipid biosynthesis were found in higher concentrations (Poulson-Ellestad et al. 2014), suggesting modification of the cell membrane with sulfolipids. Here, several transcripts involved

in lipid metabolism were down regulated in the presence *V. cholerae* (Table 3.4). except for those involved in sulfolipid biosynthesis, which were upregulated.

In algal cells, changes in light can induce alterations to the chloroplast and cellular energy balance, resulting in changes to the intracellular signaling which can affect responses to stresses (reviewed by Wilson et al. 2006). For example, in *Dunaliella tertiolecta*, when the plastoquinone pool is reduced by exposure to light, the transcription of the light harvesting complex genes (*Lhcb*) is down regulated. A decrease in the size of the light harvesting complex produces a high-light phenotype (reviewed by Wilson et al. 2006). In other research, there was a temporary spike in growth of *Heterosigma* after shifting to high light conditions, but reduced photosystem II reaction center connectivity and electron transport (Hennige et al. 2013). Those transcripts identified in *H. akashiwo* as chlorophyll and fucoxanthin binding proteins (CAB) within photosystems I and II were all down regulated in the presence of *Vibrio* (Fig. 3.5). Though high light was not used in the experiments presented here, down-regulation of these proteins can impact carbon metabolism pathways and result in a reduction of growth (reviewed by Wilson et al. 2006).

ROS may also aid in the uptake of iron in the marine environment by algal species (Garg et al. 2007). ROS are byproducts of various metabolic pathways that are localized in the chloroplast, peroxisomes, and mitochondria (Apel & Hirt 2004) and include superoxide anion radicals (O_2^-), hydrogen peroxide (H_2O_2) and hydroxyl radicals ($OH^\cdot$). Photosynthetic organisms can generate ROS by activating various enzymes in response to environmental stressors, such as pathogens, drought, light intensity, and nutrient limitation (Liu et al. 2007). Production of ROS can cause widespread damage to the cell. Plants and other organisms produce superoxide

dismutase, catalase, peroxidases, and small heat shock proteins to mediate oxidative stress (reviewed by Chi et al. 2013). In *H. akashiwo*, catalase activity was not correlated to the production of H_2O_2 (Portune et al. 2010). However, peroxidases such as glutathione peroxidase (GPX) are also capable of catalyzing the reduction of hydrogen peroxide to water (reviewed by Chi et al. 2013). Here, we identified several transcripts encoding enzymes involved in scavenging of ROS, including glutathione peroxidase (comp14318_c0_seq1, KOG1651, e-value: $4x10^{-22}$), as well as peroxidases (comp27526_c0_seq1, Uniprot: Q539E5, e-value: $7x10^{-20}$) and glutaredoxin (comp28752_c0_seq1, KOG1752, e-value: $2x10^{-29}$, Table 5), that were all up-regulated, suggesting an increase in ROS production by *H. akashiwo* in response to *Vibrio*. An increase in ROS may also influence the composition of PSI and PSII. In *Chlorella vulgaris* ROS concentration was negatively correlated with *Lhcb* abundance (Wilson et al. 2003) suggesting that the decrease in binding proteins in the presence of *V. cholerae* noted above may be due to the increase in ROS production.

A common response in bacterial:algal associations is the increased production of extracellular polymeric substances (EPS) by the algal host (Bruckner et al. 2008; Gärdes et al. 2011). The production of EPS can benefit the algal host by aiding in the sequestering of nutrients (Penna et al. 1999), as well as protection from ROS (Zhang et al. 2013). EPS may also benefit associated bacteria by increasing the diffusive boundary layer around the cell and thereby decreasing the flux of nutrients away from the cell (Lazier & Mann 1989). In phytoplankton, EPS is secreted via exocytotic pathways in which the components are first assembled in vesicles and then discharged from the cell by fusion of the vesicular membrane with the outer cellular membrane (Chin et al. 2004; Linde et al. 2001). This process is mediated by changes in cytosolic

Ca^{2+}, a secondary messenger which regulates several physiological activities in response to external stimuli (Chin et al. 2004). Previous studies have shown that quorum sensing signals from bacteria can elicit an increase in cytosolic Ca^{2+} in plant and macroalgal cells (Joint et al. 2007; Karlsson et al. 2012). In zoospores of the macroalga *Ulva*, for example, response to quorum sensing signals from bacterial biofilms resulted in a Ca^{2+} mediated decrease in swimming rate and exocytosis of adhesive compounds, increasing settlement of the zoospores at the source of signal (Joint et al. 2007). In our transcriptome, however, transcripts for calcium ATPase (comp28396_c0_seq1), responsible for exporting calcium from the cell, were significantly up regulated in the presence of *V. cholerae* (KOG class T, BIN 30.3, Fig. 3.6). Calmodulin and calmodulin-like proteins (comp23377_c0_seq1), which transduce Ca^{2+} signals within the cell (Linde et al. 2001), were also down-regulated in response to *V. cholerae*. Since the microscopic images of *H. akashiwo* show substantial EPS production in the presence of *V. cholerae*, it can be assumed that proteins responsible for Ca^{2+} -mediated exocytosis were transiently upregulated prior to RNA isolation. The increase in transcripts for Ca^{2+}-ATPase and down regulation of calmodulin genes may indicate a response to return Ca^{2+} levels to normal.

In summary, our data suggests a remodeling of *Heterosigma akashiwo* in the presence of *Vibrio cholerae* and a rebalancing of energy distribution, potentially affecting carbon assimilation pathways and light-induced ROS production. In addition, microscopic evaluation showed an increase in EPS production, which may also increase toxicity in *Heterosigma*. Associations between *H. akashiwo* and *Vibrio cholerae* may have important human health implications as well, as blooms of *H. akashiwo* may be a vector for pathogenic *Vibrio.*

Chapter 4

EFFECTS OF GROWTH PHASE, DIEL CYCLE AND MACRONUTRIENT STRESS ON THE QUANTIFICATION OF *HETEROSIGMA AKASHIWO* USING QPCR AND SHA

4.1 Abstract

The development of molecular probe technologies over the last several decades has enabled more rapid and specific identification and enumeration of phytoplankton species compared to traditional technologies, such as light microscopy. Direct comparisons of these methods with respect to physiological status, however, are sparse. Here we directly compare quantitative real-time PCR (qPCR) and sandwich hybridization assay (SHA) for enumerating the raphidophyte Heterosigma akashiwo at several points during its growth phase, over a diel cycle and with macronutrient stress in laboratory cultures. To ensure consistency between comparisons, a single cellular homogenate was generated from each culture and split for analysis by qPCR and SHA. Since the homogenate was generated from the same number of cells during each experiment, results reflect changes in nucleic acid content (rRNA and DNA) at each time point or in response to environmental conditions relative to a reference sample. Results show a greater level of precision in SHA results which contributed to significant (2-3 fold) differences in rRNA content per cell in several of these analyses. There was significantly greater rRNA content during lag and exponential phases compared to stationary phase cultures, and a significant decrease in rRNA content during the light cycle compared to cells harvested in the dark. In contrast, there were

no significant differences in DNA content per cell as determined by qPCR over a diel cycle or during different growth phases. However, both rRNA and DNA content per cell were significantly lower under N stress when compared to nutrient replete conditions. Results of this study suggest that growth stage, nutrient stress and cell cycle may impact qPCR and SHA analysis.

4.2 Introduction

A fundamental requirement for any harmful algal bloom (HAB) monitoring program is the accurate determination of both species and abundance. Light microscopy has historically been the method of choice for detection, identification, and enumeration of HAB species, but this technique can be time consuming and may require specialized training for accurate identification between species or strains. In addition, the use of microscopy for monitoring HAB species may not be sensitive enough to detect organisms that are a minor component of the assemblage (Anderson et al. 2005; Godhe et al. 2007). Further identification to the species level may also require the use of electron microscopy (Anderson 1995), which is not amendable to high-throughput analysis (Culverhouse et al. 2003). Over the past couple of decades, development of molecular probe technologies have enabled rapid and specific identification of phytoplankton species that also provide increased sensitivity of detection (Godhe et al. 2007; Greenfield et al. 2006; Coyne et al. 2001; Coyne et al. 2005). As a result, the use of molecular approaches in HAB research and monitoring programs has increased (Anderson et al. 2012; Anderson et al. 2005; Rhodes et al. 2001; Haywood et al. 2009).

Quantitative real-time PCR (qPCR) and sandwich hybridization assay (SHA) are two molecular approaches that have been developed for detection and

quantification of HAB species (Coyne et al. 2005; Tyrrell et al. 2002; Haywood et al. 2007; Greenfield et al. 2008). Each approach uses targeted molecular probes or non-specific fluorescent dyes for detection and quantification. The techniques differ in that qPCR typically targets DNA and requires isolation and purification of DNA from samples, whereas SHA uses direct detection of ribosomal RNA (rRNA) from unpurified and unamplified samples (Scholin et al. 2003; Greenfield et al. 2006). Both technologies have been used extensively in the marine environment for quantitative detection of HAB species including *Pseudo-nitzschia* (Scholin et al. 1997), *Aureococcus anophagefferens* (Popels et al. 2003), *Alexandrium fundyense* (Godhe et al. 2007), *Karlodinium veneficum* (Handy et al. 2008), *Karenia brevis* (Haywood et al. 2007; Gray et al. 2003), *Cochlodinium polykrikoides* (Mikulski et al. 2008), *Ostreopsis* spp. (Hariganeya et al. 2013) and several raphidophyte species, including *Heterosigma akashiwo* (Tyrrell et al. 2001; Handy et al. 2006; Coyne et al. 2005; Portune et al. 2009; Demir et al. 2008; Bowers et al. 2006; Tyrrell et al. 2002; Greenfield et al. 2008).

Heterosigma akashiwo is a globally distributed harmful alga (Li & Smayda 2000; Portune et al. 2009; O'Halloran et al. 2006; Kempton et al. 2008; Tyrrell et al. 2002) that has been implicated in fish killing blooms in China (Tseng et al. 1993), Japan (Honjo 1992), New Zealand (Chang et al. 1990), South Africa (Bates et al. 2004) and estuaries on the east (Kempton et al. 2008) and west (Rensel et al. 2010) coasts of the United States. Although both qPCR (Coyne et al., 2005; Handy et al., 2006; Bowers et al., 2006; Demir et al., 2008; Portune et al., 2009) and SHA (Tyrrell et al. 2002; Tyrrell et al. 2001; Greenfield et al. 2006; Greenfield et al. 2008) have been developed and independently validated for this HAB species, direct comparison

of these methods has only recently been carried out (Doll et al. 2014). In this recent study, Doll and co-authors directly compared the accuracy and sensitivity of each method for enumeration of *Heterosigma akashiwo* over a range of cell concentrations. In addition, several strains of *H. akashiwo* representing various geographic origins were assessed using qPCR and SHA, with results showing a high degree of correlation between methods. These results also highlighted the capabilities and limitations of each method. For example, qPCR accurately enumerated cells over a wide range of cell concentrations but was less able to distinguish differences in small (~2-fold) changes in cell abundance. By comparison, SHA was capable of detecting small changes in cell concentrations, particularly at pre-bloom levels, but became oversaturated at higher levels of cell abundance (Doll et al. 2014).

The physiological status of the cell may also affect the accuracy of qPCR and SHA to enumerate cell abundances (e.g. Miller et al., 2002; Tyrrell et al., 2002; Haywood et al., 2007; Dittami and Edvardsen, 2012), but rigorous comparisons between these methods with respect to physiological status of HAB species have not been conducted. Changes in growth rate during bloom progression, for example, are likely to impact both DNA (Berdalet et al. 1992) and rRNA content (Ayers et al. 2005), and can contribute to an overestimation of cell abundance during exponential growth compared to stationary phase when using SHA (Tyrrell et al. 2001; Dittami & Edvardsen 2012). Diel changes in the cell cycle are also accompanied by changes in cellular DNA and rRNA content (Zachleder & Šetlík 1988; Berdalet et al. 1992). In *Heterosigma akashiwo*, replication of DNA occurs during the daylight (Satoh et al., 1987; Lee et al., 2012; Tobin et al. 2013), suggesting that enumeration of cell densities from samples collected during the light and dark cycles may yield different results by

either qPCR or SHA. Finally, nutrient stress can affect both growth rates and rRNA synthesis. In photosynthetic organisms, RNA is a major source of non-storage phosphorus (Raven 2013), and the concentrations of rRNA have been shown to decrease under phosphorus limitation in a number of phytoplankton species (Flynn et al. 2010; Elser et al. 2000; Elser et al. 2003). Nitrogen limitation, on the other hand has a direct impact on protein content, which can result in lowered growth rates and adversely affecting rRNA content per cell (Rhee 1978; Miller et al. 2002; Dittami & Edvardsen 2012; Sterner & Elser 2002). Although this has been demonstrated for *Heterosigma akashiwo* (e.g. Blanco et al., 2013), the effect of nutrient stress on DNA-based analysis such as qPCR have not been investigated for this species.

The objective of this study was to examine the potential effects of physiological status on the accuracy of qPCR compared to SHA. This research extends the study of Doll et al. (2014), by directly comparing qPCR and SHA methods for enumerating cell density with respect to (1) diel cycle, (2) growth phase, and (3) macronutrient (nitrogen and phosphorus) stress, using *H. akashiwo* as a model organism. Results of this study are broadly applicable to research and monitoring efforts for *Heterosigma akashiwo* and other HAB species.

4.3 Material and Methods

4.3.1 Culture Conditions

Heterosigma akashiwo, Center for Applied Aquatic Ecology (CAAE) strain 1663, previously isolated from an estuary in Hilton Head, South Carolina, USA (32.18N, 80.74W), was used for all experiments. Batch cultures of *H. akashiwo* were grown in 500 mL *f*/2 medium (-Si) at a salinity of 25 (Guillard & Ryther 1962).

Cultures were kept at 25 °C with 140 µE m^{-2} s^{-1} irradiance on a 12:12 hour light:dark cycle. For all experiments, cell densities were determined from replicate (5-9) counts using a light microscope and a Sedgewick-Rafter chamber, as a reference for results produced by qPCR and SHA according to previously-described methods (Greenfield et al. 2008; Doll et al. 2014). The Sedgewick-Rafter chamber detects lower concentrations of cells and replicate counts have smaller deviations than either a Palmer-Malony slide or a hemocytometer (Godhe et al. 2007).

4.3.2 Cellular Homogenization

For each experiment described below, cultures were filtered using a gentle vacuum (380 mmHg) onto 25 mm, 0.65 µm pore size hydrophilic Durapore filters (Millipore) with a minimum of 10 filters per sample. Filters were immediately placed into 2 mL cryovials (Nalgene, Rochester, NY USA), sample facing inward, and then stored in liquid nitrogen until processing. For direct comparison of qPCR and SHA, a single cellular homogenate was generated then split for use in both assays as described in (Doll et al. 2014). Frozen filters (n=5) were briefly thawed, then incubated with 2 mL of 0.2 µm filtered lysis buffer containing guanidinium thiocyanate (3 M, pH 8.9, Saigene Biotech Corporation, Marina, CA USA) at 85 °C for five minutes (Goffredi et al. 2006). Homogenate within each cryovial was then combined and syringe-filtered through a 0.22 µm Millex filter (Fisher). A 2 mL aliquot of filtered homogenate was removed and stored at -80 °C until shipped overnight on dry ice to the University of Delaware (Lewes, DE USA) for qPCR analyses as described below. A second portion of the cellular homogenate (250 µL per sample well) was analyzed for SHA as described below at the University of South Carolina (Charleston, SC USA).

4.3.3 Growth Phase and Diel Cycle

Batch cultures (n=3) were sampled at the start of the light cycle over four growth phases (lag, exponential, stationary and decline, Fig. 4.1). Growth phases were determined by cell counts of batch culture as described above. At each phase, 40,000 cells from each replicate were collected by gentle vacuum onto 0.65 µm Durapore filter. Additional sampling occurred during exponential stage for comparison of changes during the diel cycle. Sampling for diel cycle began at the start of the light cycle (T_0), and additional samples were collected at 4, 8, 12 and 20 hours after T_0. Samples were collected, filtered and stored in liquid nitrogen as above.

4.3.4 Macronutrient Stress

To examine the effects of low levels of nitrogen (N) and phosphorus (P) on quantification of *H. akashiwo*, initial batch cultures were grown to exponential stage. A pre-treatment sample in nutrient replete *f*/2 medium (-Si, 883 µM $NaNO_3$ and 36.3 µM $NaH_2PO_4 \cdot 2H_2O$) consisting of ~60,000 cells from the batch culture was collected and used for establishment of cultures in low nitrogen (low N, 1:1 N:P, 36.3 µM $NaNO_3$ and 36.3 µM $NaH_2PO_4 \cdot 2H_2O$) or low phosphorus (low P, 100:1 N:P, 883 µM $NaNO_3$ and 8.83 µM $NaH_2PO_4 \cdot 2H_2O$) media (n=3). Control cultures were nutrient replete in *f*/2 (–Si) seawater medium. Batch cultures were grown to exponential phase in low N or P media or nutrient-replete *f*/2 (control) medium and transferred a second time to minimize carryover from nutrient replete conditions. Cell counts were conducted as above, and acclimatized cultures were sampled during exponential phase at the start of the light cycle for qPCR and SHA analyses. Sample volumes containing 40,000 cells were collected, filtered and stored in liquid nitrogen as described above.

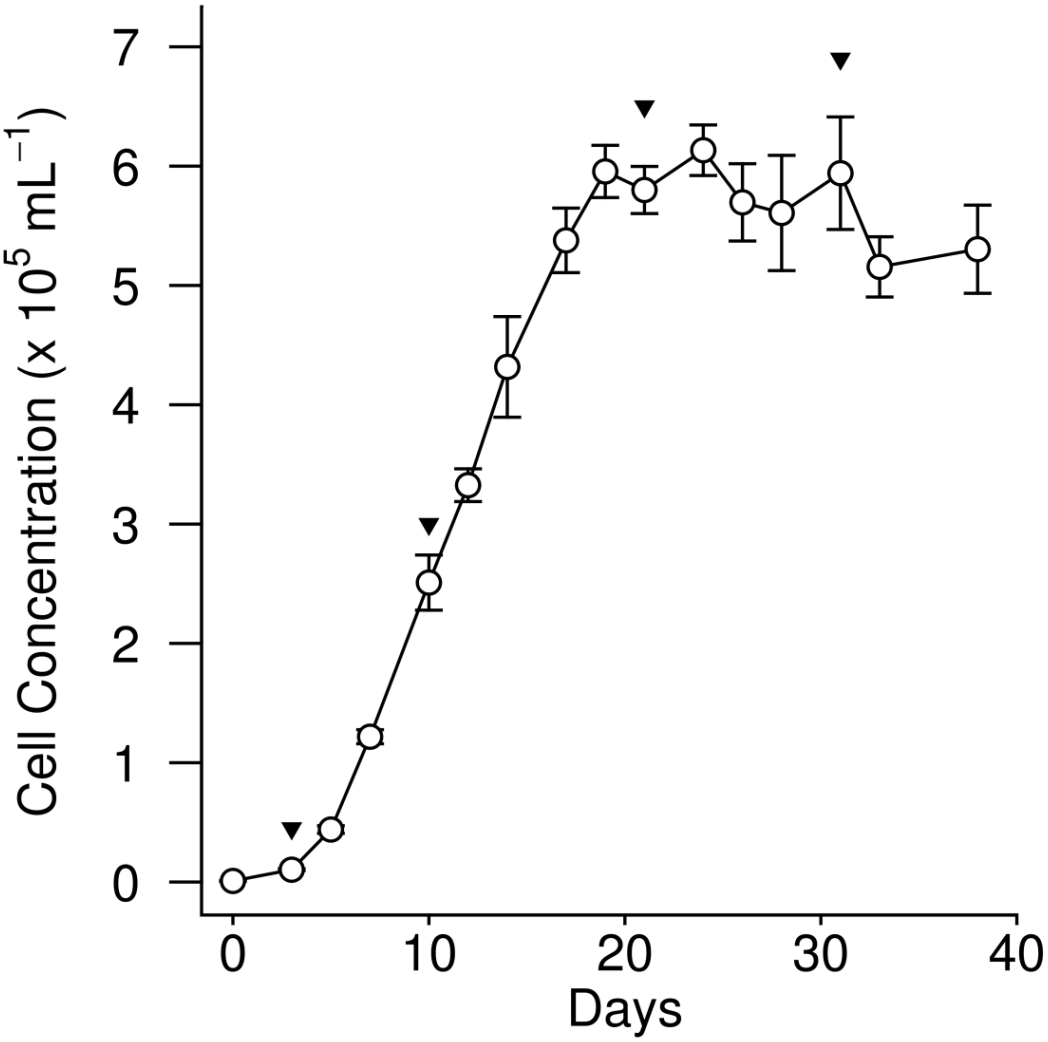

Figure 4.1. Growth curve of *Heterosigma akashiwo*. Arrow heads (▼) represent collection dates for growth phase experiment: lag phase, Day 3; exponential phase, Day 10; stationary phase, Day 22; and decline phase, Day 31.

The physiological status of *H. akashiwo* was assessed in tandem with sampling for qPCR and SHA analyses. The efficiency of photosystem II, Fv/Fm, was measured as an indicator of stress (Parkhill et al. 2001) using a Phyto-PAM fluorometer (Walz, Germany) after a 25 minute dark adaptation. Chlorophyll *a* (chl *a*) concentrations were measured after extraction with 90% acetone (Arar & Collins 1992). In addition, samples for particulate carbon (PC) and nitrogen (PN) analysis were collected to detect changes in C:N. Culture (1 mL) was concentrated onto a pre-combusted GFF and stored desiccated until analysis using a Costech Elemental Combustion System CHNS-O 4010 (Costech Analytical Technologies Inc., Valencia CA USA). An aliquot of culture was syringe-filtered through a pre-combusted GFF for dissolved nutrient (N and P) concentrations performed using a Lachat Quik-Chem-8000 autoanalyzer (Loveland, CO USA, Johnson and Petty, 1983; Hansen and Koroleff, 1999). An aliquot of 2 mL was collected in triplicate from each culture for analysis of protein and carbohydrate content. Cell pellets were obtained by centrifuging for 5 minutes at 10,600 x *g*. The supernatant was carefully removed and cell pellets were frozen immediately and stored at -80 °C until shipping over night for analyses at the University of Delaware. Proteins were extracted from pelleted algal cells by sonication in KPi buffer (200 mM potassium phosphate monobasic and 140 mM potassium hydroxide, pH 7.9). Total protein content was measured using the BCA Protein Assay Kit (Pierce, Rockford, IL USA) according to manufacturer instructions. For total carbohydrate content, algal cells were digested in phenol and sulfuric acid (final concentration 0.66% and 13 M respectively). Samples were incubated in a room temperature water bath for 30 minutes and absorbance was read at 482 nm on a FLUOstar Omega (MG LABTECH GmbH, Germany; DuBois et al., 1956).

Concentrations of each constituent (protein and carbohydrate) were determined by linear regression analysis.

4.3.5 DNA Extraction

Prior to extraction of DNA for qPCR analysis, 50 ng mL^{-1} (2µL) of pGEM plasmid (pGEM-3Z Vector, Promega, Fitchsburg, WI USA) was added to samples as an internal standard (Coyne et al. 2005). To provide concentrations of background DNA comparable to those found in environmental samples, 5 µg mL^{-1} of sheared herring sperm (Invitrogen, Grand Island, NY USA) was also added. DNA was extracted from each cellular homogenate using a DNeasy Plant Mini Kit (Qiagen, Germantown, MD USA), eluted in 100 µL of elution buffer and diluted 1:5 with LoTE (3 mM Tris-HCl, 0.2 mM EDTA, pH 7.5) prior to qPCR analysis.

4.3.6 qPCR

qPCR was performed using an Applied Biosystems 7500 Real Time PCR System (Applied Biosystems, Grand Island, NY USA). Abundances of pGEM and *H. akashiwo* 18S rDNA abundance were determined in separate qPCR reactions. DNA was amplified in 10 µL reactions for each target sequence, consisting of 5 µL of TaqMan Universal Master Mix (Applied Biosystems), 1 µL diluted template and appropriate concentrations for primers and probe. For amplification of *H. akashiwo* rDNA gene, final concentrations were 0.9 µM of each primer (Hs 1350F and Hs 1705R; Coyne et al., 2005) and 50 nM Hs Probe (Coyne et al. 2005), modified with a 5'-HEX reporter dye, an internal ZEN quencher and 3'-IBFQ1 quencher molecule (Integrated DNA Technologies, Coralville, IA USA). For amplification of the internal standard pGEM plasmid, final concentrations were 0.9 µM of each primer (M13F and

pGEMR; Coyne et al., 2005), and 0.2 µM pGEM Probe (Coyne et al. 2005). Cycling parameters for amplification of each target gene consisted of 2 min of 50 °C, 10 min at 95 °C for activation of the polymerase, followed by 40 cycles of 15s at 95 °C, 30 s at 56 °C, and 1 min at 72 °C. Relative abundance of *H. akashiwo* was determined using a standard curve generated from *H. akashiwo* 18S rRNA plasmid and normalized to the relative abundance of pGEM in each sample. Results of each analysis were then normalized to a reference sample for ease of comparison between methods.

4.3.7 SHA

Detailed methodologies for using SHA with a 96-well plate and robotic processor are described elsewhere (Goffredi et al. 2006). Briefly, homogenized samples (250 µL) were loaded in triplicate to pre-made 96-well plates (Saigene Biotech Corporation) containing the capture probe Het 1 and signal probe Raph BI DIG (Dioxygenin; Tyrrell et al., 2001, 2002; Greenfield et al., 2008). Hybridization reactions were conducted in triplicate at 30 °C with biotinylated prongs (Saigene Biotech Corporation) on an Affirm robotic processor (Microprobe Corporation, Southbury, CT USA; Goffredi et al., 2006), and lysis buffer only was used as a control. When the reaction was complete, optical density was measured using a Synergy HT plate reader (Biotek, Winooski, VT USA), and results were recorded at 450 nm using Gen 5 software (Biotek). Results of each analysis were then normalized to a reference sample as above.

4.3.8 Statistics

Statistical comparisons were performed using the R statistical package (R Core Team 2012). Outliers were determined using the Dixon's Q test, with removal of

outliers if the p-value was < 0.05. Data from growth phase, diel cycle and nutrient stress experiments were examined for significant relationships between treatment groups using a 1-way ANOVA. A difference between procedures or treatments was considered significant if the p-value was < 0.05. If a significant relationship was detected, further examination was carried out using a Tukey honest significant differences (TukeyHSD) post-hoc test to determine relationships.

4.4 Results

4.4.1 Growth Phase

Results for qPCR and SHA analyses of samples containing the same number of cells collected from lag, exponential, stationary and decline growth phases were normalized to average results of the stationary phase cultures for comparison. qPCR results were not significantly different over the four collection periods (Fig. 4.2), due in part to the large standard deviations among replicate samples. Mean optical densities from SHA analyses were not significantly different between lag and exponential phases but were significantly different ($p < 0.001$) for all other comparisons. For SHA analysis, calculated cell densities (expressed as relative rRNA content) during lag and exponential phase growth were 3.1 and 3.3 times greater, respectively, than stationary phase for SHA analysis, while cultures in stationary phase were 1.7 times greater than that of decline phase cultures.

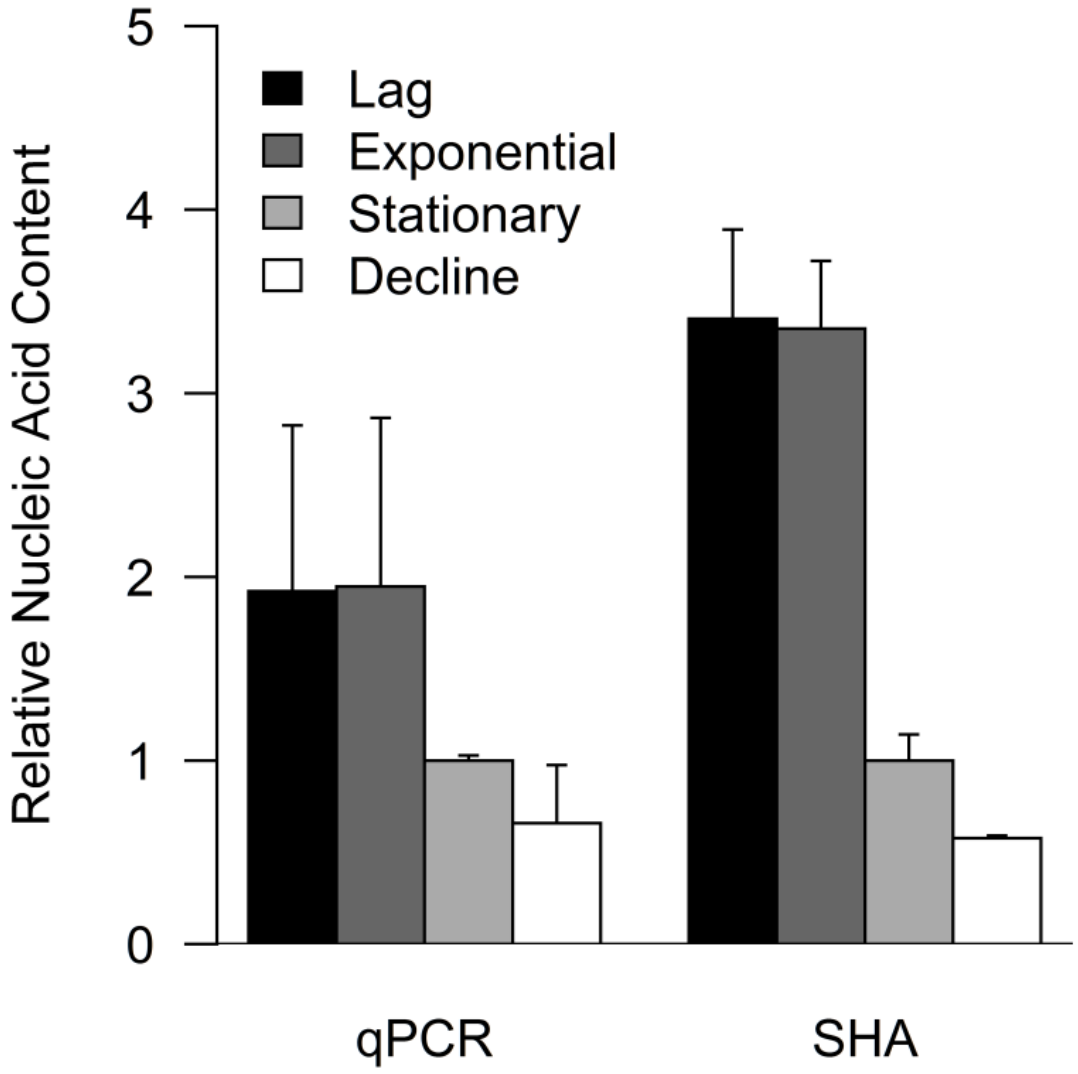

Figure 4.2 qPCR and SHA analysis during growth of *Heterosigma akashiwo*. Results were normalized to Stationary phase for ease of comparison. Error bars represent one standard deviation.

4.4.2 Diel Cycle

qPCR and SHA results were normalized to results at T_0 for the diel cycle experiment (Fig. 4.3). Results for qPCR analysis were not significantly different between sampling time points. Cell abundance as determined by SHA analysis was significantly ($p < 0.001$) between results obtained at T_0 and T_8, T_8 and T_{12}, and T_8 and T_{20}. Calculated cell densities during T_0, T_{12}, and T_{20} were 1.4, 1.5 and 1.3 times greater than cell densities at T_8.

4.4.3 Macronutrient Stress

Nutrient concentrations for low N and P cultures and control cultures are shown in Table 4.1. Several additional measurements were used to evaluate physiological status. Fv/Fm measures the quantum yield efficiency of photosystem II and has been previously shown to indicate physiological status of phytoplankton in natural and cultured samples (Jakob et al. 2005). In the current study, Fv/Fm was significantly lower ($p < 0.05$) in low N cultures compared to nutrient replete conditions (Table 4.2). Chl *a* concentrations and protein content were lower in low N and P cultures, but only low N cultures were significantly lower ($p < 0.05$) than nutrient replete conditions (Table 4.3). Carbohydrate content for low N cultures was significantly greater ($p < 0.001$) than controls, with 9.4 times more carbohydrates than nutrient replete conditions, whereas low P cultures were not significantly different than controls. Finally, pg N $cell^{-1}$ were significantly higher ($p < 0.001$) in low P cultures than replete conditions (Table 4.3) and pg C $cell^{-1}$ were significantly higher in both low N and P cultures ($p < 0.001$ and $p < 0.05$ respectively) when compared to replete cultures (Table 4.3). However, the C:N ratio of low P cultures was not significantly different from nutrient replete cultures.

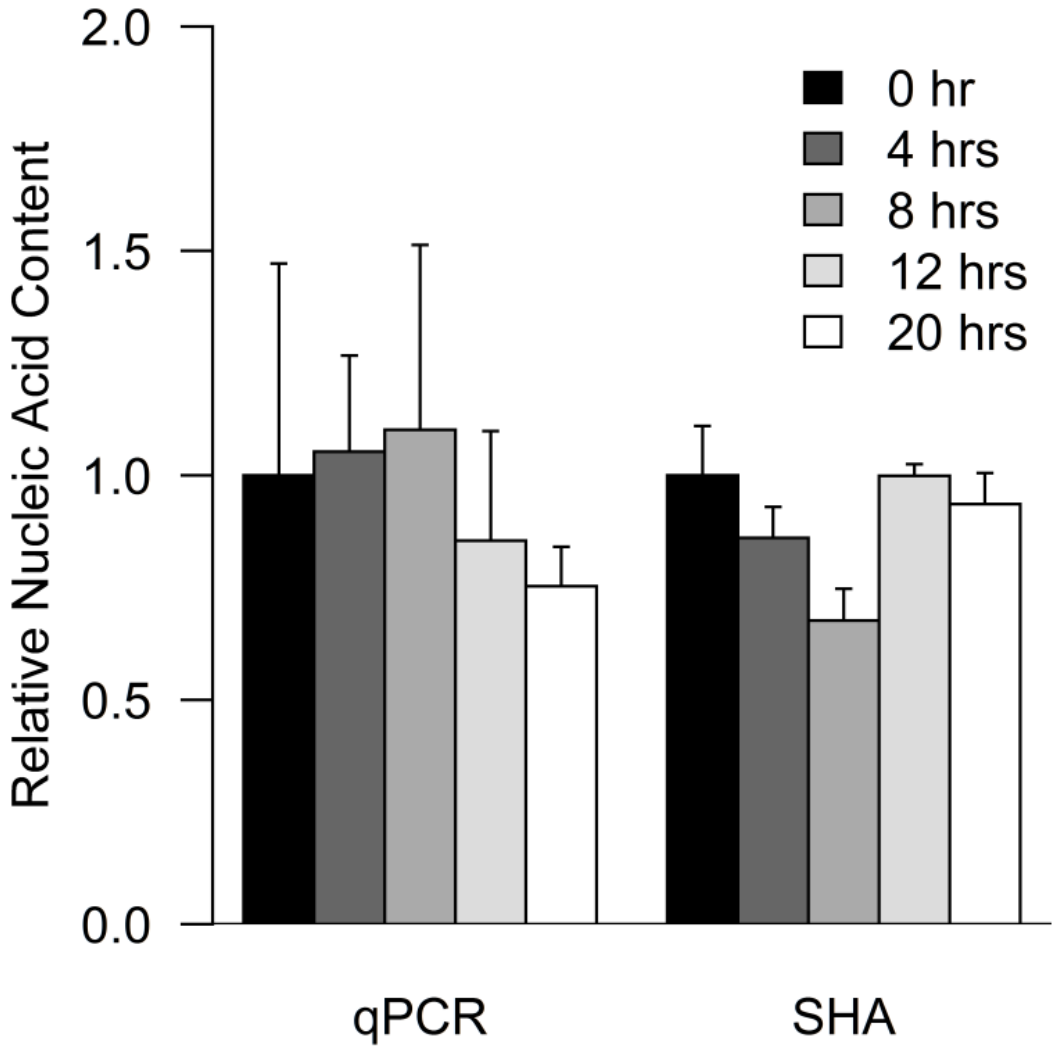

Figure 4.3 qPCR and SHA analysis during the diel cycle for *Heterosigma akashiwo*. Results were normalized to T_0 (lights on). Error bars represent one standard deviation.

Results of qPCR and SHA analyses were normalized to nutrient replete (control) samples (Fig. 4.4). qPCR results for low N cultures were significantly lower ($p < 0.05$) than nutrient replete (control) cultures, which were 1.98 times greater than low N cultures. Similar results were obtained from SHA, where replete cultures were 1.36 times greater than the low N cultures.

4.5 Discussion

In this study we examined the effects of growth phase, diel cycle, and macronutrient stress on quantification of *Heterosigma akashiwo* by qPCR and SHA in order to determine whether physiological factors may contribute to variability in results obtained by these methods. Ribosomal RNA sequences typically contain conserved and variable regions that allow for differentiation of species (Diaz et al. 2010), and both 18S rRNA and its gene sequence (rDNA) within the genome are abundant in eukaryotes, making this an ideal target for molecular methods. However, rDNA copy number within the cell changes during cell division (due to genome duplication), which may affect qPCR results during periods of rapid growth. Cellular content of 18S rRNA may also vary over the diel cycle (Berdalet et al. 1992) and can be affected by nutrient stress (Vrede et al. 2004), potentially impacting the accuracy of SHA results.

Both SHA and qPCR methods have been used to enumerate *H. akashiwo* in laboratory culture experiments (Tyrrell et al. 2001; Tyrrell et al. 2002; Bowers et al. 2006; Handy et al. 2006; Handy et al. 2008; Greenfield et al. 2008), and in field samples (Ayers et al. 2005; Coyne et al. 2005; Handy et al. 2005; Handy et al. 2008; Demir et al. 2008; Portune et al. 2009; Ryan et al. 2011; Greenfield et al. 2008), but

Table 4.1 Nutrient concentrations after transfer during the nutrient-stress experiment. Sampling occurred during exponential phase growth.

Treatment	Nitrite (µM)	Nitrate (µM)	Orthophosphate (µM)	Ammonium (µM)	N:P
Control	0.64 ± 0.01	774 ± 95	25.95 ± 0.66	4.01 ± 0.53	30.1 ± 2.6
Low N	0.33 ± 0.03	6.76 ± 11.40	38.60 ± 5.31	2.29 ± 0.52	0.22 ± 0.26
Low P	0.74 ± 0.25	820 ± 27.4	1.85 ± 2.05	2.95 ± 0.18	892 ± 617

Table 4.2 Fv/Fm and chl *a* content for nutrient-stress experiments. Sampling occurred during exponential phase.

Treatment	Fv/Fm	Chl *a* (pg cell^{-1})
Control	0.65 ± 0.01	$5.05 \times 10^{-6} \pm 0.09 \times 10^{-6}$
Low N	0.59 ± 0.02*	$3.51 \times 10^{-6} \pm 0.59 \times 10^{-6}$*
Low P	0.67 ± 0.01	$3.87 \times 10^{-6} \pm 0.65 \times 10^{-6}$

Significance levels are indicated as follows: *, $p < 0.05$.

Table 4.3 Protein (pg cell^{-1}), carbohydrate content (pg cell^{-1}), protein:carbohydrate ratio, N and C (pg cell^{-1}) and C:N ratio for nutrient-stress experiment. Sampling occurred during exponential phase.

Treatment	Proteins	Carbohydrates	Protein:Carbohydrate	N	C	C:N Ratio
Control	48.66 ± 6.47	12.10 ± 9.51	3.99 ± 2.31	52.64 ± 4.76	177.91 ± 13.99	3.95 ± 0.20
Low N	28.76 ± 9.85*	114.5 ± 101.2**	0.13 ± 0.10	NA	512.85 ± 192.40**	NA
Low P	39.04 ± 1.81	16.94 ± 10.02	2.51 ± 0.47	79.55 ± 6.49**	240.64 ± 43.07*	3.52 ± 0.48

Significance levels are indicated as follows: *, $p < 0.05$; **, $p < 0.01$. NA represents below detection limits

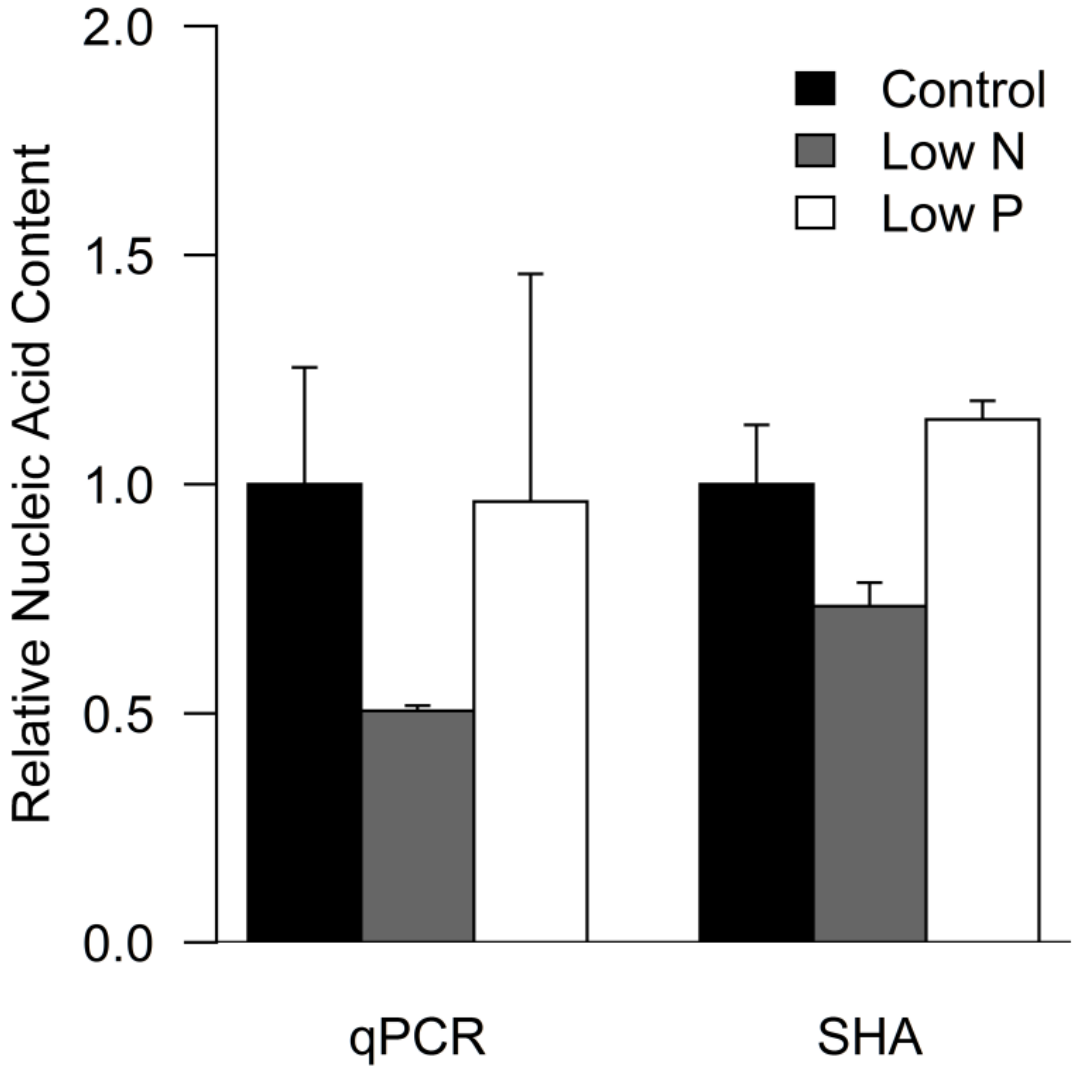

Figure 4.4 qPCR and SHA analysis for *Heterosigma akashiwo* cultures during low nutrient concentration conditions. Results were normalized to nutrient replete (control) cultures. Error bars represent one standard deviation.

rigorous comparisons between these two methods have never been carried out across a range of physiological conditions. In this study, the number of cells filtered for analysis at each sampling point was kept constant to minimize errors due to extraction efficiencies or range of detection. Results were then normalized to a reference sample to facilitate comparison between the two methods. Since the same number of cells was filtered for each time point or treatment, the results presented here are indicative of the relative nucleic acid content of DNA (for qPCR) or rRNA (for SHA) per cell.

In general, standard deviations between replicate samples were greater for qPCR compared to SHA, indicating a greater level of precision by SHA. A number of factors may contribute to errors by each of these methods. Quantification of nucleic acid content by qPCR can be influenced by the quantity and quality of DNA extracted (Boström & Simu 2004; Coyne et al. 2005). Inhibitory compounds that co-precipitated with DNA during extraction may also affect the efficiency of the PCR reaction. Addition of exogenous reference standard DNA to the extraction buffer can control for variability in extraction and amplification efficiencies, as both target and reference standard DNA are equally affected (Coyne et al. 2005). In Coyne et al. (2005), the reference standard plasmid pGEM was added to the bulk extraction buffer, resulting in a constant concentration of the reference standard between samples. In this study, we found that addition of pGEM to the buffer interfered with SHA analysis (data not shown), requiring us to add the plasmid to each split sample before extraction for qPCR analysis. Errors in pipetting when adding the exogenous reference standard to individual samples, however, may have contributed to greater standard deviation between replicates when analyzed by qPCR. In addition, PCR amplification is exponential, so that small differences in reference standard DNA content can result in

greater standard deviations between replicates. In contrast, SHA measures RNA content within the lysate and does not require further amplification of the target for detection and quantification, resulting in lower standard deviation between replicates. While the results obtained by SHA showed greater precision, Doll et al. (2014) demonstrated that qPCR had a greater range and sensitivity of detection compared to SHA without adjusting sample volume or diluting the homogenate.

For the growth phase study, results obtained by both qPCR and SHA were not significantly different between earlier growth stages for either method (Fig. 4.2). The trend to higher nucleic acid content during the early growth stages for qPCR analysis may be attributed to an increase in DNA content when a greater proportion of cells were undergoing cell division. rRNA content has also been shown to be positively related to specific growth rate (Vrede et al. 2004; Elser et al. 2000; Sterner & Elser 2002), which would contribute to the greater signal by SHA during lag and exponential growth phases compared to stationary phase. These results are consistent with those of Tyrrell et al. (2001) who previously demonstrated using SHA that *Heterosigma akashiwo* rRNA content declined by a factor of approximately 2 between exponential and stationary stages. A decline in SHA signal associated with growth phase was also noted for *Karenia* spp. (Haywood et al. 2007), where the variability in results was attributed to cell lysis of unhealthy cells during filtration, or the possible inhibition of rRNA synthesis during senescence.

Previous research demonstrated that the diel cell cycle in *Heterosigma akashiwo* is light dependent, with DNA synthesis occurring during the light cycle, and cell division occurring at night (Satoh et al. 1987; Lee et al. 2012; Kohata & Watanabe 1986). In the data presented here, qPCR and SHA data generated over a diel cycle was

normalized to T_0 (lights on). Although results obtained by qPCR were not significantly different over the course of the day, the trend toward higher nucleic acid content during the light phase may be due to the higher proportion of cells that were synthesizing DNA (Lee et al. 2012). A discrepancy in qPCR results over a diel period has also been noted in other species. In the dinoflagellate *Lingulodinium polyedrum*, for example, cell division caused an asynchrony between microscopic counts and abundances determined by qPCR (Moorthi et al. 2006). In contrast, results obtained by SHA showed a decrease in rRNA during the daylight which returned to levels similar to the initial time point at T_{12} and T_{20} (Fig. 4.3). This may be due to circadian patterns of transcription, with greater rRNA content required at the beginning of light and dark phases (T_0 and T_{12}). A similar pattern of diel variability in rRNA content was observed in *Synechococcus* cultures entrained in a 12:12 light:dark cycle (Lepp & Schmidt 1998). In this case, a decrease in rRNA content during daylight hours due to the circadian control of transcription was not considered plausible, because of the large number of genes that were differentially expressed during the light compared to dark phases. Instead, the diel pattern was attributed to a rate of cell division that exceeded rRNA transcription. Results presented here agree with the pattern observed in *Synechococcus*, but not with the explanation. Instead, rRNA synthesis in *Heterosigma* appears to keep pace with cell division, so that rRNA levels at T_{12} and T_{20} are similar to levels at T_0. The decrease in rRNA content during the day may be a consequence of cells managing internal resources. *Heterosigma akashiwo* has a very large nuclear genome (~2.9 pg DNA cell $^{-1}$; Cattolico et al., 1976), suggesting that shared cellular resources such as P, that are typically incorporated into RNA may be diverted to dNTP synthesis, resulting in lower rRNA content.

Nitrogen (N) and phosphorus (P) concentrations are potential limiting nutrients for primary producers in aquatic environments (Beardall et al. 2001), and their concentrations can vary substantially over the course of a bloom. Low concentrations of N and/or P can have an effect on cellular DNA and rRNA content. Several studies, for example, demonstrate that regulation of rRNA synthesis is coupled to nutrient availability in yeast and mammalian cells (reviwed by Grummt 2003). Although little is known about the molecular regulation of rRNA synthesis in phytoplankton, several studies have shown a relationship between N and P limitation and decreases in rRNA content in phytoplankton species. In *Alexandrium fundyense*, for example, N and P limitation resulted in a 4-fold decrease of rRNA fluorescence intensity when compared to nutrient replete conditions (Anderson et al. 1999). Similar results were noted in a recent study on *Heterosigma akashiwo* (Blanco et al. 2013), where N depletion significantly lowered cellular rRNA content after 72 hours when compared to controls. N and P are also required for DNA synthesis, and limitation of either or both of these nutrients will result in lower growth and average DNA content per cell (Berdalet et al. 1996). In work presented here, we evaluated cell status at N:P ratios that deviated considerably from the Redfield ratio of 16:1 as a metric for assessing whether cells were stressed by N or P availability. In this study, Fv/Fm values for cultures with low concentrations of N were significantly lower when compared to nutrient replete cultures (Table 4.2). Chl *a* measurements have often been used as a metric of cell density, but chl *a* content per cell can vary with nutrient status (Moore et al. 2008; Geider et al. 1993; Geider & La Roche 2002). In this study, chl *a* content of cells in low N cultures of *H. akashiwo* was significantly lower than controls (Table 4.2). Finally, protein to carbohydrate ratios may be used as indicators of nutrient limitation

(Pick 1987), with ratios > 1.2 indicative of no deficiency while ratios < 0.7 as an indicator of extreme deficiency. In our study, the protein to carbohydrate ratio of low N cultures was 0.13, confirming that N stress had a significant effect on carbon partitioning in *Heterosigma* (Table 4.3). There was no indication from the protein to carbohydrate ratios that the low P cultures were under P-stress. The half-saturation constant (K_s) for growth on orthophosphate for other strains of *H. akashiwo* (Zhang et al. 2006) were lower than the concentrations used here, suggesting that these cultures may not have been truly P limited. Likewise, cellular carbon to nitrogen ratios were not significantly different for low P cultures compared to controls whereas particulate N in low N cultures was below the level of detection (Table 4.3).

The level of nutrient stress as demonstrated by Fv/Fm, C:N and carbohydrate:protein ratios proved to be a good indicator for qPCR and SHA results. Calculated cell abundances in low N cultures were significantly lower than controls for both qPCR and SHA analyses, whereas results for low P cultures were similar to nutrient replete conditions. For qPCR, the decrease in nucleic acid content under low N conditions was likely due to decreased growth rates, as noted above. It was surprising, however, that SHA results were more significantly affected by low N concentrations than low P concentrations. RNA is a major source of non-storage P in photosynthetic organisms, and therefore a decline in RNA content would be expected under low or limiting P conditions (Raven 2013). The data presented here do not demonstrate this, suggesting further that cultures were not truly P-stressed. Instead, it was likely that decreased rRNA under low N conditions was a function of decreased growth, as proposed by the Growth Rate Hypothesis (GRH; Sterner & Elser 2002). GRH suggests that rRNA content is linked to cellular requirements for protein

synthesis, which is reduced during periods of low growth (Elser et al. 2000). While there is some controversy about that application of GRH to phytoplankton taxa (Flynn et al. 2010), the general assumption that decreases in rRNA content under N-stress are a consequence of low growth rate is supported by a number of investigations. Several studies, (e.g. Rhee 1978; Worden & Binder 2003) for example, have demonstrated that RNA is reflective of growth rate in phytoplankton. Zachleder & Šetlík (1988), also demonstrated a decline in the abundance of RNA for nitrate starved cells of the freshwater alga *Scenedesmus quadricauda*. In *Hymenomonas carterae* and *Thalassiosira weissflogii*, RNA content during nitrogen limitation decreased to one third of replete conditions (Olson et al. 1986). Finally, Berdalet et al. (1994) showed that N starvation led to parallel decreases in RNA and protein concentrations in *Heterocapsa* sp..

Previous results examining qPCR and SHA methods individually indicated that these methods could be used for accurate identification and quantification of *Heterosigma akashiwo* in laboratory and field samples (Handy et al. 2006; Handy et al. 2008; Tyrrell et al. 2002; Greenfield et al. 2008; Tyrrell et al. 2001; Ryan et al. 2011). However, this investigation demonstrates that growth stage, nutrient stress, and cell cycle may also impact results of molecular analysis, suggesting that resource managers should consider these factors when evaluating results from either method. Our results suggest that "calibrator" samples, consisting of a sample collected under similar conditions and for which a cell count has been done, may be necessary to accurately ground-truth molecular methods (Coyne et al. 2005). However, exact cell abundances may not be required by resource managers, since often the 2 – 3 fold difference in cell abundances shown here may be within acceptable limits of

variability. Batch cultures used here were not exposed to environmental conditions such as changes in temperature or nutrient flux, or inter- or intraspecific competition for resources, which may also impact results. Future work will examine these factors using field collected samples in order to determine their effects on qPCR and SHA results.

Chapter 5

CONCLUSIONS

The increasing frequency of harmful algal blooms (HABs) in the marine environment has the potential to greatly impact societal and environmental costs for the future. This apparent increase of HABs may be caused by several factors: anthropogenic eutrophication of coastal waters, increased aquaculture or the shift of focus to HABs in the scientific community. Understanding the biology and ecology of bloom dynamics in the environment will lead to better monitoring and potential mitigation strategies. Furthermore, understanding the dynamics of HAB-associated bacterial communities will lead to a better understanding of factors that influence phytoplankton ecology and impact bloom progression by stimulating or inhibiting growth. However, little is known about bacteria:algal interactions in the marine environment or their influence on the microbial community as a whole. A requirement for monitoring of HABs is an accurate determination of both species and abundance. Development of molecular techniques for both enumeration and species detection is vital in managing resource practices in the coastal environment. This dissertation adds to this understanding of interaction between the potential pathogenic bacteria species *Vibrio* and algal groups in Delaware's inland bays, as well as examining the effects of physiological status on enumeration of HAB species using two molecular methods. Results of this research are broadly applicable to research and monitoring of *Vibrio* and harmful algae in the Mid-Atlantic region.

Chapter two investigated the community and species-specific interactions between *Vibrio* sp. and three algal classes (diatoms, dinoflagellates, and raphidophytes) during naturally occurring blooms in Delaware's inland bays (DIB). Total relative *Vibrio* abundance was strongly correlated with all three algal class abundances. Previous research has noted correlations between total *Vibrio* spp. abundance and phytoplankton abundance (Takemura et al. 2014 and references therein), suggesting growth of *Vibrio* may be enhanced by exudates produced during algal blooms and/or this association may provide *Vibrio* a refuge from predation. However, few studies have examined the changes at the community level and advantages of potential refuge from grazing that association with algal species may confer. The overarching tren0d in these experiments demonstrated a close association between diatoms and raphidophytes and that this association may be species-specific. Moreover, a novel outcome of this research demonstrated that changes in the *Vibrio* community suggest an association of several *Vibrio* species with *H. akashiwo* despite an increased grazing pressure. Overall, chapter two revealed important baseline information on potential species-specific dynamics between *Vibrio* and algal classes in the DIB. These results provide an important context for the results presented in chapter 3 of this dissertation.

Chapter 3 built on the results of chapter 2 to examine the dynamics between *Heterosigma akashiwo* and *Vibrio cholerae* in a laboratory setting. Building on previous research showing a strong correlation between *H. akashiwo* and *Vibrio* species, including an increase in abundance of *Vibrio* during grazing experiments, this dissertation presented one of the first transcriptomes for a raphidophyte species. As

organisms are never alone in their environment, the presence of bacteria may affect the cellular mechanisms within the cell (see Moustafa et al. 2010). Thus, understanding how *Heterosigma* responds to the presence of *V. cholerae* can give insight into how *Heterosigma* responds to changes in its environment and interactions with the associated microbial community. The overall trends in this research demonstrated a potential increase in extracellular polymer substances produced by *Heterosigma*. This may increase the toxicity of this species. For example, extracellular organics isolated from *Heterosigma* were demonstrated to lyse erythrocyte cells (Ling & Trick 2010). In addition, production of EPS by *Heterosigma* may change the swimming dynamics of *Heterosigma* by increasing sinking of the algal cells, resulting in increased toxicity (Powers et al. 2012). However, the marine environment is not occupied by a single species, thus the effects of *V. cholerae* by itself may not have the impacts on *Heterosigma* in the environment as what was observed in a laboratory setting. Furthermore, the concentration of cells inoculated in the laboratory setting may exceed those found in the natural environment.

Examination of the transcriptional response by *Heterosigma* will begin to give insight into the potential dynamics occurring during a bloom. Further research based on this transcriptome can examine changes in the cellular mechanisms over the course of a bloom and allow insight into the drivers of bloom dynamics of *Heterosigma*.

Chapter 4 examined the effects of physiological status on the enumeration of *Heterosigma akashiwo* on two molecular methods quantitative real-time PCR (qPCR) and sandwich hybridization assay (SHA). With an increase in sampling of the marine environment, the use of molecular techniques has increased over more traditional

techniques for identification and enumeration of potential harmful algal species. In recent years adoption of molecular techniques in the scientific and management realms has increased as increased as cost has decreased. However, physiological status has the potential to skew results determined by molecular techniques. Therefore understanding how such factors of physiological status as growth phase, diel cycle and macronutrient stress can affect enumeration by molecular techniques is required. To accomplish this, cellular homogenate was generated from the same number of cells and split for use between qPCR and SHA. A greater level of precision for SHA was observed when compared with qPCR. However, responses to growth phase or the diel cycle were indifferent for qPCR, while macronutrient stress under low N affected both equally. Overall, results suggest that cell cycle, growth stage and nutrient stress may impact enumeration with either molecular technique and should be considered when examining either option for environmental sample processing.

This dissertation examined the interactions between algal groups and *Vibrio* in Delaware's inland bays, as well as species-specific interactions between *Vibrio cholerae* and *Heterosigma akashiwo*. Furthermore, the effects of stress on *H. akashiwo* in regards to enumerating by either qPCR or SHA were also explored. Results of this work will lead to an increased knowledge of consequences in increased harmful algal blooms and their association with potential pathogenic *Vibrio*. Results will also increase our understanding of the influence of *Vibrio* on the cell physiology of *Heterosigma akashiwo* and the associated implications of those physiological changes within the bloom dynamics of *H. akashiwo*.

REFERENCES

Absalon, C., Van Dellen, K. & Watnick, P.I., 2011. A communal bacterial adhesin anchors biofilm and bystander cells to surfaces. *PLoS Pathogens*, 7(8), p.e1002210.

Adhikari, B.N. et al., 2013. Comparative genomics reveals insight into virulence strategies of plant pathogenic oomycetes. *PloS One*, 8(10), p.e75072.

Alavi, M. et al., 2001. Bacterial community associated with *Pfiesteria*-like dinoflagellate cultures. *Environmental Microbiology*, 3(6), pp.380–96.

Altschul, S.F. et al., 1990. Basic local alignment search tool. *Journal of Molecular Biology*, 215(3), pp.403–10.

Amin, S.A., Parker, M.S. & Armbrust, E.V., 2012. Interactions between diatoms and bacteria. *Microbiology and Molecular Biology Reviews*, 76(3), pp.667–84.

Anderson, D.M. et al., 1999. Detection of the toxic dinoflagellate *Alexandrium fundyense* (Dinophyceae) with oligonucleotide and antibody probes: variability in labeling intensity with physiological condition. *Journal of Phycology*, 35(4), pp.870–883.

Anderson, D.M. et al., 2008. Harmful algal blooms and eutrophication: Examining linkages from selected coastal regions of the United States. *Harmful algae*, 8(1), pp.39–53.

Anderson, D.M. et al., 2005. Identification and enumeration of *Alexandrium* spp. from the Gulf of Maine using molecular probes. *Deep Sea Research Part II*, 52(19-21), pp.2467–2490.

Anderson, D.M., 1995. Identification of harmful algal species using molecular probes: an emerging perspective. In *Harmful Marine Algal Blooms*. LAVOISIER, PARIS(FRANCE), pp. 3–13.

Anderson, D.M., Cembella, A.D. & Hallegraeff, G.M., 2012. Progress in Understanding Harmful Algal Blooms: Paradigm Shifts and New Technologies

for Research, Monitoring, and Management. *Annual Review of Marine Science*, 4(1), pp.143–176.

Apel, K. & Hirt, H., 2004. Reactive oxygen species: metabolism, oxidative stress, and signal transduction. *Annual Review of Plant Biology*, 55, pp.373–99.

Arar, E. & Collins, G., 1992. In vitro determination of chlorophyll a and phaeophytin a in marine and freshwater phytoplankton by fluorescence—USEPA Method 445.0. *USEPA Methods for Determination of Chemical Substances in Marine and Estuarine Environmental Samples. Cincinnati, OH*.

Armbrust, E.V. et al., 2004. The genome of the diatom *Thalassiosira pseudonana*: ecology, evolution, and metabolism. *Science*, 306(5693), pp.79–86.

Asplund, M.E. et al., 2011. Water column dynamics of *Vibrio* in relation to phytoplankton community composition and environmental conditions in a tropical coastal area. *Environmental Microbiology*, 13(10), pp.2738–51.

Ayers, K. et al., 2005. International accreditation of sandwich hybridisation assay format DNA probes for micro-algae. *New Zealand Journal of Marine and Freshwater Research*, 39, pp.1225–1231.

Bates, S.S. et al., 2004. Interaction between bacteria and the domoic-acid-producing diatom *Pseudo-nitzschia multiseries* (Hasle) Hasle; can bacteria produce domoic acid autonomously? *Harmful Algae*, 3(1), pp.11–20.

Beardall, J., Young, E. & Roberts, S., 2001. Approaches for determining phytoplankton nutrient limitation. *Aquatic Sciences*, 63, pp.44–69.

Beardsley, C. et al., 2003. Are Readily Culturable Bacteria in Coastal North Sea Waters Suppressed by Selective Grazing Mortality? *Applied and Environmental Microbiology*, 69(5), pp.2624–2630.

Berdalet, E., Latasa, M. & Estrada, M., 1994. Effects of nitrogen and phosphorus starvation on nucleic acid and protein content of *Heterocapsa* sp. *Journal of Plankton Research*, 16(4), pp.303–316.

Berdalet, E., Latasa, M. & Estrada, M., 1992. Variations in biochemical parameters of *Heterocapsa* sp. and *Olisthodiscus luteus* grown in 12:12 light:dark cycles I. Cell cycle and nucleic acid composition. *Hydrobiologia*, 238(1), pp.139–147.

Berdalet, E., Marrasé, C. & Estrada, M., 1996. Microbial community responses to nitrogen-and phosphorus-deficient nutrient inputs: microplankton dynamics and

biochemical characterization. *Journal of Plankton Research*, 18(9), pp.1627–1641.

Blackwell, K.D. & Oliver, J.D., 2008. The ecology of *Vibrio vulnificus*, *Vibrio cholerae*, and *Vibrio parahaemolyticus* in North Carolina estuaries. *Journal of Microbiology (Seoul, Korea)*, 46(2), pp.146–53.

Blanco, E.P. et al., 2013. Detection of *Heterosigma akashiwo* (Hada) using specific RNA probes: Variability of RNA content with environmental conditions. *Harmful Algae*, 24, pp.80–88.

Boeckmann, B. et al., 2005. Protein variety and functional diversity: Swiss-Prot annotation in its biological context. *Comptes Rendus Biologies*, 328(10-11), pp.882–99.

Bolger, A.M., Lohse, M. & Usadel, B., 2014. Trimmomatic: a flexible trimmer for Illumina sequence data. *Bioinformatics*, 30(15), pp.2114–2120.

Boström, K. & Simu, K., 2004. Optimization of DNA extraction for quantitative marine bacterioplankton community analysis. *Limnology and Oceanography: Methods*, (1988), pp.365–373.

Bowers, H.A. et al., 2006. Raphidophyceae [Chadefaud ex Silva] systematics and rapid identification: Sequence analyses and real-time PCR assays. *Journal of phycology*, 42(6), pp.1333–1348.

Bricker, S.B. et al., 2008. Effects of nutrient enrichment in the nation's estuaries: A decade of change. *Harmful Algae*, 8(1), pp.21–32.

Bruckner, C.G. et al., 2008. Bacteria associated with benthic diatoms from Lake Constance: phylogeny and influences on diatom growth and secretion of extracellular polymeric substances. *Applied and Environmental Microbiology*, 74(24), pp.7740–9.

Caron, D.A., 1987. Grazing of attached bacteria by heterotrophic microflagellates. *Microbial Ecology*, 13(3), pp.203–18.

Cattolico, R.A. et al., 2008. Chloroplast genome sequencing analysis of *Heterosigma akashiwo* CCMP452 (West Atlantic) and NIES293 (West Pacific) strains. *BMC Genomics*, 9, p.211.

Cattolico, R.A., Boothroyd, J.C. & Gibbs, S.P., 1976. Synchronous Growth and Plastid Replication in the Naturally Wall-less Alga *Olisthodiscus luteus*. *Plant Physiology*, 57(4), pp.497–503.

Chang, F.H., Anderson, C. & Boustead, N.C., 1990. First record of a *Heterosigma* (Raphidophyceae) bloom with associated mortality of cage-reared salmon in Big Glory Bay, New Zealand. *New Zealand Journal of Marine and Freshwater Research*, 24(4), pp.461–469.

Chi, Y.H. et al., 2013. Redox-dependent functional switching of plant proteins accompanying with their structural changes. *Frontiers in Plant Science*, 4(July), p.277.

Chin, W.-C. et al., 2004. Secretion in Unicellular Marine Phytoplankton: Demonstration of Regulated Exocytosis in Phaeocystis globosa. *Plant and Cell Physiology*, 45(5), pp.535–542.

Connell, L.B., 2002. Rapid identificationof marine algae (Raphidophyceae) using three-primer PCR amplification of nuclear internal transcribed spacer (ITS) regions from fresh and archived material. *Phycologia*, 41(1), pp.15–21.

Cottrell, M.T. & Kirchman, D.L., 2004. Single-cell analysis of bacterial growth, cell size, and community structure in the Delaware estuary. *Aquatic Microbial Ecology*, 34, pp.139–149.

Coyne, K.J. et al., 2001. Assessing temporal and spatial variability in *Pfiesteria piscicida* distributions using molecular probing techniques. *Aquatic Microbial Ecology*, 24, pp.275–285.

Coyne, K.J. et al., 2005. Improved quantitative real-time PCR assays for enumeration of harmful algal species in field samples using an exogenous DNA reference standard. *Limnology and Oceanography: Methods*, 3, pp.381–391.

Coyne, K.J., 2010. Nitrate reductase (NR1) sequence and expression in the harmful alga *Heterosigma akashiwo* (Raphidophyceae). *Journal of Phycology*, 46(1), pp.135–142.

Crosby, L.D. & Criddle, C.S., 2003. Understanding bias in microbial community analysis techniques due to rrn operon copy number heterogeneity. *BioTechniques*, 34(4), pp.790–4, 796, 798 passim.

Culman, S.W. et al., 2009. T-REX: software for the processing and analysis of T-RFLP data. *BMC Bioinformatics*, 10, p.171.

Culverhouse, P. et al., 2003. Do experts make mistakes? A comparison of human and machine identification of dinoflagellates. *Marine Ecology Progress Series*, 247, pp.17–25.

Dalmasso, A. et al., 2009. Development of a PCR Assay Targeting the rpoA Gene for the Screening of Vibrio Genus. *Food Analytical Methods*, 2(4), pp.317–324.

Dang, H. & Lovell, C.R., 2000. Bacterial primary colonization and early succession on surfaces in marine waters as determined by amplified rRNA gene restriction analysis and sequence analysis of 16S rRNA genes. *Applied and Environmental Microbiology*, 66(2), pp.467–75.

Davidson, K. et al., 2014. Anthropogenic nutrients and harmful algae in coastal waters. *Journal of Environmental Management*, 146C, pp.206–216.

Deeds, J. & Place, A., 2006. Sterol-specific membrane interactions with the toxins from *Karlodinium micrum* (Dinophyceae) — a strategy for self-protection? *African Journal of Marine Science*, 28(2), pp.421–425.

Demir, E. et al., 2008. Assessment of microzooplankton grazing on *Heterosigma akashiwo* using a species-specific approach combining quantitative real-time PCR (QPCR) and dilution methods. *Microbial Ecology*, 55(4), pp.583–94.

Demir-Hilton, E. et al., 2012. Description of *Viridilobus marinus* (Gen. et ep. nov.), a new raphidophye from Delaware's inland bays. *Journal of Phycology*, 48(5), pp.1220–1231.

Dempster, E.L. et al., 1999. Rapid DNA extraction from ferns for PCR-based analyses. *BioTechniques*, 27(1), pp.66–8.

Diaz, M.R. et al., 2010. Molecular detection of harmful algal blooms (HABs) using locked nucleic acids and bead array technology. *Limnology and Oceanography: Methods*, 8, pp.269–284.

Dickschat, J.S., 2010. Quorum sensing and bacterial biofilms. *Natural Product Reports*, 27(3), pp.343–69.

Dittami, S.M. et al., 2011. Mannitol in six autotrophic stramenopiles and *Micromonas*. *Plant Signaling & Behavior*, 6(8), pp.1237–9.

Dittami, S.M. & Edvardsen, B., 2012. Culture conditions influence cellular RNA content in ichthyotoxic flagellates of the genus *Pseudochattonella* (Dictyochophyceae). *Journal of Phycology*, 48(4), pp.1050–1055.

Doll, C. et al., 2014. Comparison of sandwich hybridization assay and quantitative PCR for the quantification of live and preserved cultures of *Heterosigma akashiwo* (Raphidophyceae). *Limnology and Oceanography: Methods*, 12(12), pp.230–243.

DuBois, M. et al., 1956. Colorimetric Method for Determination of Sugars and Related Substances. *Analytical Chemistry*, 28(3), pp.350–356.

Edgar, R.C., 2010. Search and clustering orders of magnitude faster than BLAST. *Bioinformatics*, 26(19), pp.2460–1.

Eiler, A. et al., 2007. Growth response of *Vibrio cholerae* and other *Vibrio* spp. to cyanobacterial dissolved organic matter and temperature in brackish water. *FEMS Microbiology Ecology*, 60(3), pp.411–8.

Eiler, A. & Bertilsson, S., 2006. Detection and quantification of *Vibrio* populations using denaturant gradient gel electrophoresis. *Journal of Microbiological Methods*, 67(2), pp.339–48.

Eiler, A., Johansson, M. & Bertilsson, S., 2006. Environmental influences on *Vibrio* populations in northern temperate and boreal coastal waters (Baltic and Skagerrak Seas). *Applied and Environmental Microbiology*, 72(9), pp.6004–11.

Elser, J.J. et al., 2000. Biological stoichiometry from genes to ecosystems. *Ecology Letters*, 3(6), pp.540–550.

Elser, J.J. et al., 2003. Growth rate-stoichiometry couplings in diverse biota. *Ecology Letters*, 6(10), pp.936–943.

Erken, M. et al., 2011. In situ grazing resistance of *Vibrio cholerae* in the marine environment. *FEMS Microbiology Ecology*, 76(3), pp.504–12.

Ferrier, M., Martin, J.L. & Rooney-varga, J.N., 2002. Stimulation of *Alexandrium fundyense* growth by bacterial assemblages from the Bay of Fundy. *Journal of Applied Microbiology*, 92(4), pp.706–16.

Flemming, H.-C. & Wingender, J., 2010. The biofilm matrix. *Nature Reviews Microbiology*, 8(9), pp.623–33.

Flynn, K.J. et al., 2010. Is the Growth Rate Hypothesis Applicable To Microalgae? *Journal of Phycology*, 46(1), pp.1–12.

Freter, R., O'Brien, P.C. & Macsai, M.S., 1979. Effect of chemotaxis on the interaction of cholera vibrios with intestinal mucosa. *The American Journal of Clinical Nutrition*, 32(1), pp.128–32.

Frias-Lopez, J. et al., 2008. Microbial community gene expression in ocean surface waters. *Proceedings of the National Academy of Sciences of the United States of America*, 105(10), pp.3805–10.

Frischkorn, K.R. et al., 2014. De novo assembly of *Aureococcus anophagefferens* transcriptomes reveals diverse responses to the low nutrient and low light conditions present during blooms. *Frontiers in Microbiology*, 5(July), p.375.

Frischkorn, K.R., Stojanovski, A. & Paranjpye, R., 2013. *Vibrio parahaemolyticus* type IV pili mediate interactions with diatom-derived chitin and point to an unexplored mechanism of environmental persistence. *Environmental Microbiology*, 15(5), pp.1416–27.

Froelich, B. et al., 2013. Mechanistic and statistical models of total *Vibrio* abundance in the Neuse River Estuary. *Water Research*, 47(15), pp.5783–93.

Gärdes, A. et al., 2011. Diatom-associated bacteria are required for aggregation of *Thalassiosira weissflogii*. *The ISME Journal*, 5(3), pp.436–45.

Garg, S. et al., 2007. Iron uptake by the ichthyotoxic *Chattonella marina* (Raphidophyceae): impact of superoxide generation. *Journal of Phycology*, 43(5), pp.978–991.

Garren, M. et al., 2006. Patterns of association between *Symbiodinium* and members of the *Montastraea annularis* species complex on spatial scales ranging from within colonies to between geographic regions. *Coral Reefs*, 25(4), pp.503–512.

Geider, R. & La Roche, J., 2002. Redfield revisited: variability of C:N:P in marine microalgae and its biochemical basis. *European Journal of Phycology*, 37(1), pp.1–17.

Geider, R.J. et al., 1993. Response of the photosynthetic apparatus of *Phaeodactylum tricornutum* (Bacillariophyceae) to nitrate, phosphate or iron starvation. *Journal of Phycology*, 29(6), pp.755–766.

Gibson, U.E., Heid, C.A. & Williams, P.M., 1996. A novel method for real time quantitative RT-PCR. *Genome Research*, 6(10), pp.995–1001.

Gifford, S.M. et al., 2013. Expression patterns reveal niche diversification in a marine microbial assemblage. *The ISME Journal*, 7(2), pp.281–98.

Giorgi, F.M., 2012. Mefisto. Available at: http://www.usadellab.org/cms/index.php?page=mefisto.

Gobler, C.J. et al., 2011. Niche of harmful alga *Aureococcus anophagefferens* revealed through ecogenomics. *Proceedings of the National Academy of Sciences of the United States of America*, 108(11), pp.4352–7.

Godhe, A. et al., 2007. Intercalibration of classical and molecular techniques for identification of *Alexandrium fundyense* (Dinophyceae) and estimation of cell densities. *Harmful Algae*, 6(1), pp.56–72.

Goffredi, S.K. et al., 2006. Molecular detection of marine invertebrate larvae. *Marine Biotechnology*, 8(2), pp.149–60.

Granéli, E. & Turner, J.T., 2007. *Ecology of Harmful Algae* M. M. Caldwell, ed., New York: Springer Verlag.

Gray, M. et al., 2003. Molecular detection and quantitation of the red tide dinoflagellate *Karenia brevis* in the marine environment. *Applied and Environmental Microbiology*, 69(9), pp.5726–5730.

Greenfield, D.I. et al., 2006. Application of environmental sample processor (ESP) methodology for quantifying *Pseudo-nitzschia australis* using ribosomal RNA-targeted probes in sandwich and fluorescent in situ hybridization formats. *Limnology and Oceanography: Methods*, 4, pp.426–435.

Greenfield, D.I. et al., 2008. Field applications of the second-generation Environmental Sample Processor (ESP) for remote detection of harmful algae. *Limnology and Oceanography: Methods*, 6, pp.667–679.

Grimes, D.J., 1991. Ecology of estuarine bacteria capable of causing human disease: a review. *Estuaries and Coasts*, 14(4), pp.345–360.

Grossart, H.-P., Riemann, L. & Azam, F., 2001. Bacterial motility in the sea and its ecological implications. *Aquatic Microbial Ecology*, 25, pp.247–258.

Grummt, I., 2003. Life on a planet of its own: regulation of RNA polymerase I transcription in the nucleolus. *Genes & Development*, 17(14), pp.1691–702.

Guillard, R.R.L. & Ryther, J.H., 1962. Studies of marine planktonic diatoms: I. *Cyclotella nana* Hustedt, and *Detonula confervacea* (Cleve) Gran. *Canadian Journal of Microbiology*, 8(2), pp.229–239.

Haas, B.J. et al., 2013. De novo transcript sequence reconstruction from RNA-seq using the Trinity platform for reference generation and analysis. *Nature Protocols*, 8(8), pp.1494–512.

Hada, H. et al., 1984. *Vibrio tubiashii* sp. nov., a Pathogen of Bivalve Mollusks. *International Journal of Systematic Bacteriology*, (2), pp.1–4.

Hallegraeff, G.M., Anderson, D.M. & Cembella, A.D., 2003. *Manual on Harmful Marine Microalgae* G. M. Hallegraeff, D. . Anderson, & A. . Cembella, eds., Paris: United Nations Educational, Scientific and Cultural Organization.

Handy, S.M. et al., 2005. Evaluating vertical migration behavior of harmful raphidophytes in the Delaware Inland Bays utilizing quantitative real-time PCR. *Aquatic Microbial Ecology*, 40, pp.121–132.

Handy, S.M. et al., 2006. Simultaneous enumeration of multiple raphidophyte species by quantitative real-time PCR: capabilities and limitations. *Limnology and Oceanography: Methods*, 4, pp.193–204.

Handy, S.M. et al., 2008. Using quantitative real-time PCR to study competition and community dynamics among Delaware Inland Bays harmful algae in field and laboratory studies. *Harmful Algae*, 7(5), pp.599–613.

Hansen, H.P. & Koroleff, F., 1999. Determination of nutrients. In *Methods of Seawater Analysis*. John Wiley & Sons, Ltd, pp. 159–228.

Hara, Y. & Chihara, M., 1987. Morphology, ultrastructure and taxonomy of the raphidophycean alga *Heterosigma akashiwo*. *The Botanical Magazine Tokyo*, 100(2), pp.151–163.

Hariganeya, N. et al., 2013. Quantitative PCR Method for Enumeration of Cells of Cryptic Species of the Toxic Marine Dinoflagellate *Ostreopsis* spp. in Coastal Waters of Japan. *PLoS One*, 8(3), p.e57627.

Haywood, A.J. et al., 2009. Detection of *Karenia brevis* in Florida coastal waters using sandwich hybridization assays in two formats. In *Proceedings of the 6th International Conference on Molluscan Shellfish Safety*. pp. 95–100.

Haywood, A.J. et al., 2007. Molecular detection of the brevetoxin-producing dinoflagellate *Karenia brevis* and closely related species using rRNA-targeted probes and a semiautomated sandwich hybridization assay. *Journal of Phycology*, 43(6), pp.1271–1286.

Hennige, S.J. et al., 2013. The photobiology of *Heterosigma akashiwo*. Photoacclimation, diurnal periodicity, and its ability to rapidly exploit exposure to high light. *Journal of Phycology*, 49(2), pp.349–360.

Hoffmann, M. et al., 2010. PCR-based method for targeting 16S-23S rRNA intergenic spacer regions among Vibrio species. *BMC Microbiology*, 10(90), pp.1–14.

Honjo, T., 1992. Harmful red tides of *Heterosigma akashiwo*. *National Oceanic Atmospheric Administration Tech. Rep. National Marine Fisheries Service*, 111, pp.27–32.

Hood, M.A. & Winter, P.A., 1997. Attachment of *Vibrio cholerae* under various environmental conditions and to selected substrates. *FEMS Microbiology Ecology*, 22, pp.215–223.

Huq, A. et al., 2005. Critical factors influencing the occurrence of *Vibrio cholerae* in the environment of Bangladesh. *Applied and Environmental Microbiology*, 71(8), pp.4645–54.

Jakob, T. et al., 2005. Estimation of chlorophyll content and daily primary production of the major algal groups by means of multiwavelength-excitation PAM chlorophyll fluorometry: performance and methodological limits. *Photosynthesis Research*, 83(3), pp.343–61.

Jeong, H.J., 2011. Mixotrophy in red tide algae raphidophytes. *The Journal of Eukaryotic Microbiology*, 58(3), pp.215–22.

Johnson, C.N. et al., 2012. Ecology of *Vibrio parahaemolyticus* and *Vibrio vulnificus* in the coastal and estuarine waters of Louisiana, Maryland, Mississippi, and Washington (United States). *Applied and Environmental Microbiology*, 78(20), pp.7249–57.

Johnson, K. & Petty, R., 1983. Determination of nitrate and nitrite in seawater by flow injection analysis. *Limnology and Oceanography*, 28(6), pp.1260–1266.

Joint, I., Tait, K. & Wheeler, G., 2007. Cross-kingdom signalling: exploitation of bacterial quorum sensing molecules by the green seaweed *Ulva*. *Philosophical*

Transactions of the Royal Society of London. Series B, Biological Sciences, 362(1483), pp.1223–33.

Karlsson, T. et al., 2012. N-Acylhomoserine lactones are potent neutrophil chemoattractants that act via calcium mobilization and actin remodeling. *Journal of leukocyte biology*, 91(1), pp.15–26.

Kawano, I., Oda, T. & Ishimatsu, A., 1996. Inhibitory effect of the iron chelator Desferrioxamine (Desferal) on the generation of activated oxygen species by *Chattonella marina*. *Marine Biology*, 126, pp.765–771.

Keeling, P.J. et al., 2014. The Marine Microbial Eukaryote Transcriptome Sequencing Project (MMETSP): Illuminating the Functional Diversity of Eukaryotic Life in the Oceans through Transcriptome Sequencing. *PLoS Biology*, 12(6), p.e1001889.

Kempton, J. et al., 2008. A novel *Heterosigma akashiwo* (Raphidophyceae) bloom extending from a South Carolina bay to offshore waters. *Ecology*, 7, pp.235–240.

Kiddon, J.A. et al., 2003. Ecological condition of US Mid-Atlantic estuaries, 1997-1998. *Marine Pollution Bulletin*, 46(10), pp.1224–44.

Kim, D. et al., 1999. Toxic potential of the raphidophyte *Olisthodiscus luteus*: mediation by reactive oxygen species. *Journal of Plankton Research*, 21(6), pp.1017–1027.

Klie, S. & Nikoloski, Z., 2012. The Choice between MapMan and Gene Ontology for Automated Gene Function Prediction in Plant Science. *Frontiers in Genetics*, 3(June), p.115.

Kohata, K. & Watanabe, M., 1986. Synchronous division and the pattern of diel vertical migration of *Heterosigma akashiwo* (Hada) Hada (Raphidophyceae) in a laboratory culture tank. *Journal of Experimental Marine Biology and Ecology*, 100, pp.209–224.

Landry, M.R. & Hassett, R.P., 1982. Estimating the grazing impact of marine micro-zooplankton. *Marine Biology*, 67(3), pp.283–288.

Langmead, B. et al., 2009. Ultrafast and memory-efficient alignment of short DNA sequences to the human genome. *Genome Biology*, 10(3), p.R25.

Lazier, J.R.N. & Mann, K.H., 1989. Turbulence and the diffusive layers around small organisms. *Deep Sea Research Part A. Oceanographic Research Papers*, 36(11), pp.1721–1733.

Lee, J. et al., 2012. Application of tyramide signal amplification-fluorescence in situ hybridisation and flow cytometry to detection of *Heterosigma akashiwo* (Raphidophyceae) in natural waters. *New Zealand Journal of Marine and Freshwater Research*, 46(1), pp.137–148.

Lepp, P.W. & Schmidt, T.M., 1998. Nucleic acid content of *Synechococcus* spp. during growth in continuous light and light/dark cycles. *Archives of Microbiology*, 170(3), pp.201–207.

Li, Y. & Smayda, T.J., 2000. *Heterosigma akashiwo* (Raphidophyceae): On prediction of the week of bloom initiation and maximum during the initial pulse of its bimodal bloom cycle in Narragansett Bay. *Plankton Biology and Ecology*, 47(2), pp.80–84.

Linde, J., Morse, L. & Domozych, D.S., 2001. Calmodulin and Its Role in the Secretory Apparatus of the Desmid *Closterium*. *International Journal of Plant Sciences*, 162(1), pp.15–27.

Ling, C. & Trick, C.G., 2010. Expression and standardized measurement of hemolytic activity in *Heterosigma akashiwo*. *Harmful Algae*, 9(5), pp.522–529.

Liu, J. et al., 2008. The association of algicidal bacteria and raphidophyte blooms in South Carolina brackish detention ponds. *Harmful Algae*, 7(2), pp.184–193.

Liu, W. et al., 2007. Effects of nutrients, salinity, pH and light:dark cycle on the production of reactive oxygen species in the alga *Chattonella marina*. *Journal of Experimental Marine Biology and Ecology*, 346(1-2), pp.76–86.

Lizárraga-Partida, M.L. et al., 2009. Association of *Vibrio cholerae* with plankton in coastal areas of Mexico. *Environmental Microbiology*, 11(1), pp.201–8.

Lobitz, B. et al., 2000. Climate and infectious disease: use of remote sensing for detection of *Vibrio cholerae* by indirect measurement. *Proceedings of the National Academy of Sciences of the United States of America*, 97(4), p.1438.

Lohse, M. et al., 2014. Mercator: a fast and simple web server for genome scale functional annotation of plant sequence data. *Plant, Cell & Environment*, 37(5), pp.1250–8.

Lovejoy, C., Bowman, J.P. & Hallegraeff, G.M., 1998. Algicidal effects of a novel marine pseudoalteromonas isolate (class Proteobacteria, gamma subdivision) on harmful algal bloom species of the genera *Chattonella*, *Gymnodinium*, and *Heterosigma*. *Applied and Environmental Microbiology*, 64(8), pp.2806–13.

Lutz, C. et al., 2013. Environmental reservoirs and mechanisms of persistence of *Vibrio cholerae*. *Frontiers in Microbiology*, 4(December), p.375.

Ma, S. et al., 2006. Removal of H_2S via an iron catalytic cycle and iron sulfide precipitation in the water column of dead end tributaries. *Estuarine, Coastal and Shelf Science*, 70(3), pp.461–472.

Marsan, D. et al., 2014. Draft Genome Sequence of *Synechococcus* sp. Strain CB0101, Isolated From the Chesapeake Bay Estuary. *Genome Announcements*, 2(1), pp.2011–2012.

Marshall, J.-A. et al., 2003. Ichthyotoxicity of *Chattonella marina* (Raphidophyceae) to damselfish (*Acanthochromis polycanthus*): the synergistic role of reactive oxygen species and free fatty acids. *Harmful Algae*, 2(4), pp.273–281.

Marshall, J.-A. et al., 2002. Photosynthesis does influence superoxide production in the ichthyotoxic alga *Chattonella marina* (Raphidophyceae). *Journal of Plankton Research*, 24(11), pp.1231–1236.

Martinez, R.M., Megli, C.J. & Taylor, R.K., 2010. Growth and laboratory maintenance of *Vibrio cholerae*. *Current Protocols in Microbiology*, Chapter 6(603), p.Unit 6A.1.

Martinez-Garcia, M. et al., 2012. Unveiling in situ interactions between marine protists and bacteria through single cell sequencing. *The ISME Journal*, 6(3), pp.703–7.

Matz, C. et al., 2005. Biofilm formation and phenotypic variation enhance predation-driven persistence of *Vibrio cholerae*. *Proceedings of the National Academy of Sciences of the United States of America*, 102(46), pp.16819–16824.

Matz, C. & Kjelleberg, S., 2005. Off the hook--how bacteria survive protozoan grazing. *Trends in Microbiology*, 13(7), pp.302–7.

Mayali, X. et al., 2008. Bacteria-induced motility reduction in *Lingulodinium polyedrum* (Dinophyceae). *Journal of Phycology*, 44(4), pp.923–928.

Mayali, X. & Azam, F., 2004. Algicidal Bacteria in the Sea and their Impact on Algal Blooms. *The Journal of Eukaryotic Microbiology*, 51(2), pp.139–144.

Mayali, X., Franks, P. & Azam, F., 2007. Bacterial induction of temporary cyst formation by the dinoflagellate *Lingulodinium polyedrum*. *Aquatic Microbial Ecology*, 50, pp.51–62.

Middelboe, M. et al., 1995. Attached and free-living bacteria: production and polymer hydrolysis during a diatom bloom. *Microbial Ecology*, 29, pp.231–248.

Mieszkin, S., Callow, M.E. & Callow, J. A., 2013. Interactions between microbial biofilms and marine fouling algae: a mini review. *Biofouling*, 29(9), pp.1097–113.

Mikulski, C.M. et al., 2008. Development and field application of rRNA-targeted probes for the detection of *Cochlodinium polykrikoides* Margalef in Korean coastal waters using whole cell and sandwich hybridization formats. *Harmful Algae*, 7(3), pp.347–359.

Miller, P.E. et al., 2002. Variation in reactivity of rRNA-targeted probes towards *Pseudo-nitzschia multiseries* grown in nitrate-and silicate-limited continuous cultures. In K. A. Steidinger et al., eds. *Proceedings of the Xth International Conference on Harmful Algae*. St. Petersburg, Florida, USA: Florida Fish and Wildlife Conservation Commission, Florida Institute of Oceanography, and Intergovernmental Oceanographic Commission of UNESCO, pp. 270–272.

Miller, P.E. & Scholin, C.A., 1998. Identification and enumeration of cultured and wild *Pseudo-nitzschia* (Bacillariophyceae) using species-specific LSU rRNA-targeted fluorescent probes and filter-based whole cell hybridization. *Journal of Phycology*, 382(March 1997), pp.371–382.

Miralto, A. et al., 1999. The insidious effect of diatoms on copepod reproduction. *Nature*, 402, pp.173–176.

Moore, C.M. et al., 2008. Relative influence of nitrogen and phosphorus availability on phytoplankton physiology and productivity in the oligotrophic sub-tropical North Atlantic Ocean. *Limnology and Oceanography*, 53(1), pp.291–305.

Moore, J.W., Schindler, D.E. & Scheuerell, M.D., 2004. Disturbance of freshwater habitats by anadromous salmon in Alaska. *Oecologia*, 139(2), pp.298–308.

Moorthi, S.D. et al., 2006. Use of quantitative real-time PCR to investigate the dynamics of the red tide dinoflagellate *Lingulodinium polyedrum*. *Microbial Ecology*, 52(1), pp.136–50.

Motes, M.L. et al., 1998. Influence of water temperature and salinity on *Vibrio vulnificus* in Northern Gulf and Atlantic Coast oysters (Crassostrea virginica). *Applied and Environmental Microbiology*, 64(4), pp.1459–65.

Mouriño-Pérez, R.R., Worden, A.Z. & Azam, F., 2003. Growth of *Vibrio cholerae* O1 in red tide waters off California. *Applied and Environmental Microbiology*, 69(11), pp.6923–6931.

Moustafa, A. et al., 2010. Transcriptome profiling of a toxic dinoflagellate reveals a gene-rich protist and a potential impact on gene expression due to bacterial presence. *PLoS One*, 5(3), p.e9688.

Müller, D.G. et al., 1971. Sex attractant in a brown alga: chemical structure. *Science*, 171(3973), pp.815–7.

Muyzer, G., De Waal, E.C. & Uitierlinden, A.G., 1993. Profiling of Complex Microbial Populations by Denaturing Gradient Gel Electrophoresis Analysis of Polymerase Chain Reaction-Amplified Genes Coding for 16S rRNA. *Applied and Environmental Microbiology*, 59(3), pp.695–700.

O'Halloran, C. et al., 2006. *Heterosigma akashiwo* in central California waters. *Harmful Algae*, 5(2), pp.124–132.

O'Toole, G., Kaplan, H.B. & Kolter, R., 2000. Biofilm formation as microbial development. *Annual Review of Microbiology*, 54, pp.49–79.

O'Toole, R. et al., 1999. The chemotactic response of *Vibrio anguillarum* to fish intestinal mucus is mediated by a combination of multiple mucus components. *Journal of Bacteriology*, 181(14), pp.4308–17.

Oda, T. et al., 1992. Oxygen-radical-mediated toxic effects of the red tide flagellate *Chattonella marina* on *Vibrio alginolyticus*. *Marine Biology*, 112, pp.505–509.

Ogier, J.-C. et al., 2002. Identification of the Bacterial Microflora in Dairy Products by Temporal Temperature Gradient Gel Electrophoresis. *Applied and Environmental Microbiology*, 68(8), pp.3691–3701.

Olson, R.J., Vaulot, D. & Chisholm, S.W., 1986. Effects of environmental stresses on the cell cycle of two marine phytoplankton species. *Plant Physiology*, 80(4), pp.918–25.

Parkhill, J.-P., Maillet, G. & Cullen, J.J., 2001. Fluorescence-based maximal quantum yield for PSII as a diagnostic of nutrient stress. *Journal of Phycology*, 37(4), pp.517–529.

Penna, A. et al., 1999. Influence of nutrient ratios on the in vitro extracellular polysaccharide production by marine diatoms from the Adriatic Sea. *Journal of Plankton Research*, 21(9), pp.1681–1690.

Pick, F.R., 1987. Carbohydrate and Protein Content of Lake Seston in Relation to Plankton Nutrient Deficiency. *Canadian Journal of Fisheries and Aquatic Sciences*, 44(12), pp.2095–2101.

Pohnert, G. & Boland, W., 2002. The oxylipin chemistry of attraction and defense in brown algae and diatoms. *Natural Product Reports*, 19(1), pp.108–122.

Popels, L.C. et al., 2003. The use of quantitative polymerase chain reaction for the detection and enumeration of the harmful alga *Aureococcus anophagefferens* in environmental samples along the United States East Coast. *Limnology and Oceanography: Methods*, 1, pp.92–102.

Portune, K.J. et al., 2009. Quantitative real-time PCR for detecting germination of *Heterosigma akashiwo* and *Chattonella subsalsa* cysts from Delaware's Inland Bays, USA. *Aquatic Microbial Ecology*, 55, pp.229–239.

Portune, K.J., Craig Cary, S. & Warner, M.E., 2010. Antioxidant Enzyme Response and Reactive Oxygen Species Production in Marine Raphidophytes. *Journal of Phycology*, 46(6), pp.1161–1171.

Poulson-Ellestad, K.L. et al., 2014. Metabolomics and proteomics reveal impacts of chemically mediated competition on marine plankton. *Proceedings of the National Academy of Sciences*, 111(34), pp.12568–12568.

Powers, L., Creed, I.F. & Trick, C.G., 2012. Sinking of *Heterosigma akashiwo* results in increased toxicity of this harmful algal bloom species. *Harmful Algae*, 13, pp.95–104.

Pratt, J.T., McDonough, E. & Camilli, A., 2009. PhoB regulates motility, biofilms, and cyclic di-GMP in *Vibrio cholerae*. *Journal of Bacteriology*, 191(21), pp.6632–42.

Price, K., 1998. A framework for a Delaware Inland Bays environmental classification. *Environmental Monitoring and Assessment*, 51(1-2), pp.285–298.

Quiñones, B., Dulla, G. & Lindow, S.E., 2005. Quorum sensing regulates exopolysaccharide production, motility, and virulence in *Pseudomonas syringae*. *Molecular plant-microbe interactions : MPMI*, 18(7), pp.682–93.

R Core Team, 2012. R: A language and environment for statistical computing.

Radakovits, R. et al., 2012. Draft genome sequence and genetic transformation of the oleaginous alga *Nannochloropis gaditana*. *Nature Communications*, 3, p.686.

Randa, M.A., Polz, M.F. & Lim, E., 2004. Effects of temperature and salinity on *Vibrio vulnificus* population dynamics as assessed by quantitative PCR. *Applied and Environmental Microbiology*, 70(9), p.5469.

Raven, J.A., 2013. RNA function and phosphorus use by photosynthetic organisms. *Frontiers in Plant Science*, 4(December), p.536.

Rensel, J.E.J., Haigh, N. & Tynan, T.J., 2010. Fraser river sockeye salmon marine survival decline and harmful blooms of *Heterosigma akashiwo*. *Harmful Algae*, 10(1), pp.98–115.

Rhee, G.-Y., 1978. Effects of N:P atomic ratios and nitrate limitation on algal growth, cell composition, and nitrate uptake. *Limnology and Oceanography*, 23(1), pp.10–25.

Rhodes, L.L. et al., 2001. Harmful algae and mariculture in New Zealand. *ICES Journal of Marine Science*, 58(2), pp.398–403.

Van Rijssel, M. et al., 2007. Evidence for inhibition of bacterial luminescence by allelochemicals from *Fibrocapsa japonica* (Raphidophyceae), and the role of light and microalgal growth rate. *Hydrobiologia*, 596(1), pp.289–299.

Rooney-Varga, J.N. et al., 2005. Links between phytoplankton and bacterial community dynamics in a coastal marine environment. *Microbial Ecology*, 49(1), pp.163–75.

Rosenbaum, J.L. & Witman, G.B., 2002. Intraflagellar transport. *Nature Reviews. Molecular Cell Biology*, 3(11), pp.813–25.

Ryan, J. et al., 2011. Harmful phytoplankton ecology studies using an autonomous molecular analytical and ocean observing network. *Limnology and Oceanography*, 56(4), pp.1255–1272.

Sakami, T. et al., 1999. Effects of epiphytic bacteria on the growth of the toxic dinoflagellate *Gambierdiscus toxicus* (Dinophyceae). *Journal of Experimental Marine Biology and Ecology*, 233(2), pp.231–246.

Salcher, M.M. et al., 2005. Succession of bacterial grazing defense mechanisms against protistan predators in an experimental microbial community. *Aquatic Microbial Ecology*, 38, pp.215–229.

Sallade, Y.E. & Sims, J.T., 1997. Phosphorus Transformations in the Sediments of Delaware's Agricultural Drainageways: II. Effect of Reducing Conditions on Phosphorus Release. *Journal of Environment Quality*, 26(6), p.1579.

Sapp, M. et al., 2007. Species-specific bacterial communities in the phycosphere of microalgae? *Microbial Ecology*, 53(4), pp.683–99.

Satoh, E., Watanabe, M.M. & Fujii, T., 1987. Photoperiodic Regulation of Cell Division and Chloroplast Replication in *Heterosigma akashiwo*. *Plant and Cell Physiology* , 28 (6), pp.1093–1099.

Scholin, C. et al., 2003. Detection of HAB species using lectin, antibody and DNA probes. In G. M. Hallegraeff, D. M. Anderson, & A. D. Cembella, eds. *Manual on Harmful Marine Microalgae*. Paris, pp. 131–163.

Scholin, C.A. et al., 1997. Detection and quantification of *Pseudo-nitzschia australis* in cultured and natural populations using LSU rRNA-targeted probes. *Limnology and Oceanography*, 42(5_part_2), pp.1265–1272.

Scholin, C.A. et al., 1996. Identification of *Pseudo-nitzschia australis* (Bacillariophyceae) using rRNA-targeted probes in whole cell and sandwich hybridization formats. *Phycologia*, 35(3), pp.190–197.

Seymour, J.R., Ahmed, T. & Stocker, R., 2009. Bacterial chemotaxis towards the extracellular products of the toxic phytoplankton *Heterosigma akashiwo*. *Journal of Plankton Research*, 31(12), pp.1557–1561.

Simon, N. et al., 2009. Diversity and evolution of marine phytoplankton. *Comptes Rendus Biologies*, 332(2-3), pp.159–70.

Singleton, F.L. et al., 1982. Effects of Temperature and Salinity Growth *Vibrio cholerae*. *Applied and Environmental Microbiology*, 44(5), pp.1047–1058.

Skerratt, J. et al., 2002. Algicidal bacteria associated with blooms of a toxic dinoflagellate in a temperate Australian estuary. *Marine Ecology Progress Series*, 244, pp.1–15.

Smith, D.C. et al., 1995. Bacterial mediation of carbon fluxes during a diatom bloom in a mesocosm. *Deep Sea Research Part II: Topical Studies in Oceanography*, 42(1), pp.75–97.

Sournia, A., Chrdtiennot-Dinet, M.J. & Ricard, M., 1991. Marine phytoplankton: how many species in the world ocean? *Journal of Plankton Research*, 13(5), pp.1093–1099.

Sterner, R.W. & Elser, J.J., 2002. *Ecological Stoichiometry. The Biology of the Elements from Molecules to the Biosphere*, Princeton, New Jersey: Princeton University Press.

Stocker, R. & Seymour, J.R., 2012. Ecology and Physics of Bacterial Chemotaxis in the Ocean. *Microbiology and Molecular Biology Reviews*, 76(4), pp.792–812.

Su, C. et al., 2012. Culture-independent methods for studying environmental microorganisms: methods, application, and perspective. *Applied Microbiology and Biotechnology*, 93(3), pp.993–1003.

Sun, S. et al., 2011. Community cyberinfrastructure for Advanced Microbial Ecology Research and Analysis: the CAMERA resource. *Nucleic Acids Research*, 39(Database issue), pp.D546–51.

Sun, S., Kjelleberg, S. & McDougald, D., 2013. Relative contributions of *Vibrio* polysaccharide and quorum sensing to the resistance of *Vibrio cholerae* to predation by heterotrophic protists. *PLoS One*, 8(2), p.e56338.

Takemura, A.F., Chien, D.M. & Polz, M.F., 2014. Associations and dynamics of Vibrionaceae in the environment, from the genus to the population level. *Frontiers in Microbiology*, 5(February), p.38.

Tamplin, M.L. et al., 1990. Attachment of *Vibrio cholerae* serogroup O1 to zooplankton and phytoplankton of Bangladesh waters. *Applied and Environmental Microbiology*, 56(6), pp.1977–80.

Tatusov, R.L. et al., 2003. The COG database: an updated version includes eukaryotes. *BMC Bioinformatics*, 4, p.41.

Teplitski, M. et al., 2004. *Chlamydomonas reinhardtii* secretes compounds that mimic bacterial signals and interfere with quorum sensing regulation in bacteria. *Plant Physiology*, 134(1), pp.137–46.

Thimm, O. et al., 2004. Mapman: a User-Driven Tool To Display Genomics Data Sets Onto Diagrams of Metabolic Pathways and Other Biological Processes. *The Plant Journal*, 37(6), pp.914–939.

Thompson, F.L., Austin, B. & Swings, J. eds., 2006. *The Biology of Vibrios*, Washington, DC.

Thompson, J.R. et al., 2004. Diversity and Dynamics of a North Atlantic Coastal *Vibrio* Community. *Applied and Environmental Microbiology*, 70(7), pp.4103–4110.

Thompson, J.R., Marcelino, L. a & Polz, M.F., 2002. Heteroduplexes in mixed-template amplifications: formation, consequence and elimination by "reconditioning PCR." *Nucleic Acids Research*, 30(9), pp.2083–8.

Tilney, C.L. et al., 2014. Effects of a bacterial algicide, IRI-160AA, on dinoflagellates and the microbial community in microcosm experiments. *Harmful Algae*, 39, pp.210–222.

Trapnell, C. et al., 2013. Differential analysis of gene regulation at transcript resolution with RNA-seq. *Nature Biotechnology*, 31(1), pp.46–53.

Trapnell, C. et al., 2012. Differential gene and transcript expression analysis of RNA-seq experiments with TopHat and Cufflinks. *Nature Protocols*, 7(3), pp.562–78.

Trapnell, C. et al., 2010. Transcript assembly and quantification by RNA-Seq reveals unannotated transcripts and isoform switching during cell differentiation. *Nature Biotechnology*, 28(5), pp.511–5.

Tseng, C.K., Zhou, M.J. & Zou, J.Z., 1993. Toxic phytoplankton studies in China. In T. J. Smayda & Y. Shimizu, eds. *Toxic Phytoplankton Blooms in the Sea*. New York: Elsevier, pp. 347–352.

Turner, J.W. et al., 2009. Plankton composition and environmental factors contribute to *Vibrio* seasonality. *The ISME Journal*, 3(9), pp.1082–92.

Twiner, M.J. et al., 2005. Extracellular organic compounds from the ichthyotoxic red tide alga elevate cytosolic calcium and induce apoptosis in Sf9 cells. *Harmful Algae*, 4(4), pp.789–800.

Twiner, M.J. et al., 2001. Toxic Effects of *Heterosigma akashiwo* Do Not Appear to Be Mediated by Hydrogen Peroxide. *Limnology and Oceanography*, 46(6), pp.1400–1405.

Twiner, M.J. & Trick, C.G., 2000. Possible physiological mechanisms for production of hydrogen peroxide by the ichthyotoxic flagellate *Heterosigma akashiwo*. *Journal of Plankton Research*, 22(10), pp.1961–1975.

Tyrrell, J. V. et al., 2001. Detection and enumeration of *Heterosigma akashiwo* and *Fibrocapsa japonica* (Raphidophyceae) using rRNA-targeted oligonucleotide probes. *Phycologia*, 40(5), pp.457–467.

Tyrrell, J. V., Connell, L.B. & Scholin, C.A., 2002. Monitoring for *Heterosigma akashiwo* using a sandwich hybridization assay. *Harmful Algae*, 1(2), pp.205–214.

Utada, A.S. et al., 2014. *Vibrio cholerae* use pili and flagella synergistically to effect motility switching and conditional surface attachment. *Nature Communications*, 5, p.4913.

VanGuilder, H.D., Vrana, K.E. & Freeman, W.M., 2008. Twenty-five years of quantitative PCR for gene expression analysis. *BioTechniques*, 44(5), pp.619–26.

Vardi, A. et al., 2009. Viral glycosphingolipids induce lytic infection and cell death in marine phytoplankton. *Science*, 326(5954), pp.861–5.

Vrede, T. et al., 2004. Fundamental connections among organisms C:N:P stoichiometry, macromolecular composition, and growth. *Ecology*, 85(5), pp.1217–1229.

Warner, M.E. & Madden, M.L., 2007. The impact of shifts to elevated irradiance on the growth and photochemical activity of the harmful algae *Chattonella subsalsa* and *Prorocentrum minimum* from Delaware. *Harmful Algae*, 6(3), pp.332–342.

Welschmeyer, N.A., 1994. Fluorometric of chlorophyll *a* in the presence of analysis *b* and pheopigments chlorophyll. *Limnology and Oceanography*, 39(8), pp.1985–1992.

Whereat, E.B., 2013. *Phytoplankton Monitoring Report. Volunteer Phytoplankton Monitoring Group, The Inland Bays Citizen Monitoring Program*,

Wilson, K.E. et al., 2006. Energy balance, organellar redox status, and acclimation to environmental stress. *Canadian Journal of Botany*, 84(9), pp.1355–1370.

Wilson, K.E., Sieger, S.M. & Huner, N.P. a., 2003. The temperature-dependent accumulation of Mg-protoporphyrin IX and reactive oxygen species in *Chlorella vulgaris*. *Physiologia Plantarum*, 119(1), pp.126–136.

Worden, A.Z. et al., 2006. Trophic regulation of *Vibrio cholerae* in coastal marine waters. *Environmental Microbiology*, 8(1), pp.21–9.

Worden, A.Z. & Binder, B.J., 2003. Growth regulation of rRNA content in *Prochlorococcus* and *Synechococcus* (Marine cyanobacteria) measured by whole-cell hybridization of rRNA-targeted peptide nucleic acids. *Journal of Phycology*, 39(3), pp.527–534.

Wu, S. et al., 2011. WebMGA: a customizable web server for fast metagenomic sequence analysis. *BMC Genomics*, 12(1), p.444.

Yang, C.Z., Albright, L.J. & Yousif, A.N., 1995. Oxygen-radical-mediated effects of the toxic phytoplankter *Heterosigma carterae* on juvenile rainbow trout Oncorhynchus mykiss. *Diseases Of Aquatic Organisms*, 23, pp.101–108.

Yang, Y. et al., 2013. Community level physiological study of algicidal bacteria in the phycospheres of *Skeletonema costatum* and *Scrippsiella trochoidea*. *Harmful Algae*, 28, pp.88–96.

Ye, J. et al., 2012. Primer-BLAST: a tool to design target-specific primers for polymerase chain reaction. *BMC Bioinformatics*, 13, p.134.

Yildiz, F.H. & Visick, K.L., 2009. *Vibrio* biofilms: so much the same yet so different. *Trends in Microbiology*, 17(3), pp.109–18.

Ymele-Leki, P., Houot, L. & Watnick, P.I., 2013. Mannitol and the Mannitol-Specific Enzyme IIB Subunit Activate *Vibrio cholerae* Biofilm Formation. *Applied and Environmental Microbiology*, 79(15), pp.4675–83.

Zachleder, V. & Šetlík, I., 1988. Distinct controls of DNA replication and of nuclear division in the cell cycles of the chlorococcal alga *Scenedesmus quadricauda*. *Journal of Cell Science*, 91(4), pp.531–540.

Zhang, L. et al., 2013. Antioxidant activity of an exopolysaccharide isolated from *Lactobacillus plantarum* C88. *International Journal of Biological Macromolecules*, 54, pp.270–5.

Zhang, Y. et al., 2006. Bottom-up controls on a mixed-species HAB assemblage: A comparison of sympatric *Chattonella subsalsa* and *Heterosigma akashiwo* (Raphidophyceae) isolates from the Delaware Inland Bays, USA. *Harmful Algae*, 5(3), pp.310–320.

Appendix A

ENVIRONMENTAL PARAMETERS FOR DELAWARE'S INLAND BAYS 2009-2011

Table A.1 Environmental parameters for weekly samples collected from 2009 – 2011. Nutrients were not measured in 2009.

Site	Date	Temperature	Salinity	Dissolved Oxygen	Chlorophyll *a*	NO_x	NH_4	PO_4	Si	N:P Ratio
IR32	03/31/09	14.8	22.7							
SB10E	03/31/09	12.3	21.5							
RB64	03/31/09	22.4	24.4							
IR32	05/21/09	23.5	24.3							
SB10E	05/21/09	22.6	15.1							
RB64	05/21/09	23.5	23.9							
IR32	05/28/09	22.7	26.6							
SB10E	05/28/09	23.8	16.5							
RB64	05/28/09	25.5	23.6		18.93					
IR32	06/16/09	24.6	23.2		57.37					
SB10E	06/16/09	25.5	13.4		42.3					
RB64	06/16/09	26.6	26.1	3.5	20.45					
IR32	06/25/09	24.99	21.8		905.67					

Table A.1 continued

Site	Date	Temperature	Salinity	Dissolved Oxygen	Chlorophyll *a*	NO_x	NH_4	PO_4	Si	N:P Ratio
SB10E	06/25/09	25.21	15.65		64.8					
RB64	06/25/09	27.7	26.9	0.81	43.25					
IR32	07/06/09	27.7	23.2	3.8	276					
SB10E	07/06/09	26.3	17.6	1.7	40.9					
RB64	07/06/09	29.5	25.9	2.9	159					
IR32	07/22/09	26.9	27.7	2.23	386.75					
SB10E	07/22/09	28.98	21.09	3.5	45.85					
RB64	07/22/09	27.7	20.5							
IR32	08/04/09	29.4	26.1	3.6	183					
SB10E	08/04/09	29.5	19.4	5.3	200.5					
RB64	08/04/09	30.8	26.8	2.5						
IR32	08/13/09	28	18.2							
SB10E	08/13/09	28.5	15							
IR32	08/20/09	31	27.3	10.44						
RB64	08/27/09	24.8	37							
IR32	09/03/09	23.2	21.3							
SB10E	09/03/09	24	19.7							
RB64	09/03/09	22	27.4		90					
IR32	09/10/09	21.2	27.2		439.5					
SB10E	09/10/09	22.2	24.6		37.05					
RB64	09/10/09	24	25.3	14.1						
IR32	09/17/09	24.6	24.8	13.9						
SB10E	09/17/09	23.6	19.5	4.2						

Table A.1 continued

Site	Date	Temperature	Salinity	Dissolved Oxygen	Chlorophyll *a*	NO_x	NH_4	PO_4	Si	N:P Ratio
RB64	09/17/09	26.3	25.4	8.5	74.5					
IR32	09/24/09	24.8	24.8	8.3	154.5					
IR32	10/01/09	21.4	22.3	13.9	278.5					
SB10E	10/01/09	21.7	21	4	36.6					
RB64	10/01/09	22.3	25.2	2.6	28.75					
IR32	06/02/10	26.3	24.3		78.25					
SB10E	06/02/10	26.9	20.28	2.68	21.55					
RB64	06/02/10	29.06	24.41		36.35					
IR32	06/07/10	26.2	26.6	3.6	57.9	8.05	13.04	0.27		30.02
RB64	06/07/10	25	25.9	3.2	36.8	0.92	2.53	0.21		4.48
SB10E	06/08/10	26.6	21.3	3.3	32.3	5.83	3.52	0.13		44.94
IR32	06/14/10	26.2	27.7	3.3	65.2	2.12	3.11	0.64		3.34
SB10E	06/14/10	25.7	22.1	3.8	170	1.64	2.65	0.64		2.58
IR32	06/21/10	27.6	28.2	4.7	109.5	1.53	3.08	0.54		2.82
RB64	06/21/10	27.6	26.6	3.8	28.4	1.75	2.25	0.17		10.46
SB10E	06/22/10	28.1	24.2	2.6	267.5	1.03	3.1	0.78		1.31
IR32	06/28/10	29.6	27.9	2.5	42.65	1.67	29.09	0.41		4.1
SB10E	06/29/10	30.4	23.6	5.7	33.05	4.58	0.3	0.48		9.49
RB64	06/29/10	29.8	26.1	4.72	60.9	3.42	8.01	0.62		5.53
SB10E	07/06/10	28.3	25.4	1.2	13.1	1.36	0.77	0.3		4.55
IR32	07/07/10	27.7	27.5	2.1	53.9	0.42	1.22	0.4		1.06
RB64	07/07/10	29.5	27.1	1	29.4	1.18	9.74	0.57		2.08

Table A.1 continued

Site	Date	Temperature	Salinity	Dissolved Oxygen	Chlorophyll *a*	NO_x	NH_4	PO_4	Si	N:P Ratio
IR32	07/12/10	27.8	29	4.2	234	1.49	1.73	0.58		2.55
RB64	07/12/10	28.9	27	0.96	21.55	0.71	4.34	0.17		4.11
SB10E	07/13/10	29.1	25.6	1.3	28.65	1.9	2.51	0.22		8.46
IR32	07/19/10	28.6	28.3	3.4	37.1	1.55	1.27	0.18		8.62
RB64	07/19/10	30	27	5.1	22.3	2.2	0.9	0.18		12.49
SB10E	07/20/10	30	25.7	3.8	111	0.83	1.18	0.46		1.82
IR32	07/26/10	29.4	29.6	1.1	88.15	6.08	14.87	0.66		9.25
RB64	07/26/10	29.5	26.9	1.8	40.7	2.92	0.78	0.26		11.05
SB10E	07/27/10	28.3	26.3	0.02	32.3	1.04	10.81	1.11		0.94
IR32	08/02/10	25.1	30.1	1.5	34.7	3.46	1.03	0.45		7.7
RB64	08/02/10	27.2	28	0.1	161.5	0.84	0.82	0.27		3.05
SB10E	08/03/10	27.5	28.3	4.3	94.7	2.26	1.38	0.47		4.83
IR32	08/09/10	28.9	31	3.3	27.75	0.46	0.79	0.18		2.55
RB64	08/09/10	28.8	28.1	3.2	44.05	0.84	1.34	0.45		1.88
SB10E	08/10/10	29.3	28.5	2.3	70.25	1.04	1.33	0.5		2.07
IR32	08/16/10	26	30.3	0.8	74.6	1.02	0.58	0.32		3.16
RB64	08/16/10	28.7	25.9	1.5	22.9					
IR32	08/17/10		30		149	1.37	1.35	0.42		3.23
SB10E	08/17/10	28.6	28.9	1.3	25.25	2.66	0.91	0.36		7.35
IR32	08/23/10	25.3	20.8	2.98	32.15	4.35	8.05	0.73		5.98
RB64	08/23/10	27.4	24	1.39	16.65	1.59	6.94	0.33		4.77
SB10E	08/24/10	27	20.4	2.06	33.55	1.15	2.43	0.23		4.95

Table A.1 continued

Site	Date	Temperature	Salinity	Dissolved Oxygen	Chlorophyll *a*	NO_x	NH_4	PO_4	Si	N:P Ratio
IR32	08/30/10	25	25.4	2.2	34.9	17.27	17.24	0.31		55.24
RB64	08/30/10	25.6	26.1	2.2	26.45	1.26	2.73	0.28		4.46
SB10E	08/31/10	27.1	23.2	8.8	88.15	1.01	1.82	0.37		2.73
IR32	09/07/10	24.3	27.9	1.6	64.6	0.58	1.2	0.24		2.46
SB10E	09/07/10	25.4	24.7	1.7	21.45	1.53	8.48	0.34		4.56
RB64	09/07/10	25.3	26.5	2.2	28.3	1.97	1.48	0.31		6.4
IR32	09/13/10	20.9	28.9	0.6	11.4	2.63	17.91	0.47		5.57
RB64	09/13/10	21	26	2.5	15.05	3.43	20.16	0.62		5.54
SB10E	09/14/10	22.8	26.1	3.3	10.73	0.96	6.19	0.18		5.23
IR32	09/20/10	22.3	28.6	1.7	89.75	1.58	2.73	0.61		2.6
RB64	09/20/10	23.4	28.5	3.5	16.1	9.19	1.25	0.36		25.7
SB10E	09/22/10	22.6	26.1	4.1	15.55	0.93	1.86	0.22		4.19
IR32	09/27/10	23.3	27.4	2.2		3.3	15.98	0.78		4.25
SB10E	09/27/10	23.2	21.7	5.7		5.55	5.59	0.14		40.91
RB64	09/27/10	22.6	17.7	6.3		10.13	6.13	1.04		9.73
IR32	06/20/11	25.1	28.9	3.4	8.41	0.945	1.005	0.625	82.315	1.512
RB64	06/20/11	26	27	2.1	19.05	1.265	1.08	0.775	89.695	1.632
SB10E	06/21/11	24.8	27.6	1.65	5.66	1.065	5.35	1.34	51.76	0.795
IR32	06/27/11	26.9	29.3	3	14.45	0.195	2.905	0.215	53.89	0.907
RB64	06/27/11	27.6	26.9	3	6.52	0.695	0.7	0.64	73.65	1.086
SB10E	06/28/11	27.3	26.8	3.3	7.765	2.18	1.935	0.205	48.145	10.634
IR32	07/05/11	27.4	24.5	3.9	20.4	11.22	1.17	0.37	18.91	30.324
RB64	07/05/11	29	28.7	3.1	5.655	0.63	0.825	0.85	72.135	0.741

Table A.1 continued

Site	Date	Temperature	Salinity	Dissolved Oxygen	Chlorophyll *a*	NO_x	NH_4	PO_4	Si	N:P Ratio
SB10E	07/05/11	26.6	20	3.9	6.98	17.125	9.54	0.29	22.965	59.052
IR32	07/11/11	28.1	26.4	3.8	29.85	0.2	0.98	0.305	38.035	0.656
RB64	07/11/11	29.79	24.4	6.76	8.705	0.135	0.93	0.375	69.36	0.360
SB10E	07/12/11	30.1	23.7	5.8	33.15	2.275	1.54	0.47	44.06	4.840
IR32	07/18/11	25.6	27.7	2.8	13.2	0.465	0.635	0.085	26.54	5.471
RB64	07/18/11	27.2	27.5	4.02	7.905	0.295	0.41	0.95	67.76	0.311
SB10E	07/19/11	28.5	25.9	2	7.47	0.565	4.735	0.195	26.565	2.897
RB64	07/21/11	29.3	28.7	3.4	5.375	0.97	0.895	0.465	75.97	2.086
SB10E	07/21/11	31.3	26.9	3.57	47.2	1.035	1.01	0.455	20.915	2.275
IR32	07/25/11	31.3	25	3.6	25.75	1.395	5.355	0.495	37.335	2.818
RB64	07/25/11	31.4	25.3	10.5	15.05	0.705	1.515	0.79	81.785	0.892
SB10E	07/25/11	30.6	25.8	4.6	16.05	1.03	5.06	0.165	30.925	6.242
IR32	08/01/11	28.8	27.3	1.13	43.65	14.49	1.11	0.39	43.06	37.154
RB64	08/01/11	29.5	26.1	0.35	92.6	18.96	1.19	1.155	75.555	16.416
SB10E	08/02/11	29.9	26.1	2.1	28.9	0.635	1.82	0.285	16.95	2.228
IR32	08/08/11	28.7	28.5	5.3	14.75	0.885	0.865	0.365	37.49	2.425
RB64	08/08/11	28.9	27.4	1.32	23.05	0.715	1.29	1.055	68.91	0.678
SB10E	08/09/11	28.8	26.9	1.75	9.615	25.51	3.775	0.32	39.505	79.719
IR32	08/15/11	23.2	13.5	3.3	12.8	13.105	8.45	2.74	28.325	4.783
RB64	08/15/11	24.8	18.5	2.5	9.17	7.18	8.145	1.52	32.48	4.724
SB10E	08/16/11	24.3	9.3	4	7.125	12.865	5.85	0.67	19.99	19.201
IR32	08/18/11	26.4	24.82	2.62	31.35	10.435	3.545	1.6	38.205	6.522
RB64	08/18/11	28.02	27.66	3.51	12.6	36.59	1.74	2.815	39.04	12.998

Table A.1 continued

Site	Date	Temperature	Salinity	Dissolved Oxygen	Chlorophyll *a*	NO_x	NH_4	PO_4	Si	N:P Ratio
SB10E	08/18/11	28.38	15.48	4.27	15.05					
IR32	08/22/11	25.5	26	3.2	39.45	1.24	0.945	0.415	31.52	2.988
RB64	08/22/11	26.9	22.5	5.67	7.46	5.31	10.865	1.13	51.05	4.699
SB10E	08/23/11	26.5	20.6	2.3	11.9	0.715	1.66	0.27	39.815	2.648
IR32	08/30/11	23.2	16.8	1.1	2.815	49.56	37.5	1.26	46.735	39.333
RB64	08/30/11	24.5	18.5	2.2	4.625	8.575	13.175	1.985	39.275	4.320
SB10E	08/30/11	24.2	10.8	4.4	14.65	10.25	19.2	1.31	34.455	7.824
IR32	09/06/11	24.9	22.9	3.1	21.15	18.27	9.255	0.39	38.465	46.846
RB64	09/06/11	26.2	25	3.5	12.5	11.475	6.185	1.18	63.185	9.725
SB10E	09/06/11	26.3	15.9	1.3	27.1	1.67	1.25	0.54	33.765	3.093
IR32	09/08/11	25.12	24.83	2.92	5.8	7.785	11.2	0.53	21.82	14.689
RB64	09/08/11	25.88	23.34	2.57	16.9	3.2	3.375	0.765	39.565	4.183
SB10E	09/08/11	26.48	15.6	2.45	11.95					
IR32	09/12/11	25.6	25.8	4.5	20.15	6.615	3.025	0.395	38.905	16.747
RB64	09/12/11	25.7	23.6	2.49	128	1.755	0.685	0.68	56.7	2.581
SB10E	09/13/11	25.8	17.9	1.63	8.625	0.99	5.25	0.24	43.505	4.125
IR32	09/19/11	19.3	22.1	1.5	5.945	12.29	11.855	0.56	33.1	21.946
RB64	09/19/11	18.4	25.4	3.7	4.29	2.965	17.06	1.235	58.21	2.401
SB10E	09/20/11	20	22.1	4.5	4.01	7.01	8.275	0.215	39.315	32.605
RB64	09/26/11	23.4	19.4	5.6	19.2	8.6	8.84	0.74	38.605	11.622
IR32	09/26/11	22.9	23.2	2.9	8.335	24.79	20.01	0.715	44.43	34.671
SB10E	09/27/11	23.4	17.8	4.4	9.24	10.32	5.055	0.29	40.07	35.586

Appendix B

REUSE PERMISSION

ELSEVIER LICENSE
TERMS AND CONDITIONS

Dec 01, 2014

This is a License Agreement between Christopher R Main ("You") and Elsevier ("Elsevier") provided by Copyright Clearance Center ("CCC"). The license consists of your order details, the terms and conditions provided by Elsevier, and the payment terms and conditions.

All payments must be made in full to CCC. For payment instructions, please see information listed at the bottom of this form.

Supplier	Elsevier Limited The Boulevard,Langford Lane Kidlington,Oxford,OX5 1GB,UK
Registered Company Number	1982084
Customer name	Christopher R Main
Customer address	700 Pilottown Road LEWES, DE 19958
License number	3515880158639
License date	Nov 25, 2014
Licensed content publisher	Elsevier
Licensed content publication	Harmful Algae
Licensed content title	Effects of growth phase, diel cycle and macronutrient stress on the quantification of Heterosigma akashiwo using qPCR and SHA

Licensed content author	None
Licensed content date	July 2014
Licensed content volume number	37
Licensed content issue number	n/a
Number of pages	8
Start Page	92
End Page	99
Type of Use	reuse in a thesis/dissertation
Portion	full article
Format	both print and electronic
Are you the author of this Elsevier article?	Yes
Will you be translating?	No
Title of your thesis/dissertation	Molecular Assessment of Raphidophyte Species and their Association with Vibrio in Delaware's Inland Bays
Expected completion date	Dec 2014
Estimated size (number of pages)	172
Elsevier VAT number	GB 494 6272 12
Permissions price	0.00 USD
VAT/Local Sales Tax	0.00 USD / 0.00 GBP
Total	0.00 USD
Terms and Conditions	

INTRODUCTION

1. The publisher for this copyrighted material is Elsevier. By clicking "accept" in connection with completing this licensing transaction, you agree that the following terms and conditions apply to this transaction (along with the Billing and Payment terms and conditions established by Copyright Clearance Center, Inc. ("CCC"), at the time that you opened your Rightslink account and that are available at any time athttp://myaccount.copyright.com).

GENERAL TERMS

2. Elsevier hereby grants you permission to reproduce the aforementioned material subject to the terms and conditions indicated.

3. Acknowledgement: If any part of the material to be used (for example, figures) has appeared in our publication with credit or acknowledgement to another source, permission must also be sought from that source. If such permission is not obtained then that material may not be included in your publication/copies. Suitable acknowledgement to the source must be made, either as a footnote or in a reference list at the end of your publication, as follows:

"Reprinted from Publication title, Vol /edition number, Author(s), Title of article / title of chapter, Pages No., Copyright (Year), with permission from Elsevier [OR APPLICABLE SOCIETY COPYRIGHT OWNER]." Also Lancet special credit - "Reprinted from The Lancet, Vol. number, Author(s), Title of article, Pages No., Copyright (Year), with permission from Elsevier."

4. Reproduction of this material is confined to the purpose and/or media for which permission is hereby given.

5. Altering/Modifying Material: Not Permitted. However figures and illustrations may be altered/adapted minimally to serve your work. Any other abbreviations, additions, deletions and/or any other alterations shall be made only with prior written authorization of Elsevier Ltd. (Please contact Elsevier at permissions@elsevier.com)

6. If the permission fee for the requested use of our material is waived in this instance, please be advised that your future requests for Elsevier materials may attract a fee.

7. Reservation of Rights: Publisher reserves all rights not specifically granted in the combination of (i) the license details provided by you and accepted in the course of this licensing transaction, (ii) these terms and conditions and (iii) CCC's Billing and Payment terms and conditions.

8. License Contingent Upon Payment: While you may exercise the rights licensed immediately upon issuance of the license at the end of the licensing process for the transaction, provided that you have disclosed complete and accurate details of your proposed use, no license is finally effective unless and until full payment is received from you (either by publisher or by CCC) as provided in CCC's Billing and Payment terms and conditions. If full payment is not received on a timely basis, then any license preliminarily granted shall be deemed automatically revoked and shall be void as if never granted. Further, in the event that you breach any of these terms and conditions or any of

CCC's Billing and Payment terms and conditions, the license is automatically revoked and shall be void as if never granted. Use of materials as described in a revoked license, as well as any use of the materials beyond the scope of an unrevoked license, may constitute copyright infringement and publisher reserves the right to take any and all action to protect its copyright in the materials.

9. Warranties: Publisher makes no representations or warranties with respect to the licensed material.

10. Indemnity: You hereby indemnify and agree to hold harmless publisher and CCC, and their respective officers, directors, employees and agents, from and against any and all claims arising out of your use of the licensed material other than as specifically authorized pursuant to this license.

11. No Transfer of License: This license is personal to you and may not be sublicensed, assigned, or transferred by you to any other person without publisher's written permission.

12. No Amendment Except in Writing: This license may not be amended except in a writing signed by both parties (or, in the case of publisher, by CCC on publisher's behalf).

13. Objection to Contrary Terms: Publisher hereby objects to any terms contained in any purchase order, acknowledgment, check endorsement or other writing prepared by you, which terms are inconsistent with these terms and conditions or CCC's Billing and Payment terms and conditions. These terms and conditions, together with CCC's Billing and Payment terms and conditions (which are incorporated herein), comprise the entire agreement between you and publisher (and CCC) concerning this licensing transaction. In the event of any conflict between your obligations established by these terms and conditions and those established by CCC's Billing and Payment terms and conditions, these terms and conditions shall control.

14. Revocation: Elsevier or Copyright Clearance Center may deny the permissions described in this License at their sole discretion, for any reason or no reason, with a full refund payable to you. Notice of such denial will be made using the contact information provided by you. Failure to receive such notice will not alter or invalidate the denial. In no event will Elsevier or Copyright Clearance Center be responsible or liable for any costs, expenses or damage incurred by you as a result of a denial of your permission request, other than a refund of the amount(s) paid by you to Elsevier and/or Copyright Clearance Center for denied permissions.

LIMITED LICENSE

The following terms and conditions apply only to specific license types:

15. **Translation**: This permission is granted for non-exclusive world **English** rights only unless your license was granted for translation rights. If you licensed translation rights you may only translate this content into the languages you requested. A professional translator must perform all translations and reproduce the content word for word preserving the integrity of the article. If this license is to re-use 1 or 2 figures then permission is granted for non-exclusive world rights in all languages.

16. **Posting licensed content on any Website**: The following terms and conditions apply as follows: Licensing material from an Elsevier journal: All content posted to the web site must maintain the copyright information line on the bottom of each image; A hyper-text must be included to the Homepage of the journal from which you are licensing athttp://www.sciencedirect.com/science/journal/xxxxx or the Elsevier homepage for books athttp://www.elsevier.com; Central Storage: This license does not include permission for a scanned version of the material to be stored in a central repository such as that provided by Heron/XanEdu.

Licensing material from an Elsevier book: A hyper-text link must be included to the Elsevier homepage at http://www.elsevier.com . All content posted to the web site must maintain the copyright information line on the bottom of each image.

Posting licensed content on Electronic reserve: In addition to the above the following clauses are applicable: The web site must be password-protected and made available only to bona fide students registered on a relevant course. This permission is granted for 1 year only. You may obtain a new license for future website posting.

For journal authors: the following clauses are applicable in addition to the above: Permission granted is limited to the author accepted manuscript version* of your paper.

***Accepted Author Manuscript (AAM) Definition:** An accepted author manuscript (AAM) is the author's version of the manuscript of an article that has been accepted for publication and which may include any author-incorporated changes suggested through the processes of submission processing, peer review, and editor-author communications. AAMs do not include other publisher value-added contributions such as copy-editing, formatting, technical enhancements and (if relevant) pagination.

You are not allowed to download and post the published journal article (whether PDF or HTML, proof or final version), nor may you scan the printed edition to create an electronic version. A hyper-text must be included to the Homepage of the journal from which you are licensing at http://www.sciencedirect.com/science/journal/xxxxx. As part

of our normal production process, you will receive an e-mail notice when your article appears on Elsevier's online service ScienceDirect (www.sciencedirect.com). That e-mail will include the article's Digital Object Identifier (DOI). This number provides the electronic link to the published article and should be included in the posting of your personal version. We ask that you wait until you receive this e-mail and have the DOI to do any posting.

Posting to a repository: Authors may post their AAM immediately to their employer's institutional repository for internal use only and may make their manuscript publically available after the journal-specific embargo period has ended.

Please also refer to Elsevier's Article Posting Policy for further information.

18. **For book authors** the following clauses are applicable in addition to the above: Authors are permitted to place a brief summary of their work online only.. You are not allowed to download and post the published electronic version of your chapter, nor may you scan the printed edition to create an electronic version. **Posting to a repository:** Authors are permitted to post a summary of their chapter only in their institution's repository.

20. **Thesis/Dissertation**: If your license is for use in a thesis/dissertation your thesis may be submitted to your institution in either print or electronic form. Should your thesis be published commercially, please reapply for permission. These requirements include permission for the Library and Archives of Canada to supply single copies, on demand, of the complete thesis and include permission for Proquest/UMI to supply single copies, on demand, of the complete thesis. Should your thesis be published commercially, please reapply for permission.

Elsevier Open Access Terms and Conditions

Elsevier publishes Open Access articles in both its Open Access journals and via its Open Access articles option in subscription journals.

Authors publishing in an Open Access journal or who choose to make their article Open Access in an Elsevier subscription journal select one of the following Creative Commons user licenses, which define how a reader may reuse their work: Creative Commons Attribution License (CC BY), Creative Commons Attribution – Non Commercial - ShareAlike (CC BY NC SA) and Creative Commons Attribution – Non Commercial – No Derivatives (CC BY NC ND)

Please refer to Elsevier's Open Access Policy for further information.

21. **Other Conditions**:

v1.7

Questions? customercare@copyright.com or +1-855-239-3415 (toll free in the US) or +1-978-646-2777.

Gratis licenses (referencing $0 in the Total field) are free. Please retain this printable license for your reference. No payment is required.